

**Development and Test of a 1,000 Level 3C
Fiber Optic Borehole Seismic Receiver Array
Applied to Carbon Sequestration**

Final Scientific/Technical Report

**Reporting Period:
October 1, 2010 - February 28, 2015**

**Björn N.P. Paulsson, Ph.D.
Phone: +1-310-780-2219
Email: bjorn.paulsson@paulsson.com**

May 29, 2015

DOE Award Number: DE-FE0004522

**Paulsson, Inc.
16543 Arminta Street
Van Nuys, CA 91406-1745**

DISCLAIMER

This report was prepared as an account of work sponsored by an agency of the United States Government. Neither the United States Government nor any agency thereof, nor any of their employees, makes any warranty, express or implied, or assumes any legal liability or responsibility for the accuracy, completeness, or usefulness of any information, apparatus, product, or process disclosed, or represents that its use would not infringe privately owned rights. Reference herein to any specific commercial product, process, or service by trade name, trademark, manufacturer, or otherwise does not necessarily constitute or imply its endorsement, recommendation, or favoring by the United States Government or any agency thereof. The views and opinions of authors expressed herein do not necessarily state or reflect those of the United States Government or any agency thereof.

ABSTRACT

To address the critical site characterization and monitoring needs for CCS programs, US Department of Energy (DOE) awarded Paulsson, Inc. in 2010 a contract to design, build and test a fiber optic based ultra-large bandwidth clamped borehole seismic vector array capable of deploying up to one thousand 3C sensor pods suitable for deployment into high temperature and high pressure boreholes.

Paulsson, Inc. has completed a design of a unique borehole seismic system consisting of a novel drill pipe based deployment system that includes a hydraulic clamping mechanism for the sensor pods, a new sensor pod design and most important – a unique fiber optic seismic vector sensor with technical specifications and capabilities that far exceed the state of the art seismic sensor technologies.

These novel technologies were all applied to the new borehole seismic system. In combination these technologies will allow for the deployment of up to 1,000 3C sensor pods in vertical, deviated or horizontal wells. Laboratory tests of the fiber optic seismic vector sensors developed during this project have shown that the new borehole seismic sensor technology is capable of generating outstanding high vector fidelity data with extremely large bandwidth: 0.01 – 6,000 Hz. Field tests have shown that the system can record events at magnitudes much smaller than M-2.3 at frequencies up to 2,000 Hz. The sensors have also proved to be about 100 times more sensitive than the regular coil geophones that are used in borehole seismic systems today. The fiber optic seismic sensors have furthermore been qualified to operate at temperatures over 300°C (572°F).

The fibers used for the seismic sensors in the system are used to record Distributed Temperature Sensor (DTS) data allowing additional value added data to be recorded simultaneously with the seismic vector sensor data.

Table of Contents

Executive Summary	5
Key Project Tasks and Deliverables	7
The Optical Sensor Technology.....	7
The Fiber Optic Seismic Sensor (FOSS)™ Technology	10
Manufacturing of the Fiber Optic Seismic Sensors	15
Testing the Fiber Optic Seismic Sensors (FOSS)™	15
System Electronics.....	23
Deployment System	23
The Sensor Deployment Technology.....	23
Test of Deployment System Components.....	26
Pull Test of Tool Joints – Setup and Results	28
Torque Test of Tool Joints – Set Up and Results	28
Hydro Test of Tool Joints – Set Up and Results.....	32
Pull Test of Drill Pipe – Set Up and Results.....	33
Destructive Testing of Sensor Pod Housing welds – Set Up and Results	35
Non-Destructive Testing of Sensor Pod Housing welds – Set Up and Results	37
Non-Destructive and Destructive Testing of Sensor Pod Housing – Set Up and Results	38
Pressure rating of the OpticSeis® sensor pod.....	43
Operation of the OpticSeis® system.....	43
The Long Beach, CA Field Tests of the OpticSeis® system, November 2012	47
Processing of Long Beach, CA Data	53
The Pearland, TX Field Tests of the OpticSeis® system, June 2013	55
Deployment Speed of OpticSeis® System	58
Processing of Pearland, TX Data	62
Late Developments	67
Next steps.....	68
Conclusions.....	69
References	70

Executive Summary

Effective storage of CO₂ is critically dependent on a precise understanding of the complexity of the geologic formations prior to the development of the CO₂ storage site. A successful storage also depends on an accurate and robust long term monitoring program to understand the dynamic processes of the injection of the CO₂ and the interaction of the CO₂ with the geologic formation. The complex storage processes of CO₂ will thus only be understood and managed in detail if robust high-resolution reservoir imaging and monitoring technologies are available to characterize the dynamic behavior reservoirs in the early phases of the CO₂ storage field development.

High-resolution imaging, including mapping of complex high angle faults and fractures, can only be achieved if large volumes of high quality high frequency borehole seismic data can be recorded and sampled properly both spatially and temporally. 3D borehole seismic (3D VSP) P-wave images have shown routinely to have better than twice the spatial resolution than surface seismic images in areas with excellent surface seismic data. In areas with poor to very poor surface seismic data the 3D VSP technique has been proven to still be able to record the high quality P-wave data needed for high resolution P-wave 3D imaging. High-quality Converted Shear (CS) wave data are also routinely recorded during borehole seismic acquisition. Images generated using Converted Shear waves, due to their much shorter wave lengths, potentially offer a significant resolution improvement over P-wave images. Shear waves and shear wave images are also providing additional pore-pressure, directional stress, lithologic, stratigraphic, fault and fracture information about the geologic formations surveyed.

A long borehole seismic vector array is a large aperture seismic antenna where the incoming vector of the seismic energy is recorded at each 3C station. This is what is needed to effectively and precisely map the spatial distribution of natural and induced seismic events. An array with high vector fidelity is an essential component to determine the type of natural or induced seismic events that are being recorded. A correct determination of the vector of the recorded seismic events, from either active or passive seismic sources, is a critical input for both 3D imaging and 3D mapping of induced seismic events. The 3D borehole seismic P and S wave images will provide high resolution depth images far away from the borehole complementing the currently used reservoir characterization techniques. As a rule, the diameter of the 3D VSP depth images using primary reflections is equal to the image depth – example: at a depth of 3,000 m. the image diameter is 3,000 m. If secondary reflections, i.e. multiples, are used in the imaging process then the image coverage grows significantly.

The 3D VSP technique can produce much higher resolution images than surface seismic techniques and image much larger reservoir volumes than well logging techniques. The 3D VSP technique is thus filling the coverage and resolution gaps between the low resolution but large areal coverage surface seismic techniques and high resolution but limited coverage well logging techniques.

To allow the acquisition of the large volumes of high quality data required for high resolution imaging and monitoring we designed an ultra large borehole seismic array system that can deploy as many as 1,000 3C clamped sensors in deep vertical and horizontal wells. To make this

large array possible we designed high temperature fiber optic seismic sensor technology which allows the deployment of 3,000 vector sensors using only limited number of fibers. To safely deploy all these fiber optic sensors we also designed a high strength ultra-robust small diameter drill pipe based deployment system with a built-in active all-metal hydraulic clamping system.

During the design and development phase of the sensor technology, we manufactured a number of fiber optic seismic sensors using several different form factors and tested the sensors in our laboratory at different accelerations, different frequencies and at elevated temperatures. After a large number of tests we were able to arrive at a sensor design which provides an outstanding combination of sensor qualities such as sensitivity, vector fidelity, robustness and small size. We have shown that the fiber optic seismic sensors that will be used in our large 3C borehole seismic array are more sensitive, have a lower noise floor, have a broader band width and are more robust than electronic equivalents such as standard geophones and MEMS sensors. These attributes are making them an excellent choice for the demanding borehole environment. The range of data recorded in a borehole includes low frequency large amplitude data from surface seismic sources and very low amplitude high frequency data from natural and induced micro seismic events.

The fiber optic borehole seismic array will be able to monitor and map the injection of fluids into the reservoirs using 3D location of micro seismic events. The critical differences between the new fiber optic downhole array described in this paper and existing downhole receiver arrays are the large aperture, the fine spatial sampling and higher sensitivity afforded by the ultra-large 3C fiber optic array. One will routinely record broad bandwidth micro seismic data with frequencies over 1,000 Hz during monitoring of micro seismic events from natural causes or induced fracturing. This is outside the effective operational frequency range of currently used borehole seismic geophones.

The drill pipe deployment design allows the receiver array to be deployed in both vertical and horizontal wells which is an operational requirement in CO₂ injection wells since many of the wells drilled for CO₂ injection are highly deviated. The all metal clamping system for the 3C sensor pods is using drill pipe hydraulics as a power source. The fiber optic sensors are operated using light only and manufactured using high temperature fibers. This combination has allowed us to design and manufacture a receiver array that can operate to temperatures up to 300°C (572°F) at pressures up to 30,000 psi. Since no electronics or electric power will be used in either the hydraulic clamping system or for the fiber optic sensors the borehole seismic fiber optic sensor system is intrinsically safe.

To demonstrate the 3C borehole seismic system we built first a six then a sixteen level clamped array and tested the six level array in two wells, one in California and one in Texas, by recording data from both surface and borehole seismic sources. Finally we processed the data from the two borehole seismic field tests of the new fiber optics seismic vector sensor system. The field survey results show that we achieved the design goal to develop a borehole seismic array that is significantly more sensitive, has a higher bandwidth and has a better vector fidelity than the current state of the art borehole seismic arrays using geophone sensor technology.

Key Project Tasks and Deliverables

The project scope included the following technical tasks.

Task 2.0 Determine System Specifications

Task 3.0 Design of the Borehole Seismic System

Task 4.0 Manufacturing of the Prototype

Task 5.0 Environmental and Bench Test of Prototype

Task 6.0 Geophysical Test of Prototype Five Level Array Unit

Task 7.0 Test Evaluation and Report of Prototype

Task 8.0 Fabrication of the Field-scale 3C Seismic Array Demonstration System

Task 9.0 Geophysical Surveys using the Field-scale 3C Demonstration System

The remainder of the report is organized to discuss results from these tasks activities. This is followed by a Conclusion section.

The Optical Sensor Technology vs State-of-the-Art Geophones

In seismic exploration the coil geophone has been the standard sensor for exploration work in the oil and gas industry for over 70 years, Wolf et al. (1938). The coil geophone has been very successful because it combines high performance and a robust design with a reasonable price. A few years ago a new seismic sensor was introduced; the Micro Electro Mechanical Systems (MEMS) accelerometer with hopes that it would deliver a game-changing performance improvement. It was thought that the MEMS sensor would record higher fidelity and higher frequency data than the coil geophone. However, the MEMS sensors have proved to only provide similar data to the regular geophone, Hons et al. (2008), so the regular coil geophones are still the sensors of choice for seismic surveys with millions of units manufactured each year.

To judge the success of the fiber optic sensors we must compare these new sensors with geophones. The fiber optic seismic sensor technology compared with the geophones have a number of positive attributes. The positive attributes include a low noise floor, a high sensitivity, broad bandwidth, extreme robustness and reliability and high temperature capability.

The novel seismic sensor technology we are presenting is based on technology originally developed for the US Navy. The US Navy has for many decades been one of the largest and one of the most sophisticated users of sensors in its operations worldwide. In particular the US submarine fleet has deployed hydrophone sensors that have been more sophisticated and more

advanced than hydrophone sensors used for the geophysical industry for exploration applications.

After more than a decade of development work the US Navy equipped its newest members of its submarine fleet, the Virginia Class submarines, with arrays of 2,700 fiber optic hydrophones mounted on the hulls of the submarines. The array can be seen mounted on the first Virginia class submarine hull commissioned in August 2003 shown in Figure 1, Dandridge et al. (2004).

The system is called the Light Weight Wide Aperture Array (LWWAA) which is a passive Anti Submarine Warfare (ASW) sonar system which consists of three large array panels each containing 450 hydrophones mounted on either side of the submarine's hull. The Navy Research Lab (NRL) developed and demonstrated fiber optic methods based on the Michelson interferometry technique which measure the strain in fiber from dynamic acoustic signals. The primary reason for the new technology was the requirement for 30+ years of operation without maintenance. The new fiber optic sensors have proved to be much more sensitive and much more reliable than the old piezo-electric and electronic/digital hydrophone system, thus validating the fiber optic sensor choice by the US Navy for its submarines.

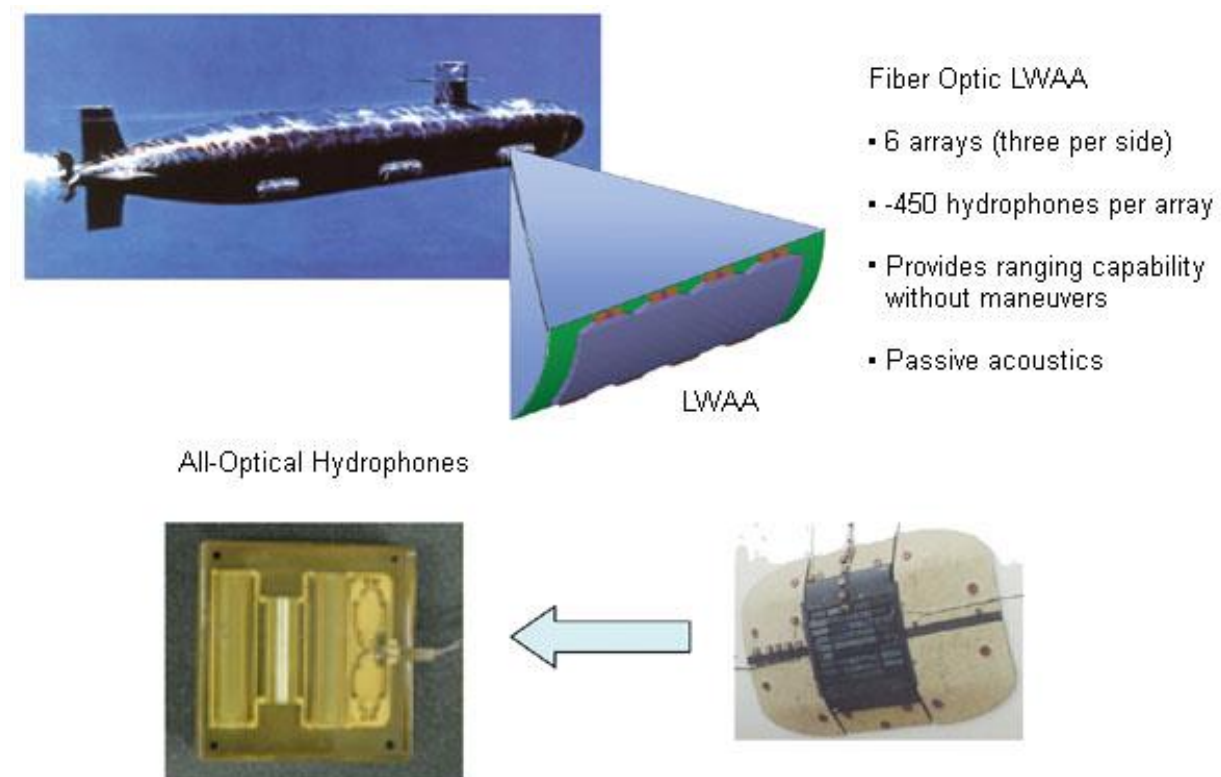


Figure 1. NSSN Virginia Class Attack submarine FOAS array shown mounted on the hull. Also shown are details of the sensors and the sensor arrays. The number of sensor for the FOAS array is similar to the Fiber Optics Seismic Sensor (FOSS)TM array. The FOAS has 2700 acoustic sensor while the FOSS is designed for 3,000 vector sensors.

An important fact is that the number of fiber optic sensors mounted on the submarine hull similar to the number of sensor that can be used for the Paulsson FOSSTM system.

The current trend for the development fiber optic sensor technology is towards simpler designs, Kirkendall et al. (2004). The Navy system is based on configurations a and b in Figure 2 while the Paulsson FOSS™ array design is based on configurations c and d shown in Figure 2.

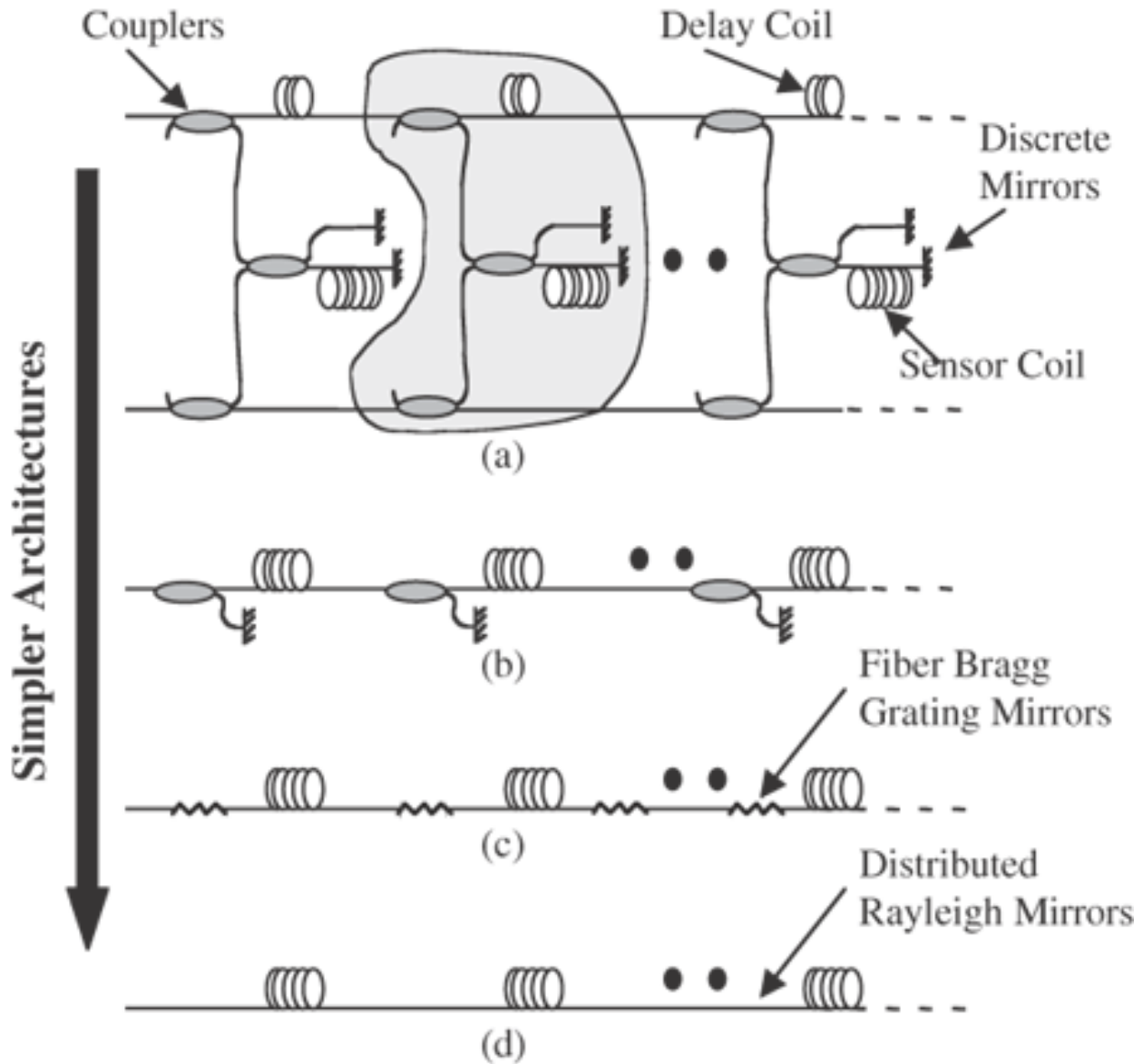


Figure 2. (Figure 4 in Kirkendall et al. 2004). The trend toward simpler fiber optic multiplexing architectures; from discrete coupler based interferometers (a), to in-line Michelson configurations (b) or Fiber Bragg Gratings (FBG) (c) with fewer components, to Rayleigh based architectures (d) which use inherent properties of the fiber itself and require no additional optical components.

The new fiber optic sensor developed for the US Navy is in principle a very simple sensor. It uses the dynamic strain of the fiber between two reference points to generate the signal. These mirrors can be seen in (a) and (b) part of figure 2. The sensor elements, or mandrels, can be configured in a number of different ways. By arranging the strain sensing fiber differently the fiber optic sensor can be configured as either:

1. A strain sensor
2. A fiber optic hydrophone
3. A fiber optic accelerometer

Paulsson, Inc. has designed and developed the third option listed above – the fiber optic accelerometer which is the key component of the 3C sensor package that is part of the OpticSeis® borehole seismic system. It is critical to use a vector sensor rather than an acoustic sensor because the medium for geophysical imaging is an elastic medium while the imaging medium for the Navy is an acoustic medium. An elastic medium is much more complex than an acoustic medium for imaging so a vector sensor is required.

The Fiber Optic Seismic Sensor (FOSS)™ Technology

The FOSS system dynamically measures the strain of the fiber between two Fiber Bragg Gratings (FBG) using an interferometric technique and a Time Domain Multiplexing (TDM) technique to transmit the dynamic fiber strain information to the recording instruments.

Time Domain Multiplexing (TDM): Interrogator System Overview

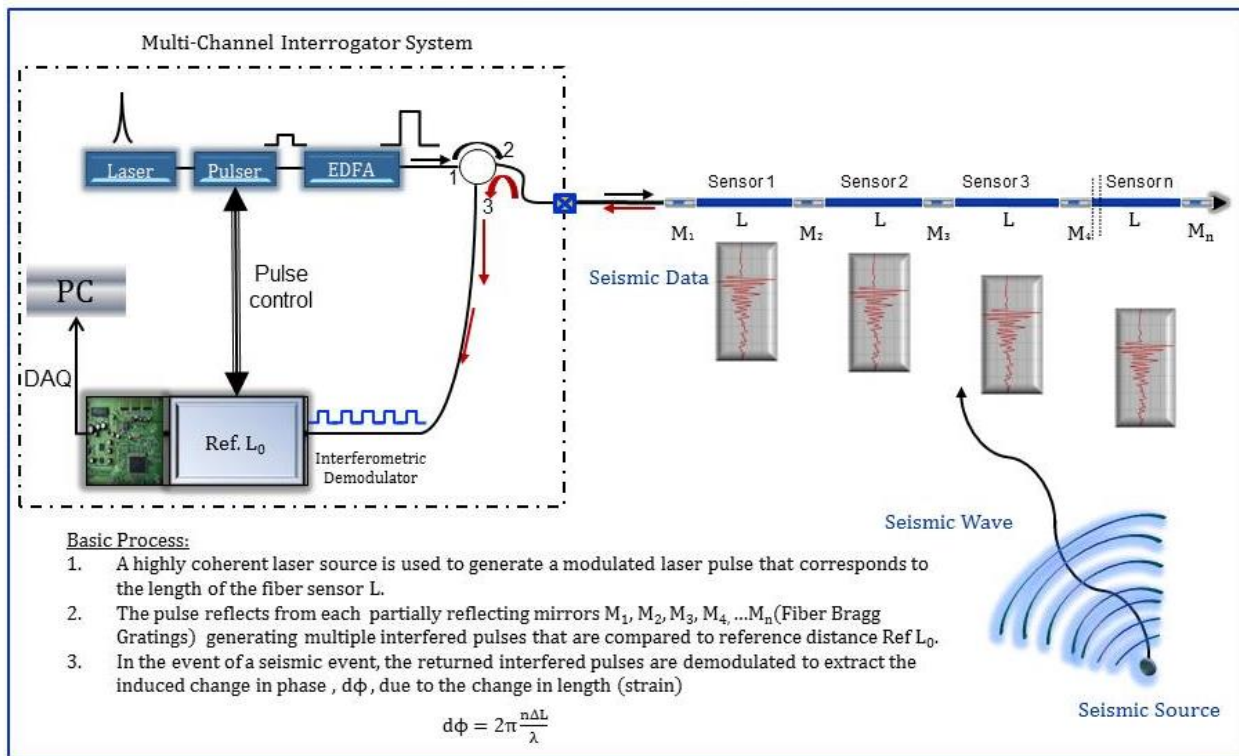


Figure 3. The Optical Interrogator Diagram. The Fiber Optic Seismic Sensor (FOSS)™ system is comprised of three basic integrated building blocks; the Fiber Optic Seismic Sensor (FOSS)™; the telemetry cable and the Optical Interrogator. The interrogator technology was first developed by US Navy Research Laboratory (USNRL).

A Fiber Bragg Grating (FBG) is a reflector in the fiber core with a low reflectivity used to separate the sections of fiber into individual sensors allowing recording and analysis of the

multiple sensors on a single fiber. A low reflectivity allows most of the light to continue to the next set of FBG's, allowing for many FBG's and thus many sensors. A schematic of the Fiber Optic Seismic Sensor (FOSS)TM system is shown in Figure 3. This use of fiber optic technologies allows a large number of seismic sensors to be deployed on one fiber while maintaining the high performance attributes of the sensors.

The Fiber Optic Seismic Sensor (FOSS)TM is immune to electric and electromagnetic interference, since the system does not require any electronics at the fiber optic sensor end. This design also makes the fiber optic seismic sensor extremely robust and able to operate in extreme environments such as temperatures up to and over 300°C. Even higher temperatures are possible using specialty fibers.

The Time Domain Multiplexing (TDM) method interrogates the sensors by sending one light pulse at a time and recording the reflections from the FBG's from each sensor in an array as seen in Figure 3. One can measure strain using a single FBG as shown in Figure 4. A single FBG sensor is however not sensitive enough for high quality seismic measurements. A much better approach for demanding seismic applications is to use pairs of FBG and use the fiber between the FBG's as the sensor. The strain in the seismic sensor is measured interferometrically by comparing the changes in the relative phase angle between the reflections of the two FBG's bracketing the section of sensing fiber. In the case of a FOSS the sensing fiber responds to seismic vibration by dynamically straining the fiber as shown in Figure 5.

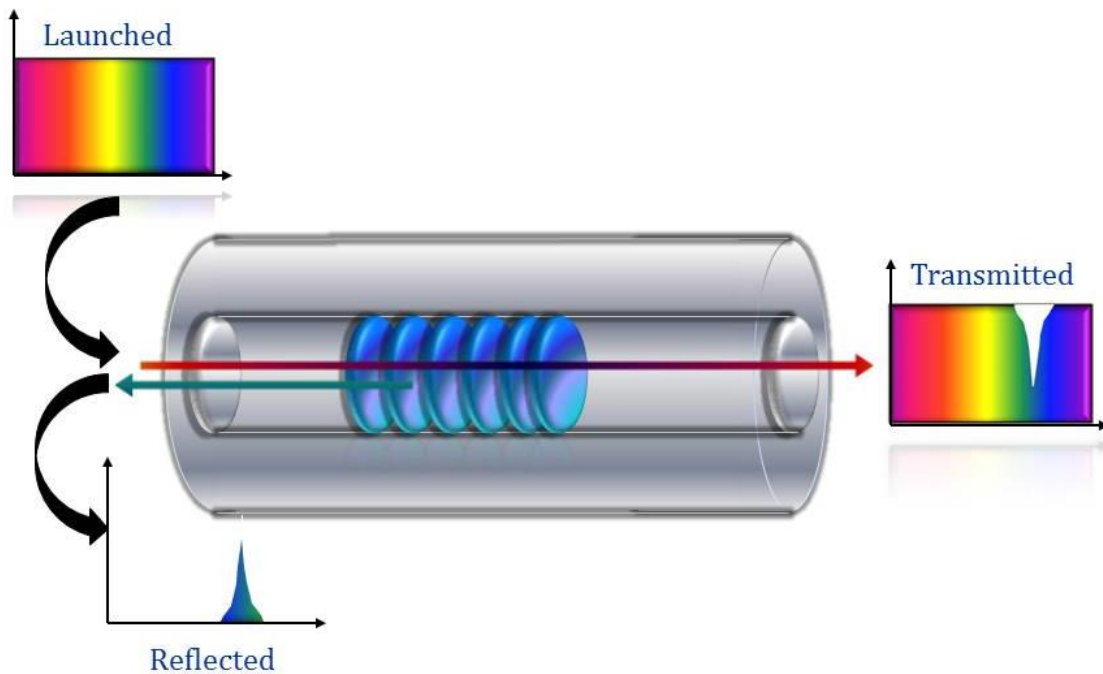


Figure 4. This figure shows a single Fiber Bragg Grating (FBG) written into an 80 μm fiber. A single FBG responds to changing pressure, temperature and to seismic waves. A single FBG is however not sensitive enough to record high quality seismic data.

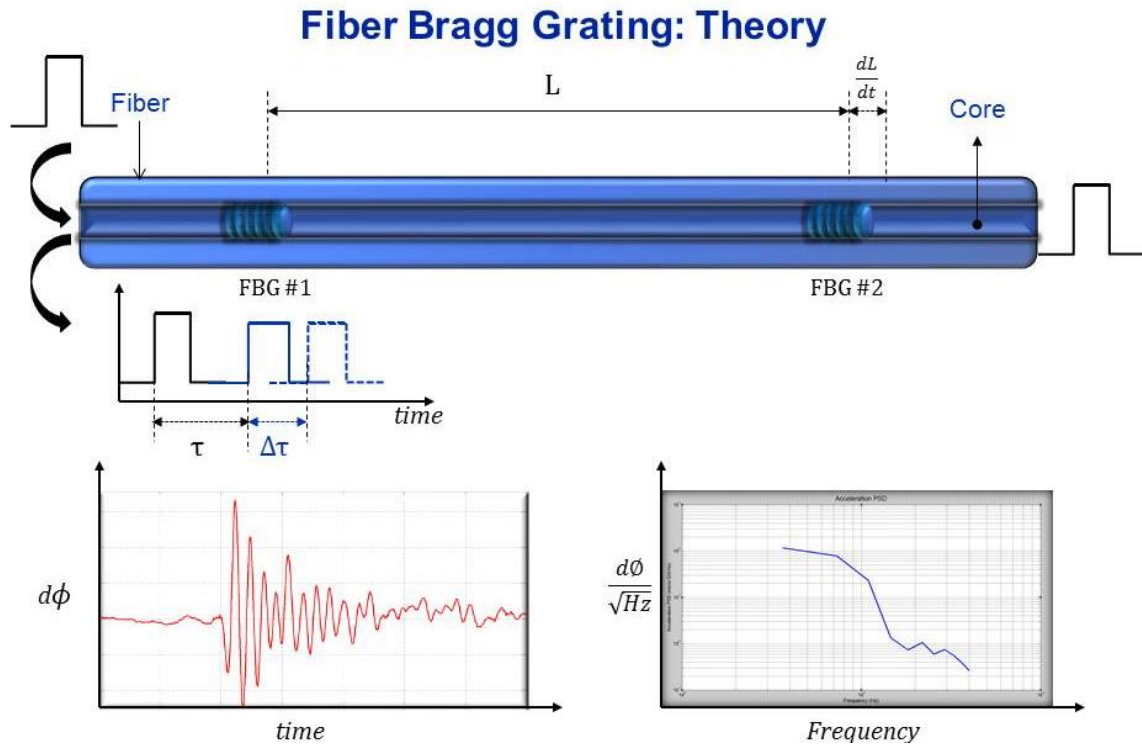


Figure 5. The fiber between a pair of Fiber Bragg Gratings (FBG's) respond to changing pressure, temperature and to seismic waves using interferometric measurements between two FBG's. While the pressure and temperature measurements are static measurements the seismic data is dynamic which allow high quality seismic to be recorded at different temperatures.

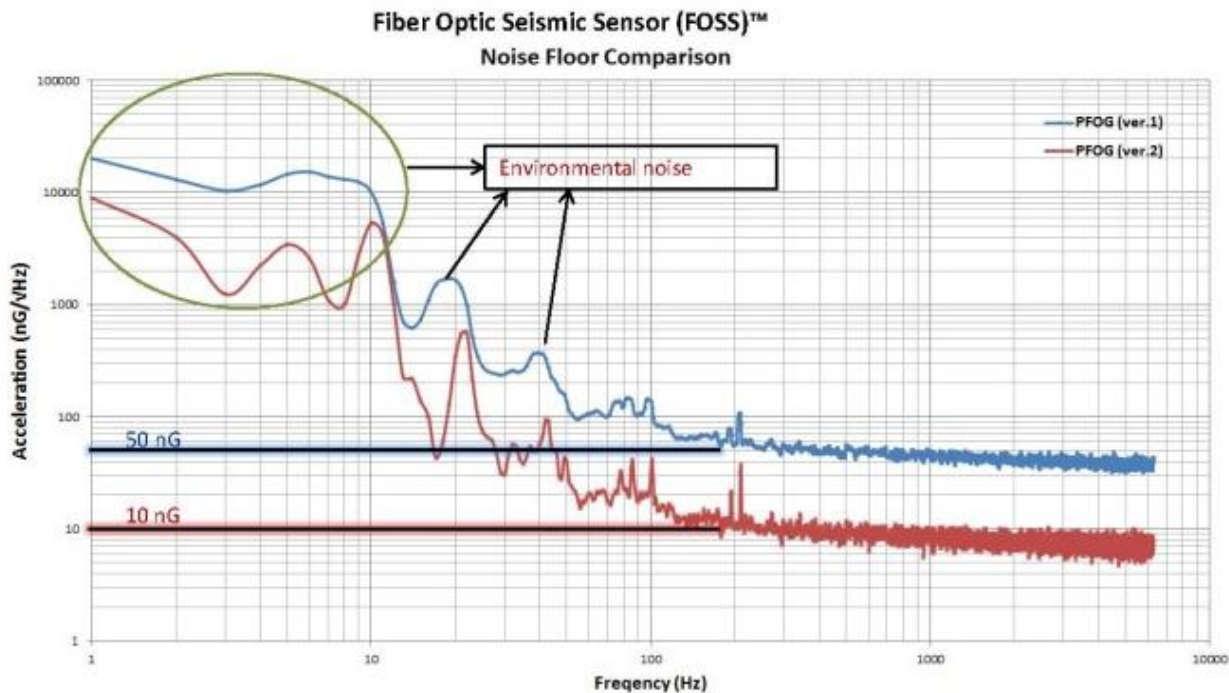


Figure 6. Noise floors for the Paulsson Fiber Optic Seismic Sensor (FOSS)TM System. The blue curve was the initial 2011 noise floor of the system when it was first assembled. After noise source and noise reduction analysis the 2012 noise floor is shown in the red curve.

The fiber optic sensor system can measure strains in the fiber with a resolution of about 1 picometer (1×10^{-12} m). The optical sensor telemetry system is inherently low noise since it does not pick up electrical noise from any source. The system also uses low noise surface electronics to convert the optical data into electric digital data.

When the fiber optic seismic sensor system developed by Paulsson, Inc. was first tested, the noise floor at frequencies above 120 Hz was measured to be $50 \text{ ng}/\sqrt{\text{Hz}}$. At frequencies below 120 Hz the noise floor was affected by environmental noise. After several months of noise source analysis and changes to the system, the system noise was reduced by 80%. The measured noise floor in the fiber optic seismic sensor system now ranges from about $50 \text{ ng}/\sqrt{\text{Hz}}$ at 20 Hz to about $10 \text{ ng}/\sqrt{\text{Hz}}$ at frequencies over 120 Hz, as seen in Figure 6. Further improvements of the electronics will extend the $10 \text{ ng}/\sqrt{\text{Hz}}$ noise floor to 10 Hz and even below 10 Hz.

The current manufacturing and testing facility is next to a busy airport with significant environmental low frequency noise, as seen in Figure 6. The noise floor from the fiber optic sensor should be compared with published noise floors from coil geophones and MEMS sensor, (Hons and Stewart, 2009), which is about $1,000 \text{ ng}/\sqrt{\text{Hz}}$ (see Figure 7 from the Hons and Stewart, (2009) paper). The desired noise floor for high resolution seismic systems is listed as $100 \text{ ng}/\sqrt{\text{Hz}}$ by Panahi et al. (2006).

The rate of the phase modulated pulses sent by the interrogator to interrogate the FBG's depends on the overall length of the fiber cable. The maximum pulse rate for the interrogator, which is the optical equivalent of sampling rate for electronic systems, is twice the light transit time in the lead-in cable and array because, in the TDM interrogation scheme, the best performance is achieved if only one pulse travels in the sensor fiber at a time. For a 10 km long fiber the maximum sampling rate is 0.1 ms, or 10,000 Hz, yielding a Nyquist frequency of 5,000 Hz which is sufficient for most geophysical applications.

For the fiber optic seismic sensor we are using a pulse width of the interrogating pulses of twice the light round trip transit time between FBG's. For a 20 m length of fiber between the FBG's, i.e. a typical length of sensor fiber in the FOSS between the FBG's, and a refractive index of the glass of 1.5, the pulse width is thus 0.2 μsec .

Pulses reflected from each FBG contains phase information from preceding adjacent sensors proportional to the fiber strain between two FBG's on each side of the fiber wound around the mandrel as a result of the acceleration of the mandrel due to the passing seismic wave. Upon returning to the interrogator, each pulse is compared to a reference interferometer, generating an intensity pulse in the interrogator. The resulting intensity pulse is converted to an electrical signal and filtered in the analog front end and then digitized. Once digitized, the electrical signal is demodulated, thus yielding a digital word representative of the instantaneous fiber strain at the sensor. A software demodulation algorithm is then used to ensure a high fidelity output with a low noise floor and large dynamic range. De-multiplexing is accomplished by tracking the pulses in the order received: each from a different sensor. A large number of fiber-optic channels can be deployed on each fiber, making a large channel count system possible in hostile environments

such as in high temperature boreholes and on the ocean floor. Currently up to about 50 fiber optic seismic sensors can be operated on one fiber without loss of fidelity.

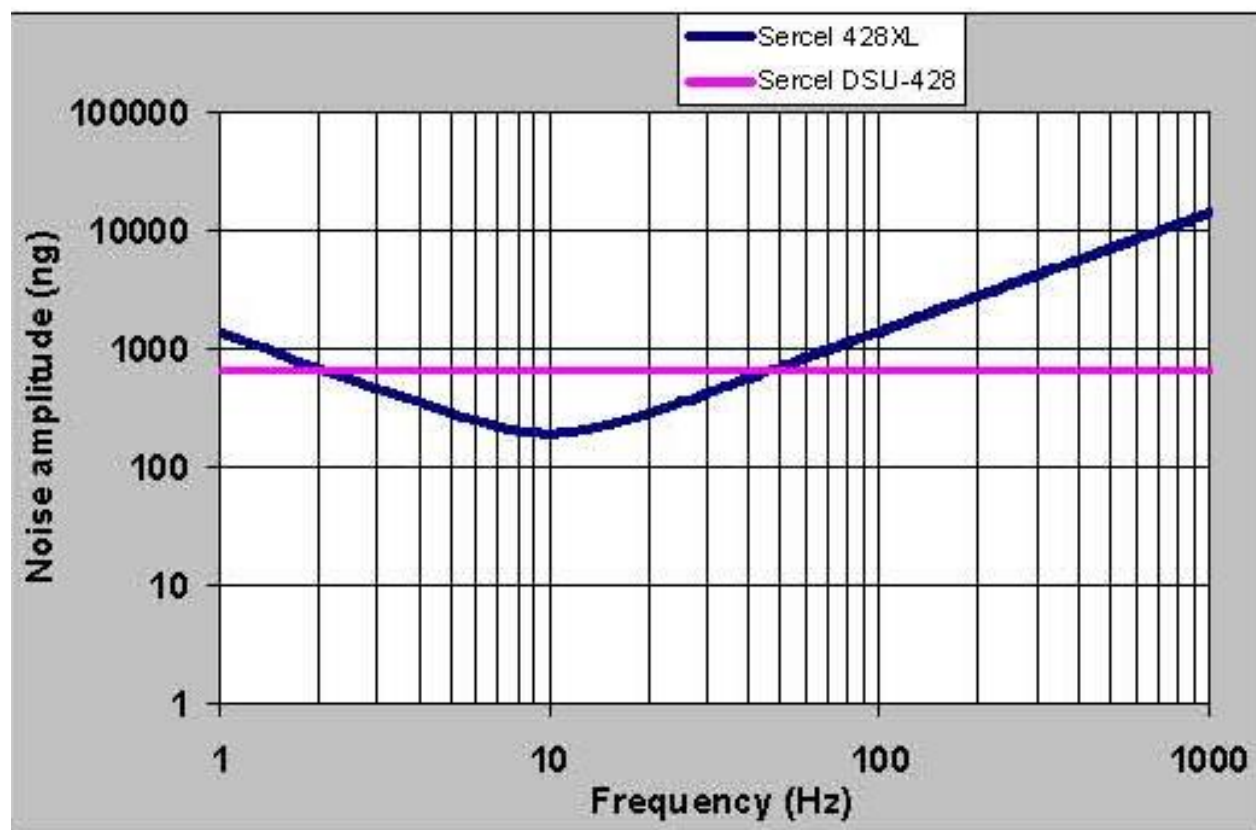


Figure 7. From Hons and Stewart, (2009). Figure 1. Modeled noise floor of a geophone and DSU recorded with the Sercel 428XL system, based published specifications of the DSU-428, the 428XL recording system and the SM24 geophone element.

One advantage fiber optic sensors have over conventional electronic based sensors is the ability to separate the electronics (preamplifiers, filters, ADC, multiplexing electronics, etc.) from the sensor without any degradation in performance. This removes the electronics from the hostile sensing environment (downhole, ocean bottom, buried, etc.), to a benign, controlled environment where they are accessible for maintenance, upgrades repairs. Thus, for permanently installed fiber optic seismic sensors, only the optical fiber, the mandrel and its associated packaging must be installed permanently. In the case of the new Fiber Optic Seismic Sensor (FOSS)TM this will significantly increase the robustness of the permanently installed sensors.

No electric power needs to be transmitted to the sensor, nor does the fiber optic sensor generate any electric signal, making the sensor intrinsically safe and immune from EMI/RFI. The high-temperature version of the Fiber Optic Seismic Sensor (FOSS)TM is manufactured using commercially available high temperature polyamide coated fiber allowing the sensor to work at temperatures as high as 320°C (608°F).

Manufacturing of the Fiber Optic Seismic Sensors

To manufacture the fiber optic sensor Paulsson, Inc. developed a new manufacturing process which included the design and manufacturing of a precision winding machine installed in a 1,000 rated clean room. The winding machine can be seen on the left side of the clean room, shown in



Figure 8. This photo shows the 1,000 rated clean room designed for the manufacturing of the Fiber Optic Seismic Sensors (FOSS)TM. The air in a 1,000 rated clean room is 1,000 time cleaner than the air outside the clean room.

Figure 8. This winding machine allows prototype manufacturing of our fiber optic sensors in a clean environment that minimizes the contamination of the fiber from air born particles. Keeping dust and dirt away from the fiber will significantly increase the life of the fiber based sensors.

Testing the Fiber Optic Seismic Sensors (FOSS)TM

To establish the absolute and relative performance of the Fiber Optic Seismic Sensors (FOSS)TM we designed and conducted a series of calibrated laboratory tests of the sensors. To establish the relative performance of the new sensors we did several of the tests concurrently on the fiber optic seismic sensor, a high quality high temperature geophone currently in use in borehole seismic tools and a high quality piezo electric based accelerometer.

The tests include:

1. Shaker test at frequencies ranging from 5 Hz to 4,000 Hz at 25°C
2. Shaker test at frequencies ranging from 5 Hz to 4,000 Hz at 200°C.
3. Low frequency test at frequencies ranging from 0.01 Hz to 10 Hz at 25°C.
4. Tap test at temperatures ranging from 25°C to 320°C.

We tested the Fiber Optic Seismic Sensor (FOSS)TM using a dynamic test system developed to test the new fiber optic sensors. This system has the shaker head installed in an environmental chamber capable of temperatures ranging from -65°C to +200°C. Figure 9 illustrates the



Figure 9. The dynamic test station for the Fiber Optic Seismic Sensors (FOSS)TM. This test station can test the sensor at both low (-65°C) and high (200°C) temperatures at frequencies from 5 Hz to 4,000 Hz.

layout of the dynamic testing system for one of the environmental chambers. The second oven shown in Figure 15 can reach 350°C. By combining the test results from several tests we thus tested the Fiber Optic Seismic Sensors (FOSS)TM at frequencies ranging from 0.01 Hz to 4,000 Hz, at temperatures ranging from 25°C to 320°C and at various accelerations. The first tests used our high frequency shaker system. We used sweeps from 5 Hz – 4,000 Hz at an acceleration of 600 μg to characterize the properties of the fiber optic seismic sensors. To compare and benchmark our Fiber Optic Seismic Sensor (FOSS)TM system we did simultaneous testing of the FOSS with a high temperature 15 Hz coil geophone currently used in borehole seismic tools and two high performance piezo electric accelerometer. We installed the four sensors on the shaker head inside the oven and attached them to our data acquisition system which is capable of simultaneous recording of all four sensors.

We first tested the sensors at 25°C in several frequency bands ranging from 5 – 4,000 Hz, followed by a 200°C test using the same frequency bands. The 10 – 200 Hz 600 μg test at 25°C is shown in Figure 10. The red curve is the piezo-electric feedback accelerometer data from 10 – 200 Hz. This accelerometer kept the shaker at 600 μg over the test frequency bands using a feedback loop system. The blue curve is the amplitude output from the regular 15 Hz geophone from 10 – 200 Hz. The green curve is from the second piezo-electric accelerometer. The purple curve is the amplitude output as function of frequency for the Fiber Optic Seismic Sensor (FOSS)TM test from 10 to 200 Hz. The test results from the 200°C tests are virtually identical to those at 25°C, showing that our fiber optic seismic sensor is stable with temperature.

Both the 25°C and the 200°C tests showed that the standard coil geophone lost most of its amplitude output at 100 Hz, while the accelerometers, both the fiber optic and the piezo- electric retained the amplitude over the entire test frequency band of 5 – 4,000 Hz.

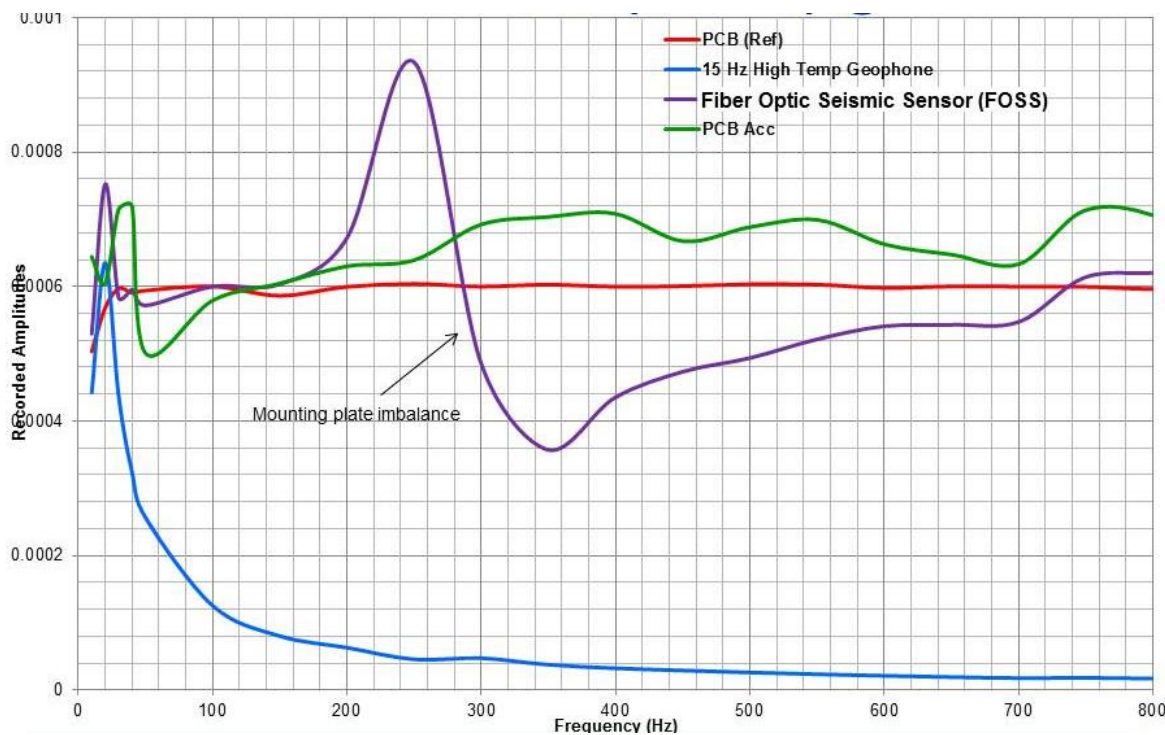


Figure 10. Results from a 10 – 800 Hz sensor test using a shaker at a fixed acceleration of $600 \mu\text{g}$ in an oven at 25°C with the test system shown in Figure 9. Four sensors were mounted on the shaker head. The four sensors included one reference accelerometer (red curve), one 15 Hz geophone (blue curve), one Fiber Optic Seismic Sensor (FOSS)TM (purple curve) and a second piezo-electric accelerometer (green curve).

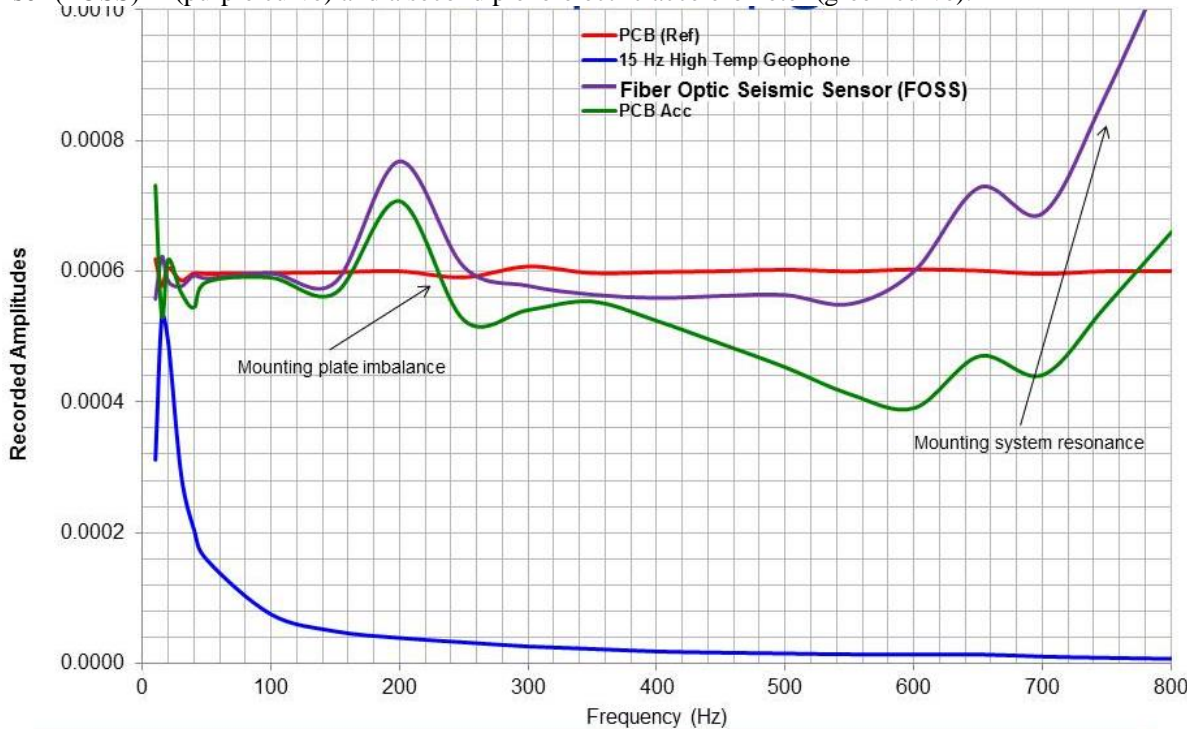


Figure 11. Results from a 10 – 800 Hz sensor test using a shaker at a fixed acceleration of $600 \mu\text{g}$ in an oven at 200°C with the test system shown in Figure 9. The same four sensors were tested as discussed in Figure 10. The purple and the green curves both show the resonances of the test set up at 200 Hz and at about 1,200 Hz which are the mounting plate resonances.

The performance tests of the sensors using the shaker were followed by tap tests of the sensors. We placed the three sensors in close proximity to each other on the top of the granite block seen in Figure 9. To isolate the test system from environmental noise the granite block was placed on active vibration isolation pads which can be seen under the granite block. The first tap test was performed at an ambient temperature of about 25°C. The tests involved comparing the performance of the FOSS with a standard high temperature borehole seismic 15 Hz coil geophone and a high performance accelerometer.

The data from the simultaneous tap test of the three sensors are shown in Figure 12. This figure shows that the first arrival of the fiber optic seismic sensor has a faster rise time, indicating a higher frequency response, than the other sensors. It is also clear from this data that the Fiber Optic Seismic Sensor (FOSS)TM has the highest signal/noise ratio. We calculated the signal-to-noise ratio by dividing the amplitude of the second positive peak with the mean amplitude of the pre-arrival data over a 5 ms window. The signal/noise ratio for the fiber optic seismic sensor is 617 (55 dB), the signal/noise ratio for the reference accelerometer is 149 (43 dB). The signal-to-noise ratio for the 15 Hz geophone is 15 (23 dB) for this particular test. The fiber optic seismic sensor thus has a 41 times larger signal-to-noise ratio than the regular coil geophone and a four times larger signal-to-noise ratio than the piezo-electric accelerometer.

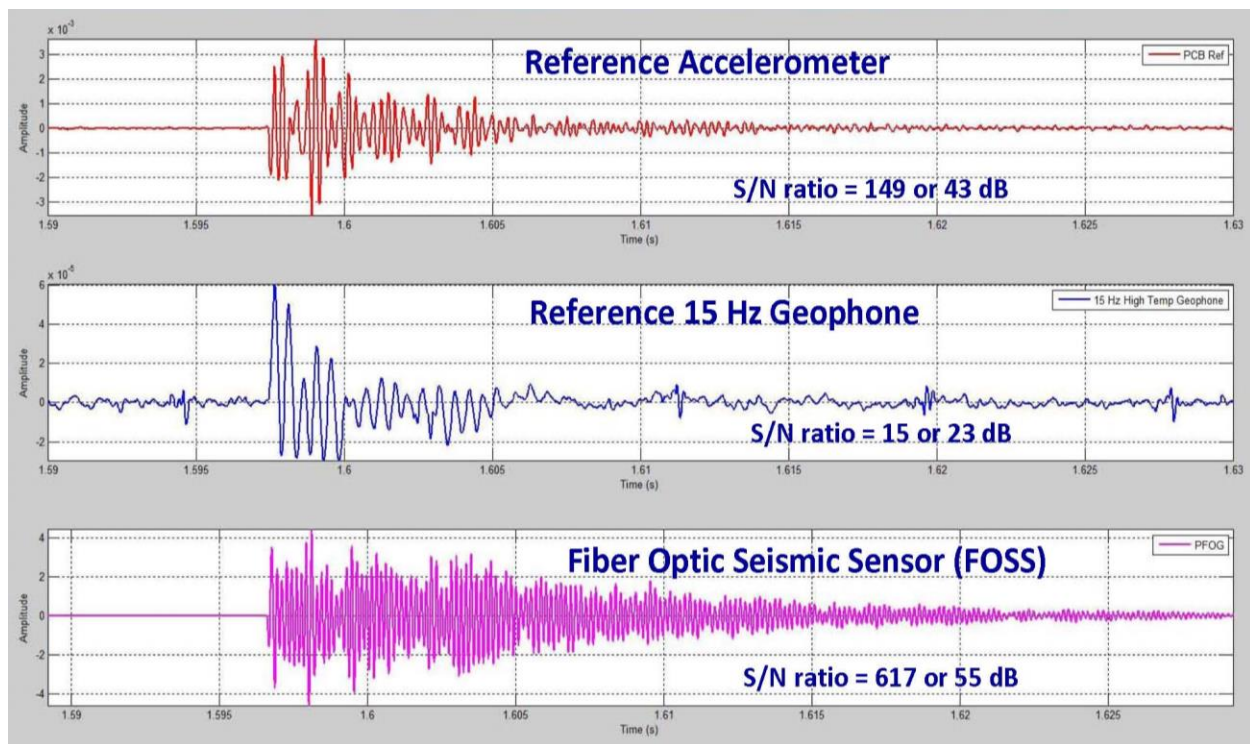


Figure 12. Seismic traces from simultaneous tap test of a reference accelerometer (top), a 15 Hz coil geophone (middle) and the Paulsson Fiber Optic Seismic Sensor (FOSS)TM (bottom). Band pass filter applied: 5 – 2,500 Hz.

We also evaluated our Fiber Optic Seismic Sensor (FOSS)TM in our low frequency test facility that is capable of testing our sensors from 0.01 Hz to 10 Hz (Period ranging from 100 seconds to 0.1 seconds). The result from one of the low frequency tests is seen in Figure 13.

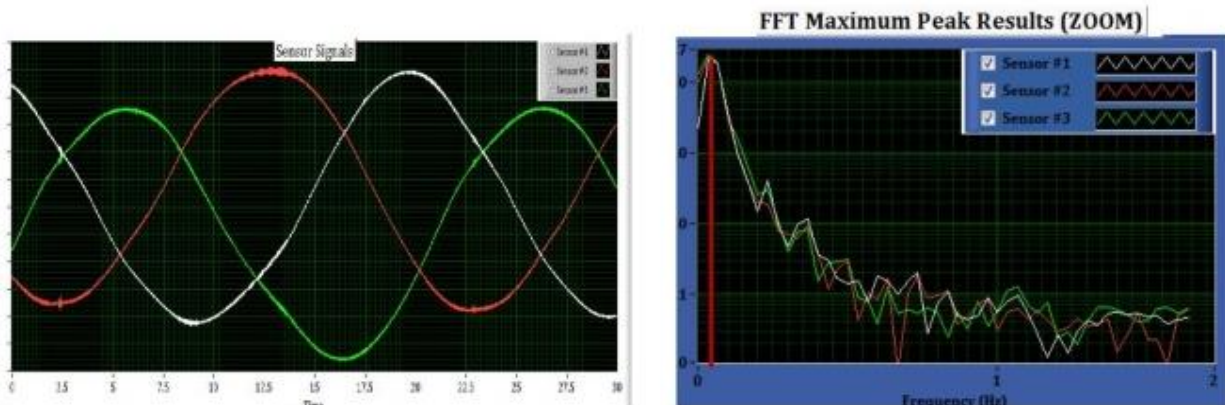


Figure 13. Simultaneous Low frequency test of three Fiber Optic Seismic Sensors at a frequency of 0.03Hz (33 second period). This system can test the sensors from 0.01 Hz – 10 Hz (Period of 100 sec. to 0.1 sec.).

During this test we were evaluating the performance of the 3C sensors at a frequency of 0.03 Hz (33 second period). We made a number of low frequency tests of the fiber optic seismic sensor. In one of the test series we tested the fiber optic sensor from 0.03 Hz to 0.9 Hz. The amplitude variation from this range of frequencies is shown in Figure 14 which shows that the amplitude response is almost flat. This particular test was performed at 25°C. High-temperature, low-frequency tests are planned for the future.

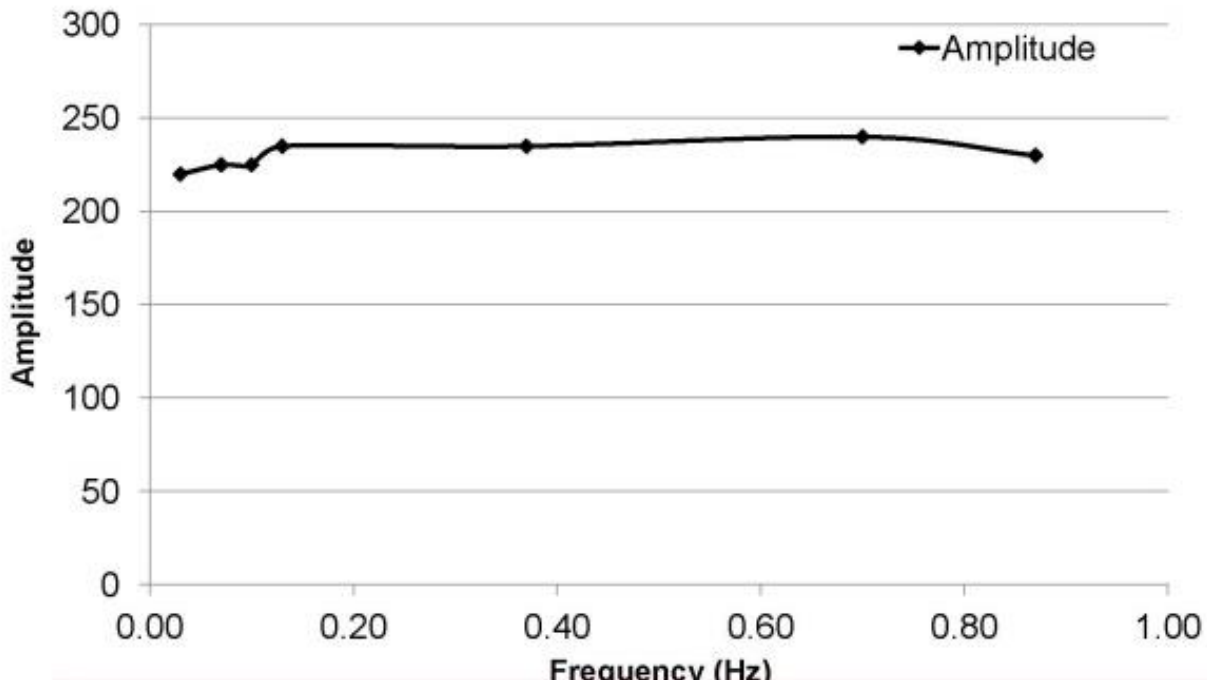


Figure 14. Seismic data amplitude variation during a low frequency test of the Fiber Optic Seismic Sensor (FOSS)TM at frequencies 0.03 – 0.9 Hz (33 – 1.1 second period).

In order to compare and benchmark the data recorded with the Fiber Optic Seismic Sensor (FOSS)TM as used in the field we mounted 3C FOSS sensors inside the sensor pod that is used for the borehole seismic systems. We then attached high temperature piezo-electric

accelerometers to the pod to generate comparative data. One external piezo-electric accelerometer was mounted parallel with the FOSS axial accelerometer near the left end of the sensor pod. The cable going to this accelerometer is seen at the left end of the fiber optic seismic sensor pod in Figure 15. The second accelerometer was mounted on the outside of the pod at the position of the radial optical seismic sensor, as illustrated in Figure 15.



Figure 15. This photo shows the 3C sensor pod inside a high-temperature oven at a measured temperature of 315°C.

A series of tap tests were performed by tapping the outside of the fiber optic seismic sensor pod at an extended range of temperatures to evaluate the performance of the fiber optic sensor while mounted inside the sensor pod. This set up allowed us to do dynamic testing of the fiber optics sensors and the pod as a system.

Figure 15 shows the sensor pod with the 3C sensors during the high-temperature test in the oven. The digital thermometer shows a temperature of 315°C on the base plate. A temperature reading on the pod itself showed a temperature of 320°C during the last tap test.

We started the tap test sequence at a room temperature of 25°C followed by increasing the temperature in a number of steps, as shown in Figure 16. For each new temperature, care was taken to make the seismic tap test measurement after the oven, the sensor pod and the fixtures reached their respective temperature equilibrium. Each temperature step took approximately two

hours. For the final test at 320°C we performed the test after the sensor pod with the three sensors had been in the oven for 54 hours.

In Figure 16, we show 20 ms records from eight different tap tests at eight different temperatures ranging from 25°C to 320°C. The data is very consistent considering manual taps were used by two different engineers. The first engineer did the tap tests from 25°C to 200°C and the second engineer the tap tests from 250°C to 320°C. No filtering was applied to the data displayed.

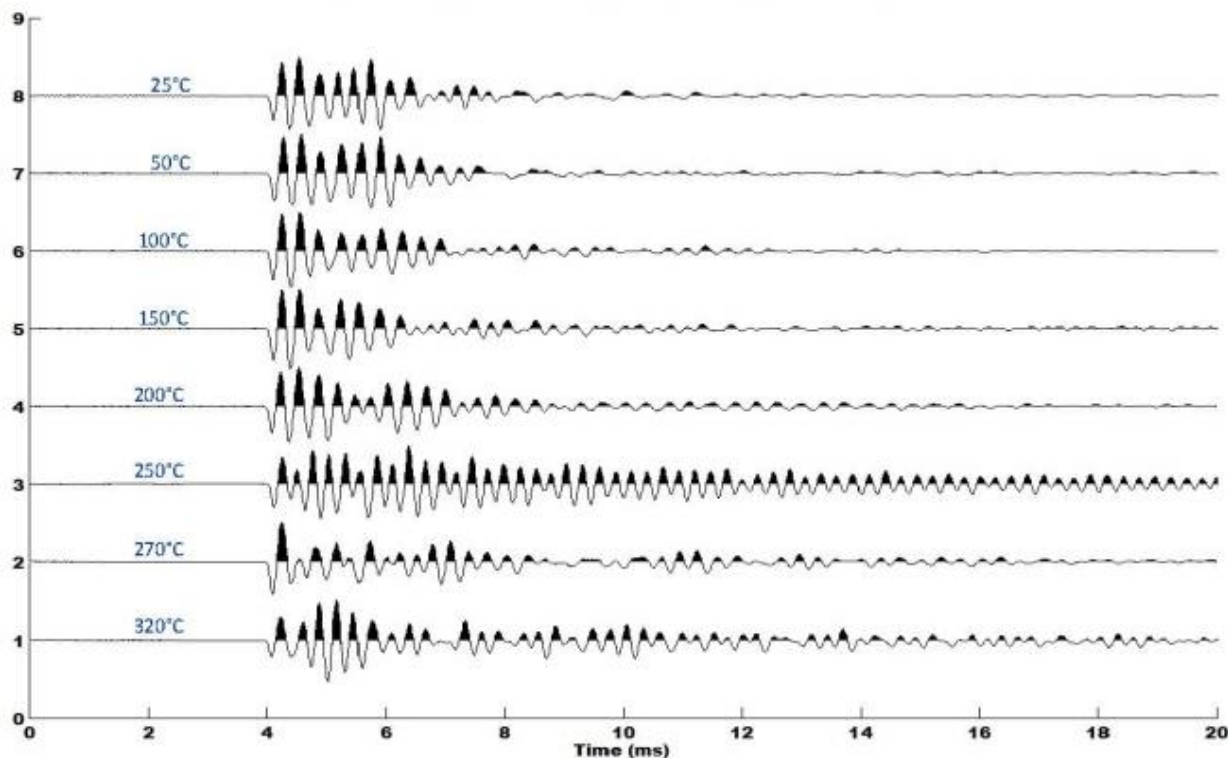


Figure 16. Tap test 20 ms data recorded on a Radial Fiber Optic Seismic Sensor (FOSS)™ installed in a 3C sensor pod at temperatures ranging from 25°C to 320°C.

In Figure 17 we show a 2 ms window including the first arrival of the data shown in Figure 16. Once again, the data is very consistent. When we analyze the spectral content of the laboratory tap test data we find high quality broad band seismic energy with the -15 dB points at ~1Hz and at ~ 6,000 Hz as shown in Figure 18. The broad band data together with the sensitivity and the high temperature capability of the sensor makes the Fiber Optic Seismic Sensor (FOSS)™ ideal for micro seismic monitoring of fluid injection and detection and mapping of fracturing reservoirs.

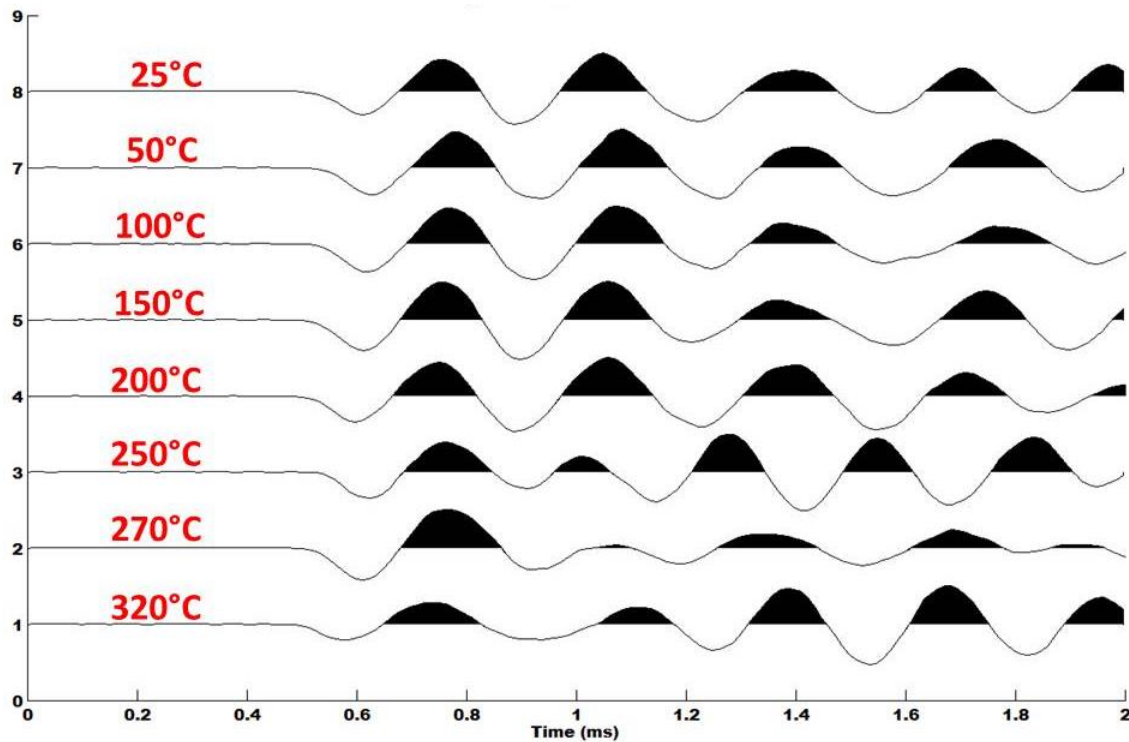


Figure 17. Tap test 2 ms data recorded on a Radial Fiber Optic Seismic Sensor (FOSS)TM installed in a 3C sensor pod at temperatures ranging from 25°C to 320°C. The 3C sensor pod can be seen in figure 15.

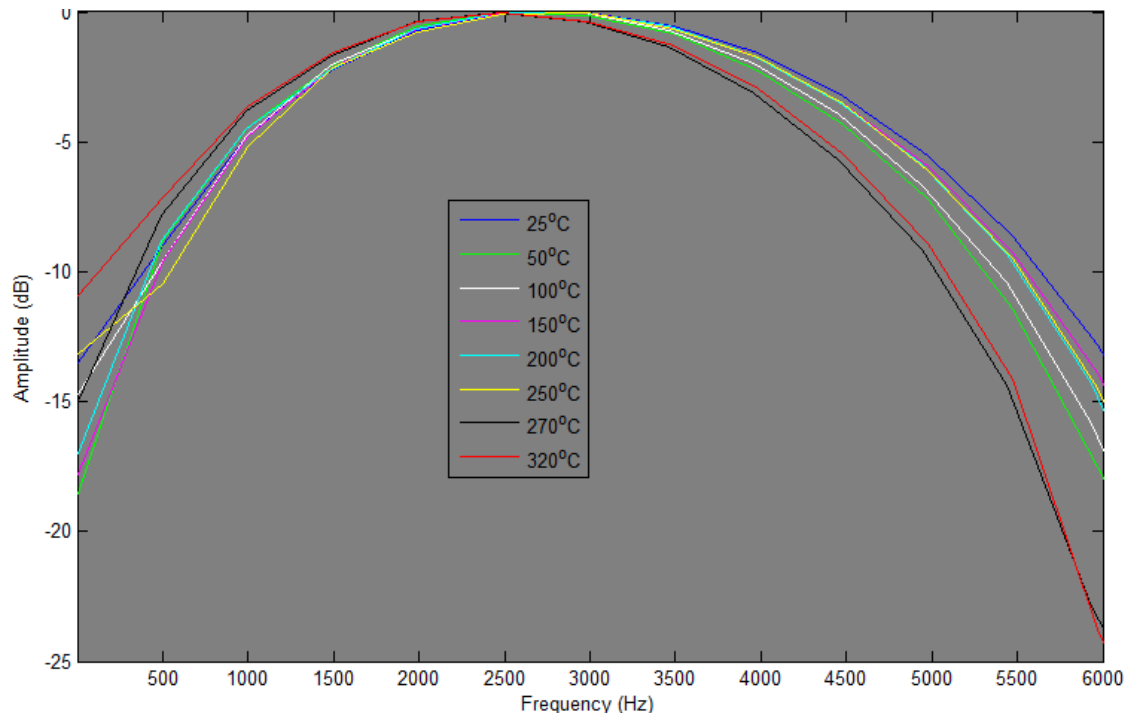


Figure 18. Spectra of the eight 2 ms waveforms of tap test data from Figure 17. The spectra demonstrate a high quality broad signal from close to 0 Hz to about 6,000 Hz.

System Electronics

The main components of the system electronics include an optical interrogator and an optical to SEGY converter. The interrogator electronics contains all the optical components including lasers, light splitters, modulators, circulators, compensators, Erbium Doped Fiber Amplifiers (EDFAs), amplifiers and A/D converters.

The Optical to SEGY is performed by streaming the digitized optical data to a high performance GPU based computer and convert the data in real time to SEGY data.

The system electronics can be seen in Figure 19. The electronics have been mounted into field racks that protect the electronics both during shipment and operations. The field rack mounting allows an efficient and safe set up of the system in the field.



Figure 19. Optical Interrogator for Paulsson OpticSeis™ system.

Deployment System

The Sensor Deployment Technology

Today commercially available borehole seismic arrays use wireline technology to deploy the sensors. Wireline technology has however a number of limitations including limited data transmission, limited power transmission, low strength and only capable of deploying the seismic tools in vertical or near vertical wells without using an expensive well tractor.

To deploy the new Fiber Optic Seismic Sensors (FOSS)™ Paulsson, Inc. designed and manufactured a deployment system that is based on small diameter high strength drill pipe. The seismic deployment system is manufactured using an S135 steel which is also used for offshore drilling. The system design and the quality of the steel used for the system allows us to deploy the borehole seismic array to a drilled depth of 30,000 ft in vertical and horizontal boreholes.

We have destructively tested the drill pipe used for the developed system and measured an axial strength of about 145,000 lbs. before exceeding the elastic yield point. The projected weight of the entire borehole system is about 5.4 lbs./ft. With a 20% safety margin the maximum weight we can use during the deployment of the borehole seismic system is 116,000 lbs. Using the measured strength of the drill pipe, the weight of the system and the assumed safety margin of 20% we can deploy a 200 level system to a drilled depth of about 21,730 ft. To deploy deeper than 21,730 ft we need to use a tapered string with heavier wall drill pipe when the load exceeds 116,000 lbs. We have designed such a pipe with the same OD but with a thicker wall capable to hold a weight of 220,000 lbs. Using the same assumptions as for the thinner wall tubing we can deploy the system until we reach a weight of 80% of 220,000 lbs. or 176,000 lbs. allowing us to deploy a 200 level system to a drilled depth of 30,000 ft.

The clamping function in the tool string is using an all-metal hydraulic actuator. This actuator is powered using tubing hydraulics controlled from the surface so the system does not use electric power in the tool for clamping purposes. A fiber optic downhole seismic sensor and a pipe hydraulic based clamping system are in combination thus intrinsically safe since no electric power is used for the sensor or the clamping system.

The deployment system consists of four sets of components:

1. Sensor pod housings as seen in Figure 20
2. Drill pipe as
 - a. spacers between the sensor pod housings, seen in Figure 20
 - b. the means to deploy and suspend the sensor array in vertical or horizontal wells
3. Bottom assembly as seen in Figure 21. The bottom assembly consists of
 - a. A Nose cone.
 - b. A Fluid Intake section - lower coupler.
 - c. A Fluid Intake section.
 - d. A Fluid Intake section - upper coupler and holder for check valve.
 - e. A Check valve holder.
 - f. A Burst disk assembly.
4. Top assembly consisting of
 - a. A 3' drill pipe pup joint. The drill pipe pup joint is capped at upper end and equipped with a number of ports to supply fluid to pressurize the drill pipe to actuate the clamping mechanisms.
 - b. Pressure gauges.

- c. Valves to supply the fluid to the drill pipe.
- d. Valves to release the clamping pressure as needed.

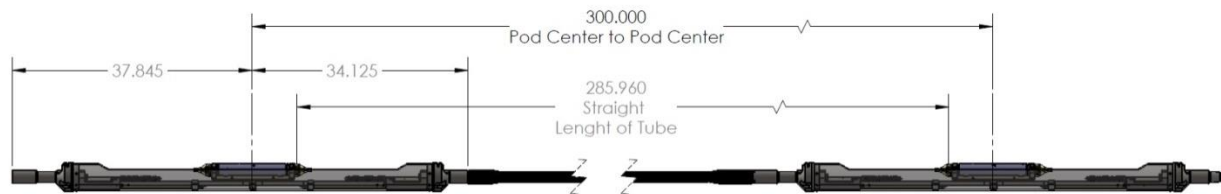


Figure 20. Two sensor pod housings showing a 300" (25 ft, 7.62 m) c/c pod spacing. The sensor pod housings serve several functions. One is to protect the sensor pods during the deployment. Second is to house the clamping mechanism. Third the sensor pod housing can also hold other sensors and functions.

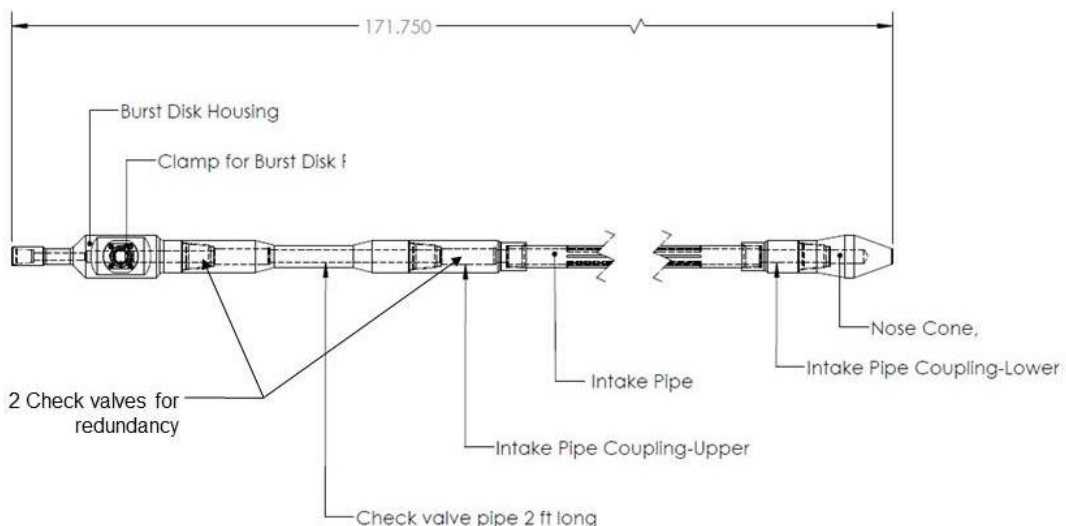


Figure 21. Bottom assembly of the array. The bottom assembly holds the nose cone, the intake pipe two check valves and a burst disk assembly.

The Sensor Pod Housing and Pod seismic Tool A in Figure 22 is shown in the vertical part of the well. Tool B is shown in the 45 degree part of the well and Tool C in the horizontal section of the well. Tool D, in the horizontal section of the well shows the last sensor pod housing and pod linked with the bottom assembly. The bottom assembly is a combination of fluid-take-in section, check valves and burst disk assemblies. This section is required for the safe operation of the clamping system for the 3C Fiber Optic Seismic Sensor (FOSS)TM pods.

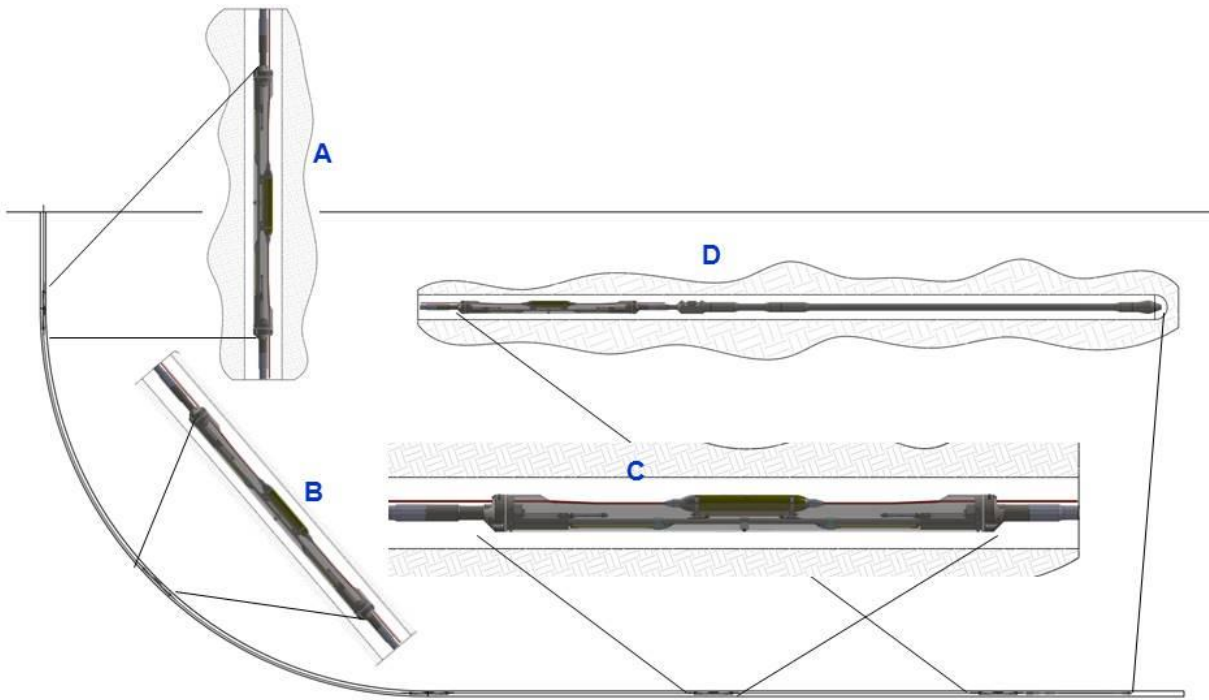


Figure 22. OpticSeis® redeployable array deployed into a well which starts vertical but is deviated to horizontal

Test of Deployment System Components

To safely operate the system in deep and very expensive wells we must demonstrate that all components are qualified to operate safely in deep wells under high loads at high pressures and high temperatures. A number of tests on the deployment system components were programmed into the design and evaluation process to qualify the system to operate to 572°F (300°C), 30,000 psi and 30,000 ft. We started by testing the system components and when the components had been qualified we continued the tests by testing subassemblies and later full assemblies.

The following tests are part of the qualification tests for the borehole seismic system:

1. Destructive pull tests of several samples of the tool joints for the drill pipe used to deploy the borehole seismic system to establish the actual load strength of the tool joints.
2. Destructive torque tests of several samples of the tool joints for the drill pipe used to deploy the borehole seismic system to establish the torque strength of the tool joints.
3. Non-destructive torque test of the tool joints for the drill pipe used to deploy the borehole seismic system to establish the makeup torque for the drill pipe.
4. Hydro test of the tool joints to establish that the tool joints can handle 10,000 psi internal pressure.
5. Destructive pull test of the drill pipe used to deploy the borehole seismic system to establish the load capability of the drill pipe. The drill pipe is expected to be the weak link in the deployment system.

6. Non-destructive hydro test of all drill pipe to 10,000 psi to establish that all drill pipe is free from structural flaws.

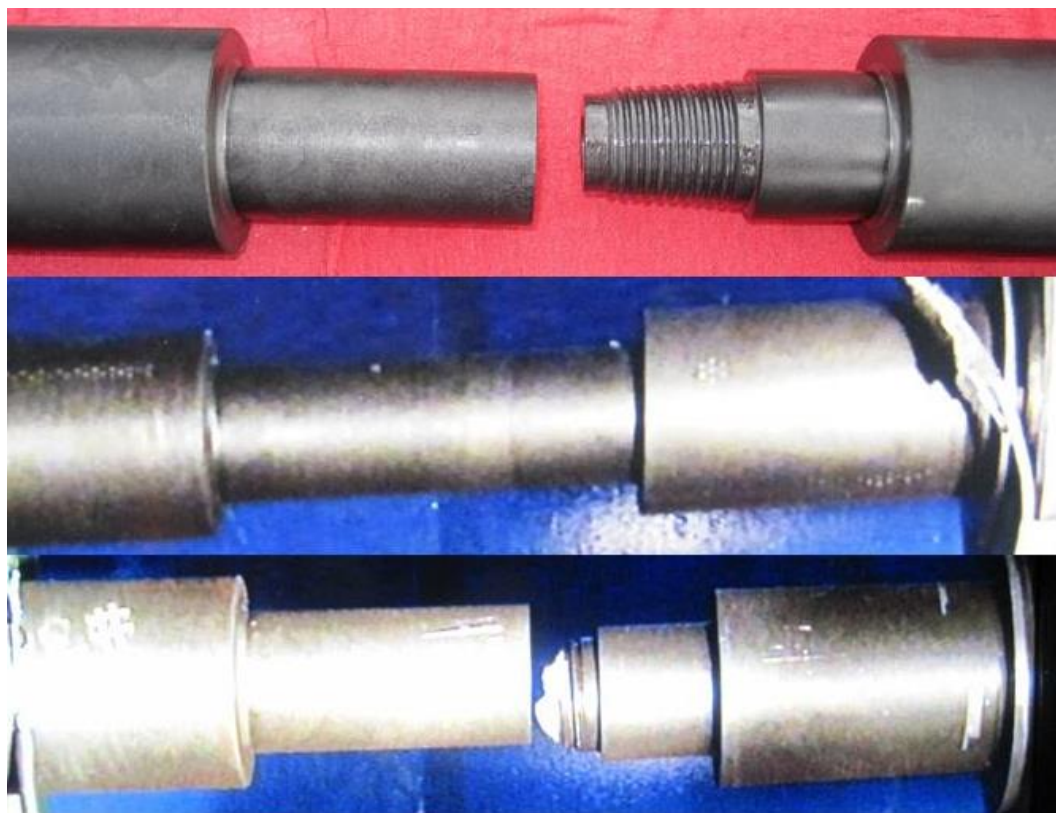


Figure 23. Destructive pull testing of the tool joints used for the FOSS deployment system

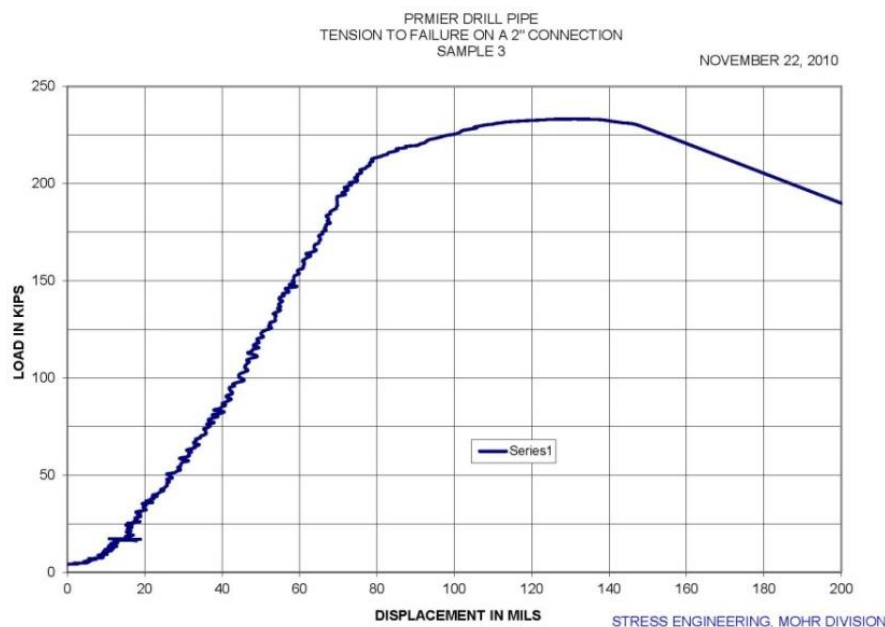


Figure 24. Destructive pull testing of the tool joints used for the FOSS deployment system. The elastic to plastic yield point was reached at about 210,000 psi. The tool joint failed at 238,000 lbs.

7. Non-destructive penetrant dye and ultra-sonic tests of the welded joint design for the sensor pod housings used to deploy the borehole seismic system.
8. Destructive pull test of the welded joint design for the sensor pod housings used to deploy the borehole seismic system
9. Non-destructive pull test of the sensor pod housings used to deploy the borehole seismic system
10. Destructive pull test of the sensor pod housings used to deploy the borehole seismic system
11. Non-destructive pressure test of the sensor pods to 30,000 psi external pressure

The following sections discuss the specific tests of the deployment components.

Pull Test of Tool Joints – Setup and Results

The pull tests were performed on several specially manufactured test specimens. One of the specimen assemblies prior to the test are shown at the top of Figure 23. At the center of Figure 23 one of the test specimens is shown after the tool joints have been screwed together using a torque of 1,000 ft-lbs.

The destructive tests were performed by Stress Engineering at their facilities in Houston. At the bottom of Figure 23 the tool joint assembly is shown after the tool joint has been pulled apart.

The tool joint went from elastic to plastic deformation at 210,000 lbs. and failed at 238,000 lbs. This behavior can be seen in Figure 24 which shows the load - displacement curve for this test.

Torque Test of Tool Joints – Set Up and Results

To establish the torque strength of the tool joint design developed for the project we commissioned a comprehensive set of torque tests. The equipment for this set of tests is shown in Figure 25. The equipment was provided by Bucking Masters in Houston.

Figure 26 show four sets of the tested tool joints after the tests. Two of the samples were torqued until the tool joints started to exhibit plastic yield seen as swelling of the tool joint. This can be clearly seen in samples 7 and 6 at the top of Figure 26. Two of the samples, 5 and 8, shown at the lower part of the Figure 26 where torqued to establish safe make up torque.

The resulting test data from samples 7 and 6 are shown in Figures 27 and 28. In figure 27 it is noticed that while the joint strength is decreasing the rotational speed is increasing. This is a clear indication of a tool joint that is failing in torque.

Samples 5 and 8 were torqued to establish a recommended make-up torque. Based on these two tests the safe makeup torque was established to be 1,000 ft-lbs. The resulting torque –strain curves are shown in Figure 29 and 30. Both sets of tool joints show linear elastic behavior up to 1,604 ft-lbs. for sample 5 and up to 1,111 ft-lbs. for sample 8.



Figure 25. Torque test machine to establish proper makeup torque and to test the tool joint torque strength.

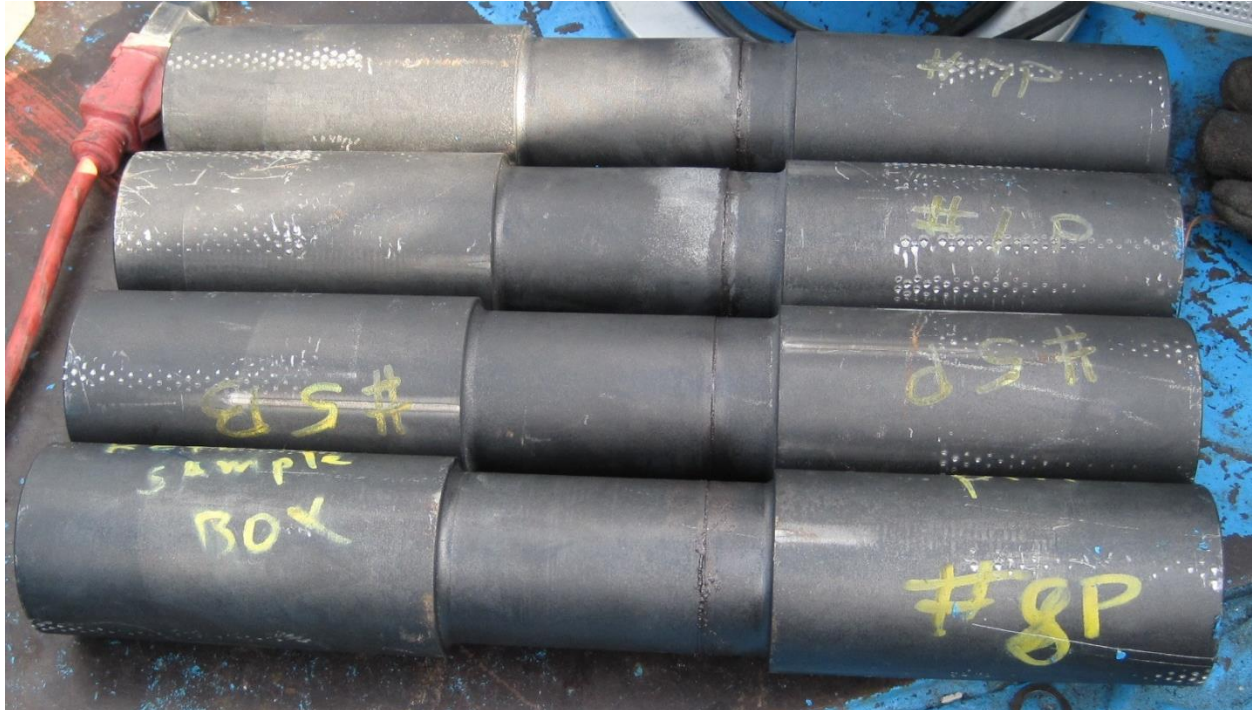


Figure 26. Samples of tool joints after destructive (#7 and #6) and non-destructive (#5 and #8) torque tests.

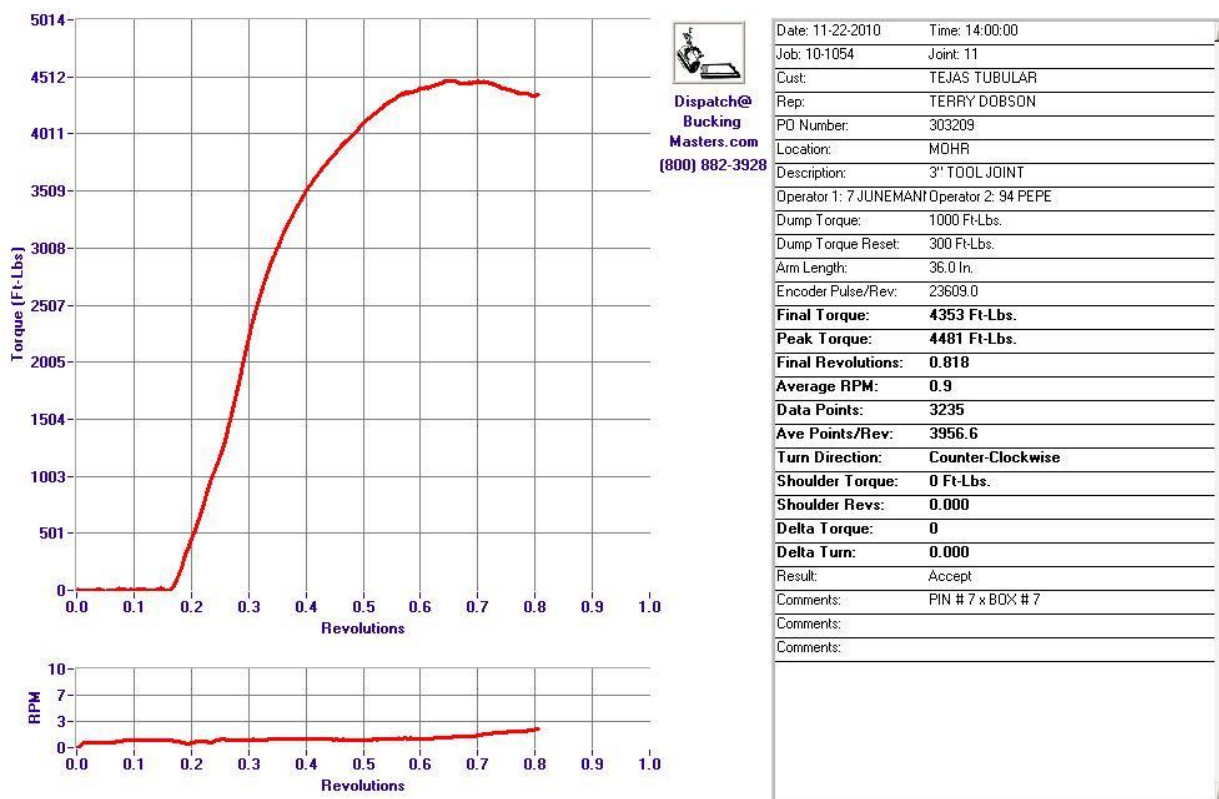


Figure 27. Strain – torque curve from destructive torque test of tool joints of sample #7.

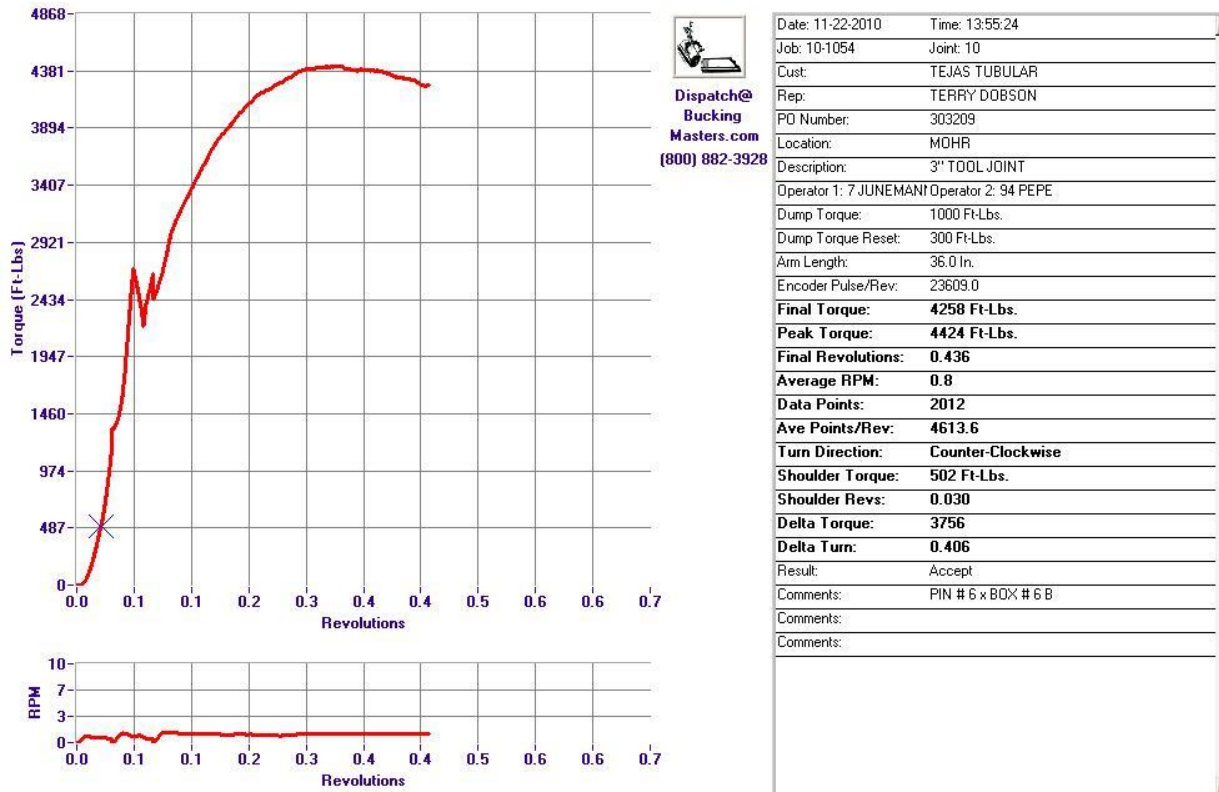


Figure 28. Strain – torque curve from destructive torque test of tool joints set #6

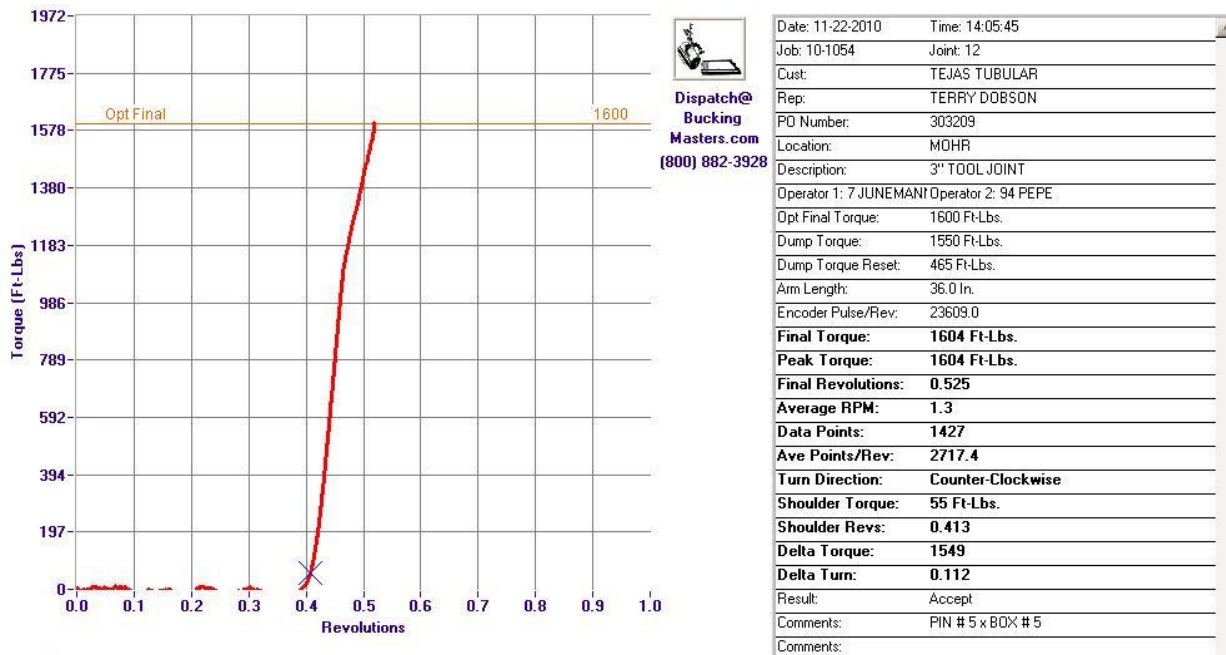


Figure 29. Strain – torque curve from non-destructive torque test of tool joints set #5 to establish recommended make up torque.

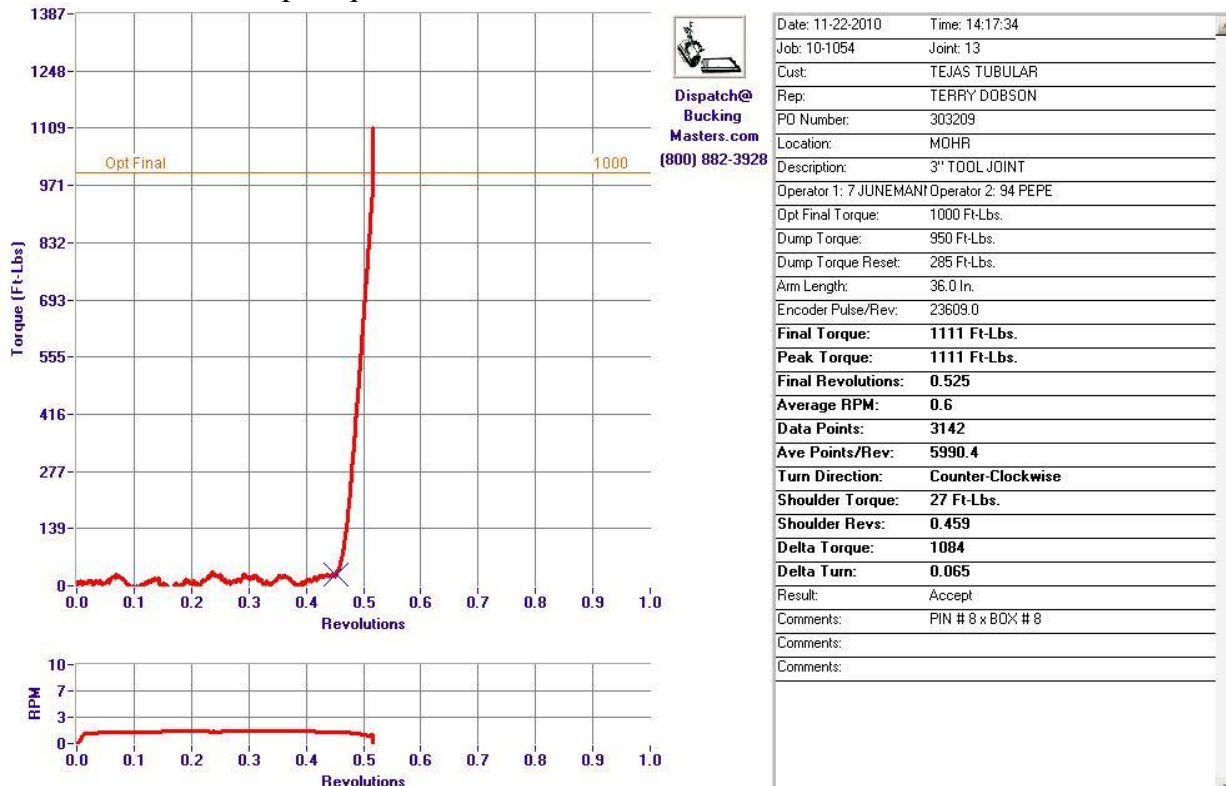


Figure 30. Strain – torque curve from non-destructive torque of tool joints set #8 to establish recommended make up torque. Based on the tests shown in Figures 29 and 30 the recommended make-up torque is set as 1,000 ft-lbs.

Hydro Test of Tool Joints – Set Up and Results



Figure 31. Two samples of Fiber Optic Seismic System tool joint prepared for hydro tests.

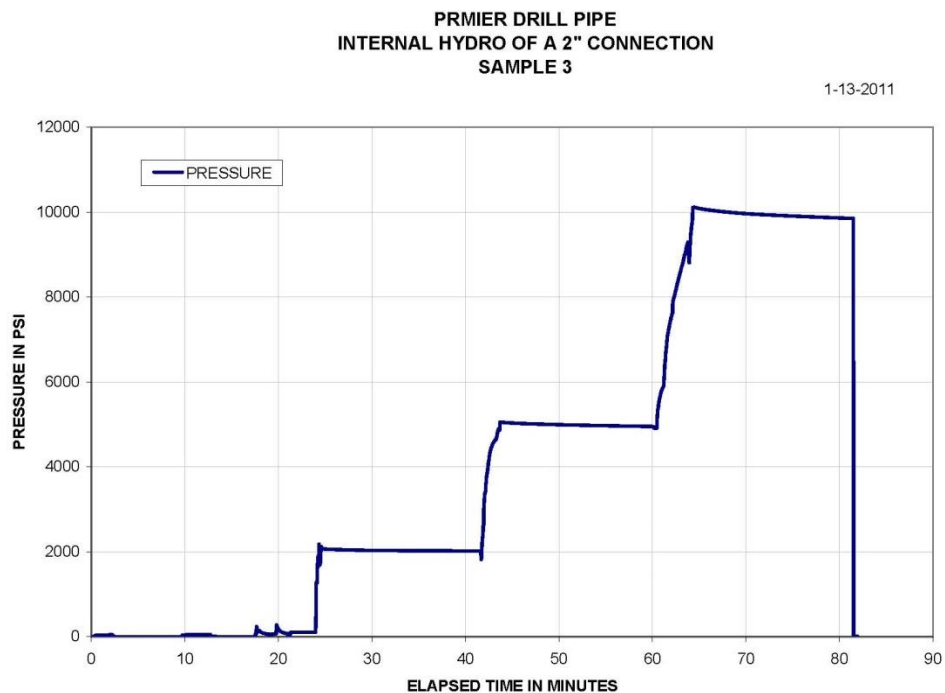


Figure 32. Results from Hydro testing one of the tool joints to 10,000 psi.

The hydro test was another test required to establish the function of the borehole seismic system. The drill pipe not only serves as the mechanical strength member of the system but also as the conduit for the fluids that operates the clamping system. It is therefore essential that the system does not leak under a wide range of operational pressures.

The result of the hydro test is shown in Figure 32 which clearly demonstrates that the tool joints hold pressure up to 10,000 psi. Since the leak test was performed using fluids even a very small leak would result in an immediate drop of pressure.

Pull Test of Drill Pipe – Set Up and Results

The small diameter based deployment system is the structural backbone of the borehole seismic array. The steel used for the drill pipe use is an S135 steel. The same steel is used in drill pipe for drilling deep offshore wells. The OD of the drill pipe is 1.660" and the pipe wall thickness is 0.24". This provides for slightly more than one square inch of steel cross section so the nominal strength of the drill pipe should be about 140,000 – 145,000 lbs.

The reason for selecting drill pipe technology vs. production tubing is that the drill pipe tool joints are designed to be deployed many 100s of times making the system cost effective. In comparison production tubing connections are only designed to be deployed a few times. Production tubing connections are considered used up after five deployments so while cheaper to manufacture they are more expensive per deployment due to their limited life span. A commercial borehole seismic system must be able to be deployed 100s of times in order to be commercially viable.

Two 5 ft samples of the drill were prepared for the destructive pull test. The test set up can be seen in Figure 33. Both samples were pulled to failure. The results from the two tests are nearly identical. Figure 34 shows the cross section where the drill pipe failed. The necking down of the pipe can also be clearly seen which is the result of plastic deformation of the drill pipe.

The drill pipe showed elastic behavior up to 145,000 lbs. as can be seen in Figure 35. Above 145,000 lbs. the deformation was plastic. The ultimate pull load at failure of the pipe was 160,000 lbs.

To assure that each drill pipe has the necessary integrity and has no structural flaws each drill pipe joint is hydro tested to 10,000 psi.



Figure 33. Destructive testing of the drill pipe used for the OpticSeis® deployment system. The steel used in the drill pipe is an S135 steel which is qualified to be used for offshore drill pipe.

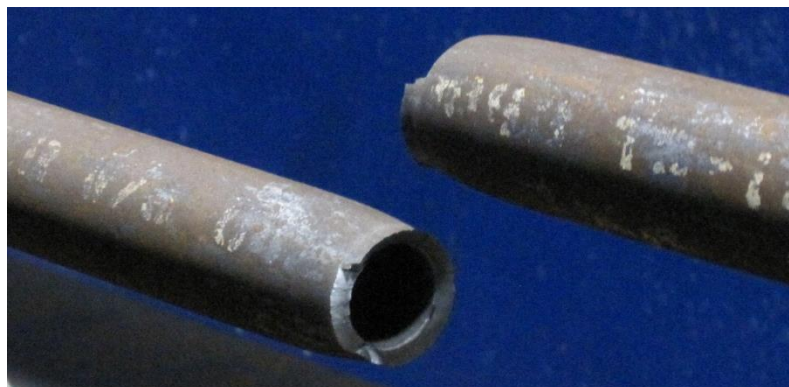


Figure 34. Destructive testing of the drill pipe used for the FOSS deployment system. The drill pipe failed at 160,000 lbs. Clearly seen is the necking down of the pipe diameter on either side of the failure point.

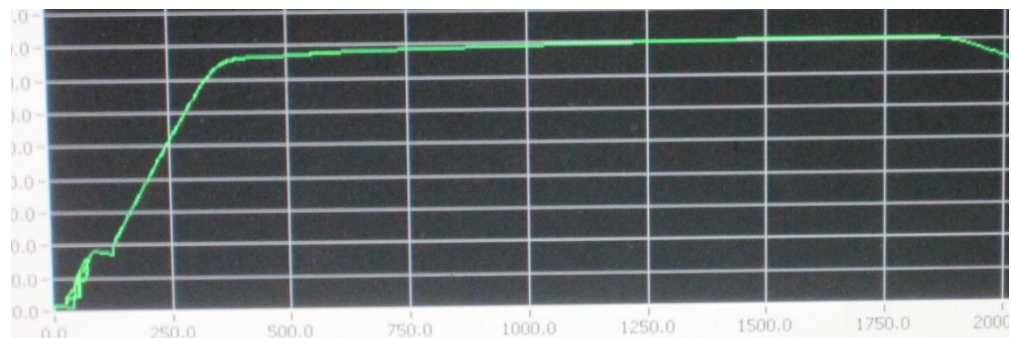


Figure 35. Destructive testing of the tool joints used for the FOSS deployment system. The transition point between elastic and plastic yield is at about 145,000 lbs. The drill pipe failed at 160,000 lbs.

Destructive Testing of Sensor Pod Housing welds – Set Up and Results

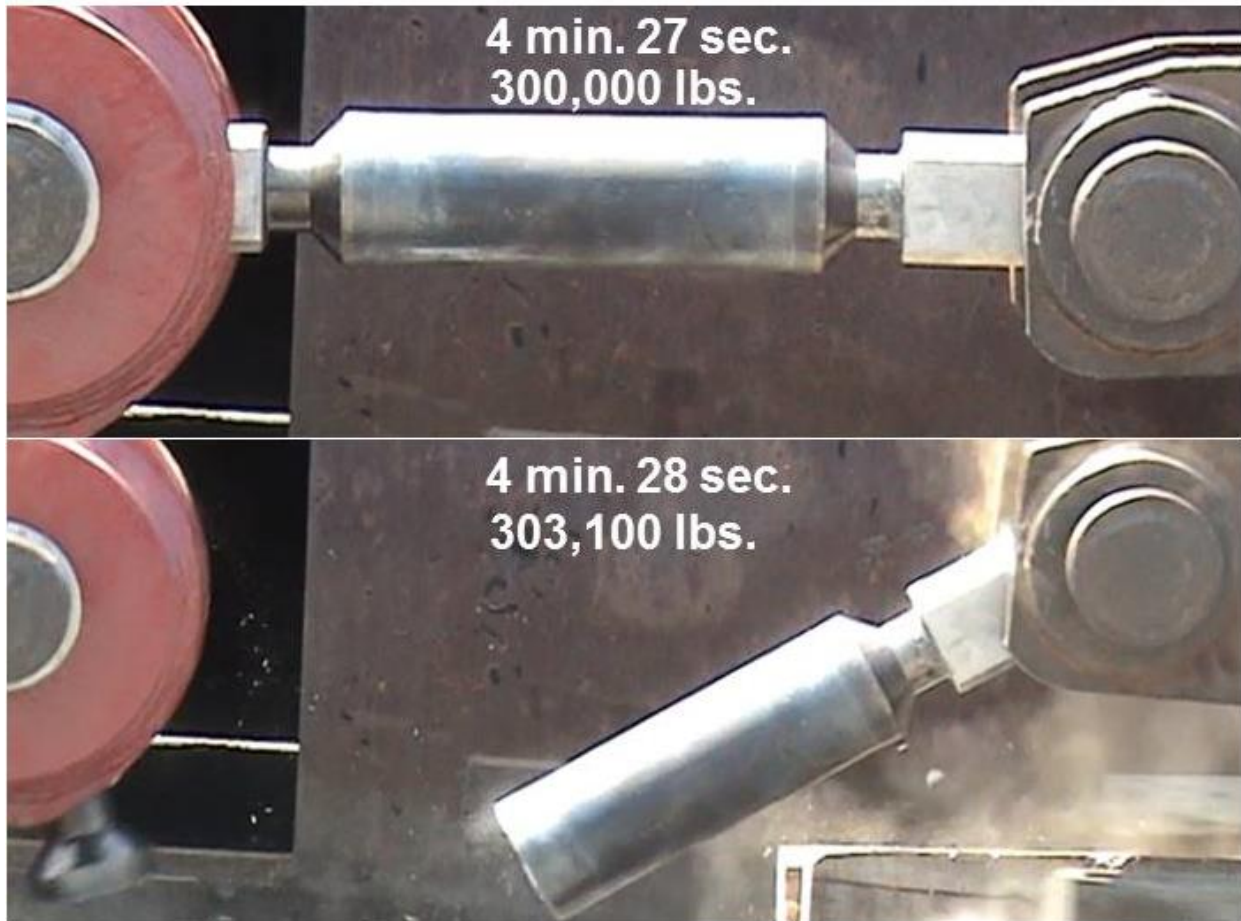


Figure 36. Destructive pull testing of welds on coupons representing sensor pod housings. The coupon welds are duplicate of the wells used on the sensor pod housings for the Fiber Optics Seismic Sensor (FOSS)TM deployment system.

It is critical that all components used for the OpticSeis[®] system are stronger than the drill pipe so in the case the system gets stuck and we need to fish the system the drill pipe is the predicted failure point allowing a fishing tool to attach to the system.

To establish the ultimate strength of the main welds used to assemble the sensor pod housing a number of test coupons were designed and manufactured. The test coupons used the same steel and the same welding procedures developed for the sensor pod housings.

One of these coupons is shown at the top of Figure 36 during to a destructive test immediately prior to failure. The necking of the failure point can be observed on the left side of the test specimen. At the bottom of Figure 36 the coupon is shown immediately after the failure. The load at failure was recorded at 303,100 lbs. The test certificate from the destructive testing of the welding coupons by Coordinated Equipment Co, Inc. in Wilmington, CA is shown in Figure 37.

CERTIFICATE OF TEST AND EXAMINATION OF CHAINS, RINGS HOOKS, SHACKLES, SWIVELS, BLOCKS AND RELATED GEAR BY COORDINATED EQUIPMENT CO., INC.			
TEST CERTIFICATE No. 16465	OUR WORK No. T-27648	<small>THIS CERTIFICATE PROPERLY EXECUTED BY A COMPETENT PERSON IS ACCEPTED BY THE GOVERNMENT OF THE UNITED STATES OF AMERICA AS BEING IN ACCORDANCE WITH THE REQUIREMENTS OF 46 CFR 91.25-25 (A) 3, 71.25-25 (A) 5, AND 29 CFR 1594.12 (A) AND I.L.O. FORM NO. 4, PRESCRIBED BY THE UNITED STATES DEPARTMENT OF LABOR FOR CERTIFICATION WHICH IS PERFORMED TO THE REQUIREMENTS OF 29 CFR PART 1505.</small>	
FOR: Paulsson, Inc.		P.O. # 407	
CERTIFICATION DATA			
DESCRIPTION OF GEAR*	Number Tested	Maximum Load Applied	Remarks
Weld Coupon 01 With Adapters, Drawing Number: B-08-006	1	303,100 lbs.	Failed at weld 4 which was connected at the anchor end of the machine.
<small>Tested in accordance with customer's specifications by attaching to the adapters threaded onto the coupon on each end, and applying an axial tensile load up to failure.</small>			
<small>Test Witnessed By:</small>  <small>7-30-12</small> <small>Jon Thonburg, Paulsson, Inc.</small>			
ATTESTATION			
<small>As an authorized signatory for Coordinated Equipment Co., Inc. which carried out the work for which this certificate is issued, I attest that on 7-30-2012, The above Gear was tested and examined by a competent person** in the manner set forth in this certificate.</small>			
<small>Signature:</small> <small>Title: David Mikhael, Chief Engineer</small> <small>Date: 7-30-2012</small>		COORDINATED EQUIPMENT CO., INC. <small>1707 E. Anaheim St., Wilmington, CA 90744</small> <small>Tel: (310) 834-8535 * Fax: (310) 834-2991</small>	
<small>NOTE: Use of this certificate by unauthorized persons is prohibited. Violators may subject themselves to the penalties provided in 33 U.S.C. 941 (P.L. 85-742). This form in substantial agreement with I.L.O. Form #4.</small>			

Figure 37. Certificate of the destructive testing of coupon welds representing sensor pod housing welds.

Non-Destructive Testing of Sensor Pod Housing welds – Set Up and Results



Figure 38. Non-destructive testing of the welded joints used for the FOSS sensor pod housing. The test shown is a penetrant dye test. Any surface fractures in the welds show up as thin red lines.



Figure 39. Non-destructive testing of the tool joints used for the FOSS deployment system. The test shown is an Ultra sonic test. Any shallow or deep fractures in the welds show up as reflection anomalies in the ultra-sonic data.

We also developed a nondestructive testing procedure using ASME Section XI Acceptance standards using both Penetrant Dye and Ultrasonic testing methods that will be used on all welds on the sensor pod housings prior to commission the sensor pod housing for commercial use. These testing procedures were applied to the welding coupons prior to the destructive test as seen in Figures 38 and 39. This type of non-destructive testing will assure that all the structural components have passed quality tests and that the system can safely be deployed.

Non-Destructive and Destructive Testing of Sensor Pod Housing – Set Up and Results

The two structural elements in the deployment system are the drill pipe and the sensor pod housings. Samples of both elements must be tested destructively to confirm and establish ultimate strength of the design. Each individual unit of the two elements in the deployment system must also undergo non-destructive testing to confirm that each individual unit has the structural integrity to withstand the heavy load during a deep deployment of a large fiber optic borehole seismic array.

To establish both the ultimate strength and operational strength of the sensor pod housings we designed a series of tests on four sensor pod housings. Two of the sensor pod housings were pulled to failure and two were pulled to the failure point for the drill pipe which is by design the weakest member of the deployment system.

In order to establish the behavior of the sensor pod housings during the destructive and non-destructive tests we instrumented the four sensor pod housings with 16 strain gauges. The strain gauges attached to the sensor pod housing can be seen in Figure 40.



Figure 40. One of four sensor pod housings instrumented with 16 strain gauges in preparation for destructive and non-destructive tests.

The setup in the pull tester is shown in Figure 41. The left side of the 6 ft long (72") sensor pod housing is attached to a fixed point while the right side of the sensor pod housing is attached to a cylinder capable of pulling up to 400,000 lbs.

The first two tests were non-destructive test to establish the behavior of the sensor pod housing up to the breaking strength of the drill pipe. We pulled the first two sensor pod housings to 150,000 lbs. Both sensor pod housings behaved well during these two pull test showing that we can safely pull 150,000 lbs. on these housings. The result of one of these tests is shown in Figure 42 where we plot the Time vs. Strain and Load curves from the 16 strain gauges. The mounting of the 16 individual strain gauges is shown in Figure 45.

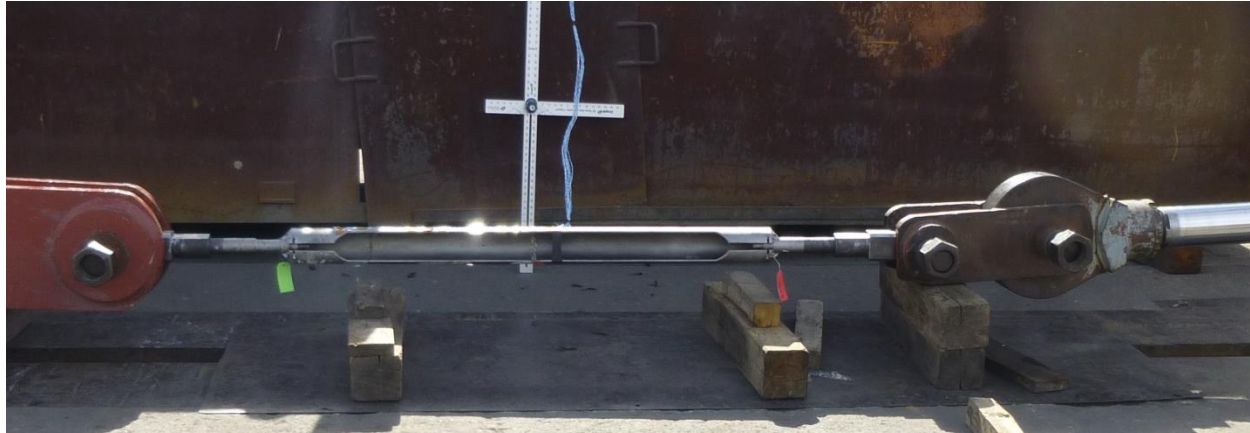


Figure 41. One of four sensor pod housings tested using destructive and non-destructive pull tests.

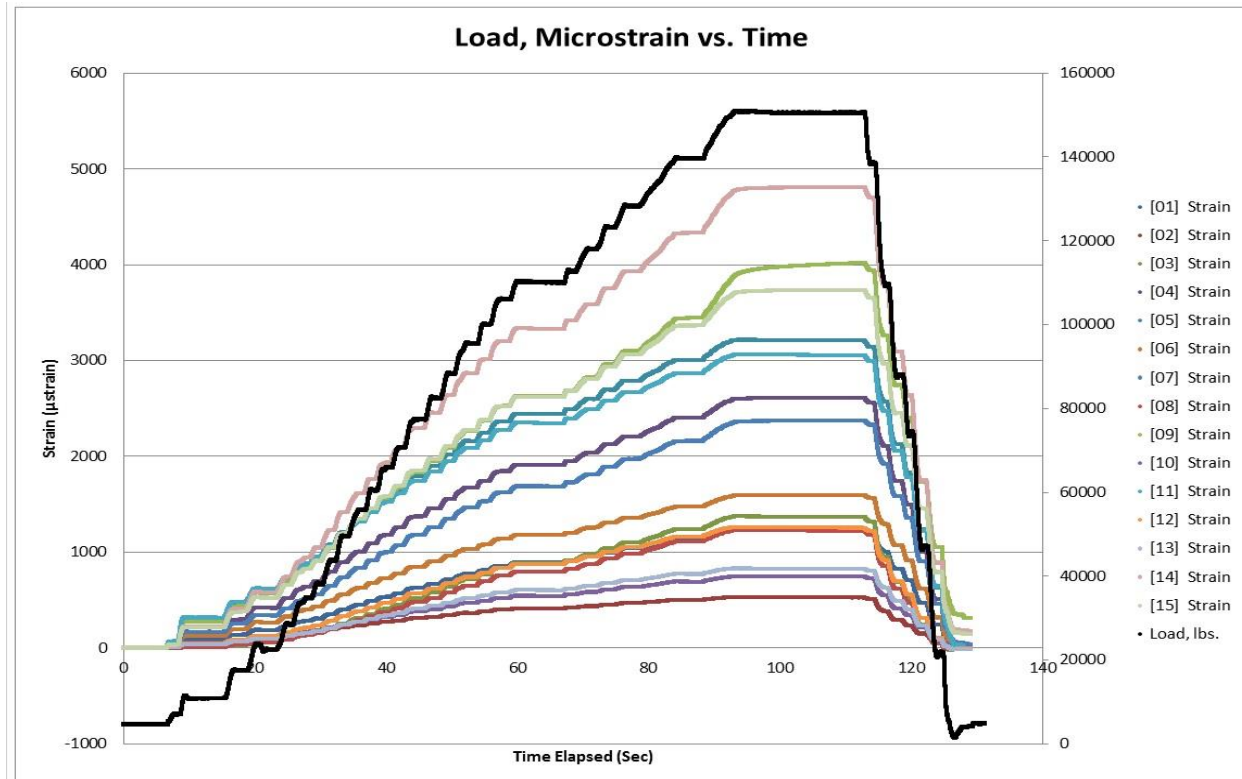


Figure 42. Time vs. Strain and load curves from one of two sensor pod housings tested using non-destructive tests.

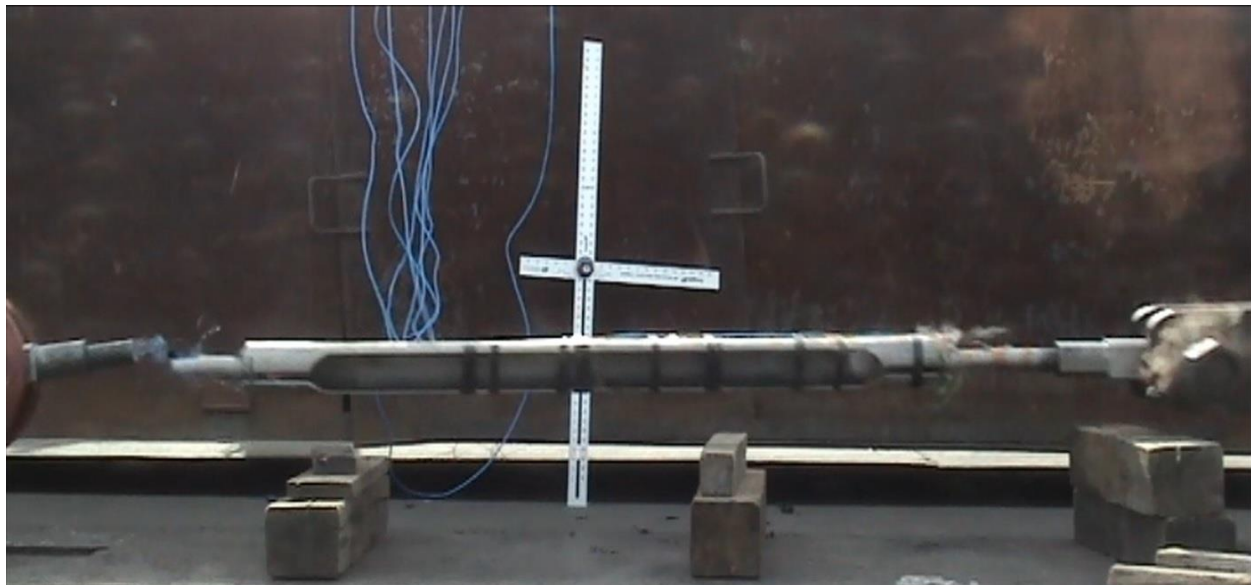


Figure 43. One of two sensor pod housings tested using destructive tests. As expected the tool joint failed at about 200,000 lbs.

The destructive tests were performed on a second set of two sensor pod housings which were pulled until they failed. Figure 43 show the moment of failure for one of the two sensor pod housings.

Figure 44 show the Time vs. Strain and Load curves for one of two destructive tests.

Prior to the actual pull test we did Finite Difference modeling of axial load (pull) – strain behavior of the sensor pod housings. The results from this modeling are shown in Figure 45. The actual results from our destructive pull test is plotted together with the model data and as shown in this figure the correlation between the model data and the actual pull- strain data is excellent.

These results validate the design of the sensor pod housing and show that we can safely deploy these housings to a load of 150,000 lbs.

In Figure 46 we show the certificate for Coordinate Equipment Co, Inc. for the non-destructive and destructive tests of the sensor pod housings.

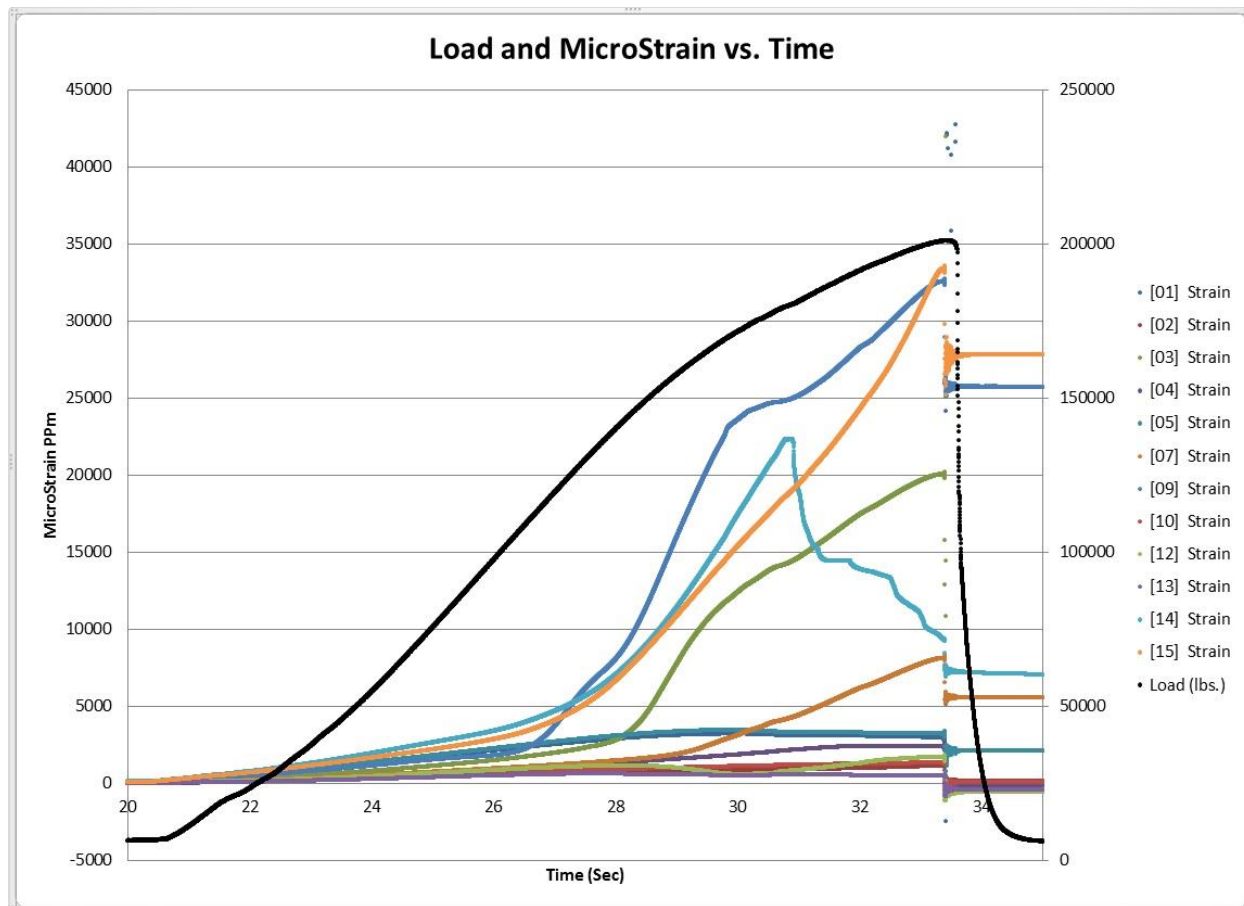


Figure 44. Time vs. Strain and Load curves from one of two sensor pod housings under destructive tests.

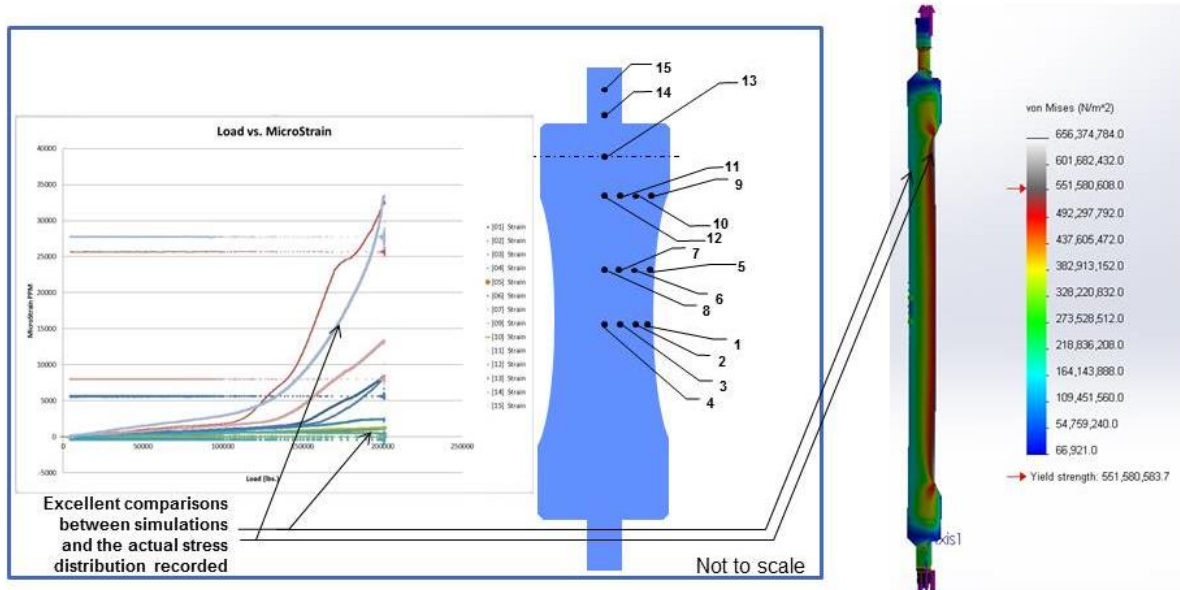


Figure 45. Load-strain curves from one of two sensor pod housings tested using destructive tests. Also shown are the simulated load-strain curves. There is an excellent agreement between the simulated and the measured load strain curves.

**CERTIFICATE OF TEST AND EXAMINATION
OF CHAINS, RINGS HOOKS, SHACKLES, SWIVELS, BLOCKS AND RELATED GEAR
BY COORDINATED EQUIPMENT CO., INC.**

FOR: Paulsson, Inc. PO Number: 667

DESCRIPTION OF GEAR*	Number Tested	Maximum Load Applied	Remarks
Mechanical Assembly for Pull Testing Drawing Number: 2013_20_12_TEMP2	1		
Tested in accordance with customer's specifications by attaching to the (2) customer furnished eye connectors, Dwg No: B-08-002, as described in Dwg No: B-08-006. The connectors were threaded onto the assembly at each end, and an axial tensile load was applied to the assembly.			
Housing Sample 1 - Proof Load Tested Only		150,000 lbs.	Load held for 5 seconds and released. See DAQ reports.
Housing Sample 2 - Proof Load Tested Only		150,000 lbs.	Load held for 5 seconds and released. See DAQ reports.
Housing Sample 3 - Loaded to Ultimate Failure		201,081 lbs.	Male thread on housing pulled out of the eye connector. See DAQ reports.
Housing Sample 4 - Loaded to Ultimate Failure		199,920 lbs.	Male thread on housing pulled out of the eye connector. See DAQ reports.
Test Witnessed By:	_____ Jon Thomburg, Paulsson, Inc.		

ATTESTATION

As an authorized signatory for Coordinated Equipment Co., Inc. which carried out the work for which this certificate is issued, I attest that on 11-07-2013 The above Gear was tested and examined by a competent person** in the manner set forth in this certificate.

Signature: 
Title: David Mikhael, Chief Engineer
Date: 11-07-2013

COORDINATED EQUIPMENT CO., INC.

1707 E. Anaheim St., Wilmington, CA 90744
Tel: (310) 834-8535 * Fax: (310) 834-2991

NOTE: Use of this certificate by unauthorized persons is prohibited. Violators may subject themselves to the penalties provided in 33 U.S.C. 941 (P.L. 85-742). This form in substantial agreement with I.L.O. Form #4.

Figure 46. Certificate of the non-destructive and destructive testing of the sensor pod housings.

Pressure rating of the OpticSeis® sensor pod

The Fiber Optic Seismic Sensors (FOSS)TM are housed in a sensor pod which is a pressure vessel designed and built to protect the sensors from the well fluids and the well pressures. The sensor pod, or pressure vessel, can be seen in Figures 15, 48a and 48b, 55, 70 and 71. In order to hold the design pressure of 30,000 psi we decided to manufacture the main sleeve using a Inconel 718 material. The decision to use Inconel 718 was taken after extensive Finite Difference modeling. The results of the modeling using Inconel 718 can be seen in Figure 47. This modeling indicate that we start to see the material reaching the elastic to plastic yield point at 38,213 psi providing ample margin for a maximum deployment pressure of 30,000 psi.

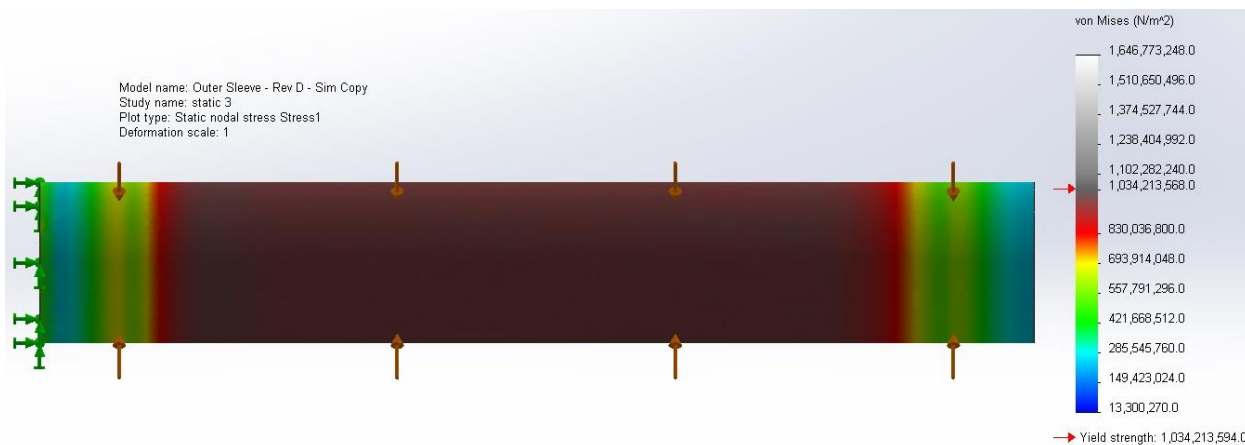


Figure 47. Results of Finite Difference modeling of the pressure housing manufactured using Inconel 718 for the Fiber Optic Seismic Sensor (FOSS)TM pod. At 38,213 psi the static stress material's yield strength appears to start propagating thru the entire wall thickness.

The next step in the process to establish the pressure rating is a test in a high pressure high temperature test facility. This test is planned for 2015.

Operation of the OpticSeis® system

During deployment in a well, the drill pipe is filled with the well fluid which enters the tool string through a fluid take in system as shown in Figure 21 and passed through two check valves as it fills the drill pipe. The fluid take-in section is a slotted liner with fine slots which filters particulates so they do not enter the drill pipe. When the deployment is complete the drill pipe is thus filled with fluid of the same density as is present outside the pipe, so the fluid pressure gradient is the same inside and outside the deployment system drill pipe.

The fluid inside the drill pipe is used to actuate the all-metal clamping mechanism used to clamp the sensor pods to the borehole wall. The pod clamping is achieved by applying a differential pressure on the fluid inside the drill pipe using the borehole seismic system surface assembly. This differential pressure moves the clamping actuator which in turn operates the clamping system. This system will produce a clamping force-to-weight ratio exceeding 50 for the sensor pod, thus providing for outstanding coupling between the sensor pod and the borehole wall. The high force is essential to provide outstanding vector fidelity for the high frequency data recorded.

A sample of the sensor pod and the sensor pod housing are shown in Figures 48a and 48b. The sensor pod holds the three component fiber optic sensors. The 3C Fiber Optic Seismic Sensor (FOSS)TM discussed in this paper has been packaged into a pod that is capable of withstanding an external pressure of 30,000 psi, allowing for deployment in the deepest and longest wells drilled in the US today. The sensor pod housing serves several functions. It serves to protect the sensor pod and the tubing containing the fibers during the deployment stage. It also contains the clamping mechanism to clamp the sensor pod to the borehole wall. The sensor pod housing also dampens the tube waves traveling in the borehole, thus increasing the signal-to-noise ratio of the recorded borehole seismic data. The sensor pod housing is also designed to deploy a $\frac{1}{4}$ " tube for a Distributed Temperature Sensor system (DTS) and a Distributed Acoustic Sensor (DAS) or FiberSeisTM simultaneously with the Fiber Optic Seismic Sensor (FOSS)TM system. The sensor pod housing is also capable of holding other instruments such as pressure gauges, EM tools and fluid sampling tools.



Figure 48a. The Sensor Pod installed into a Sensor Pod Housing. Figure 48b. The 3C Fiber Optic Seismic Sensor (FOSS)TM packaged into a 16" long and 2" in diameter pod capable of operating at an external pressure of 30,000 psi and an ambient temperature of 320°C (608°F).



Figure 49. The small diameter drill pipe with an OD 1.660" that is used to deploy the OpticSeis[®] system.

Figure 49 shows the drill pipe used to deploy the OpticSeis® system. This drill pipe was manufactured especially for OpticSeis® system at a length 19 ft \pm 0.125". The sensor pod housings are 6 ft \pm 0.125" so the combined length of one sensor pod housing and one joint of drill pipe is 25 ft \pm 0.25".

To handle the tubing with fiber and the sensor pods attached to the tubing we designed and manufactured electric spools with a large diameter drum. A sample of this spooling unit is shown in Figure 50 .

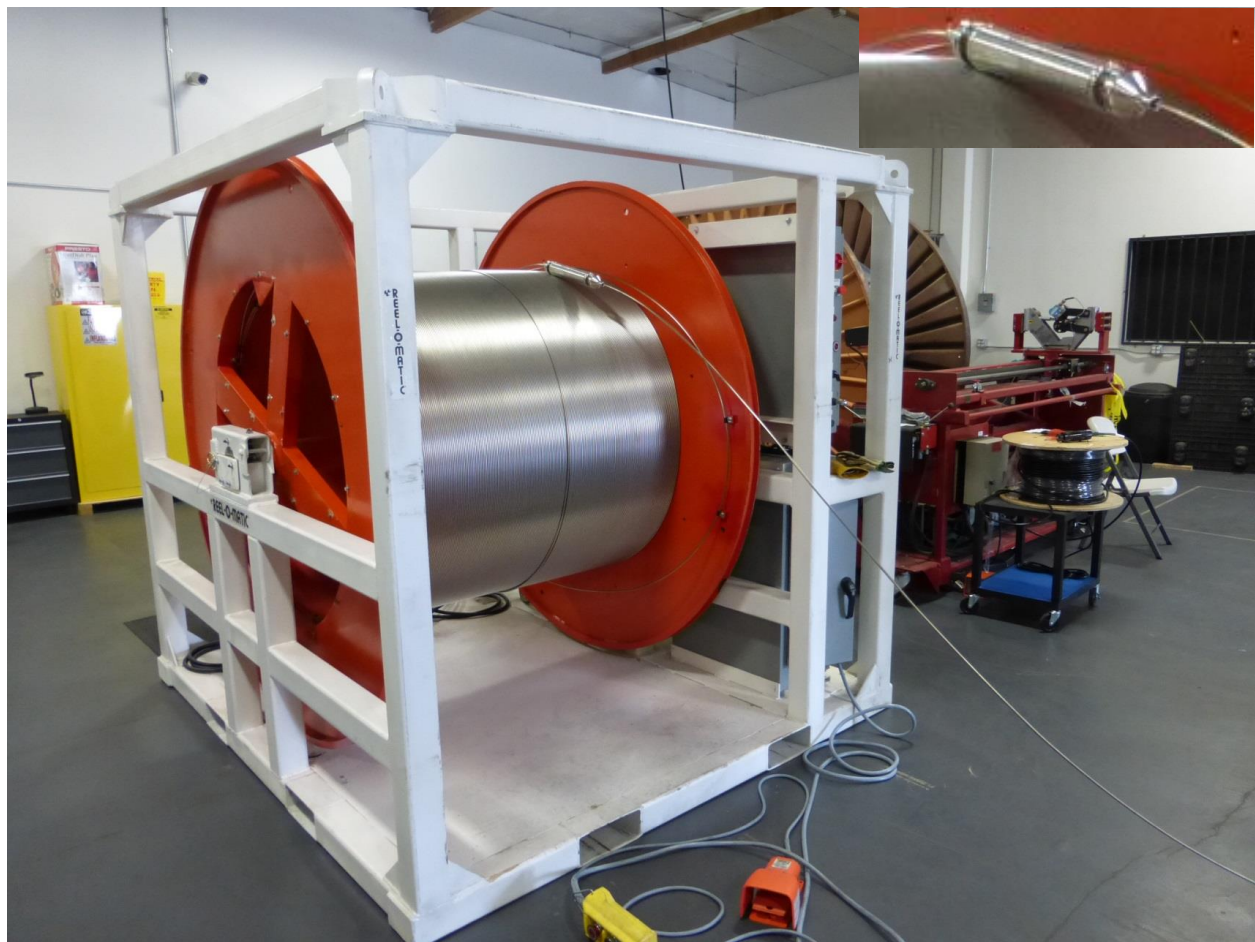


Figure 50. The powered spool for the fiber tubing for the redeployable borehole seismic system. This spool is designed to be placed in the container shown in Figure 51. This spool is specifically designed for fiber optic tubing.

This spooling unit is designed to fit inside a specially designed container shown in Figure 51. The side of this container can be fully opened to give full access to the content of the container.

The 20 ft container will also serve as the dog house for the OpticSeis® system electronics minimizing the distance from the electronics to the spool with fiber and Fiber Optic Seismic Sensors (FOSS)®



Figure 51. The specialized 20 ft field container that will serve as the doghouse for the redeployable borehole seismic system. The powered spool shown in Figure 50 is designed to fit into the container. There is also room in the container for the interrogator instruments, recording system, observers and data processors.

The Long Beach, CA Field Tests of the OpticSeis® system, November 2012

We completed the manufacturing of the first prototype five level 3C fiber optic borehole seismic array in October 2012 incorporating our high temperature Fiber Optic Seismic Sensors (FOSS)® into our high pressure sensor pods and our deployment system. We mounted the borehole seismic array onto a large spool and tested the completed system at our manufacturing facility prior to moving the array and the associated deployment equipment to the field. We mobilized the OpticSeis® system to a research well in Long Beach, CA owned by City of Los Angeles in November 2012 and conducted a test of the five level fiber optic seismic array to a depth of about 1,600 ft. The main objectives were to test the deployment components in the system and to record the first seismic field data to assess the quality of the data recorded and the process of converting the optical data to seismic data in a SEGY format.

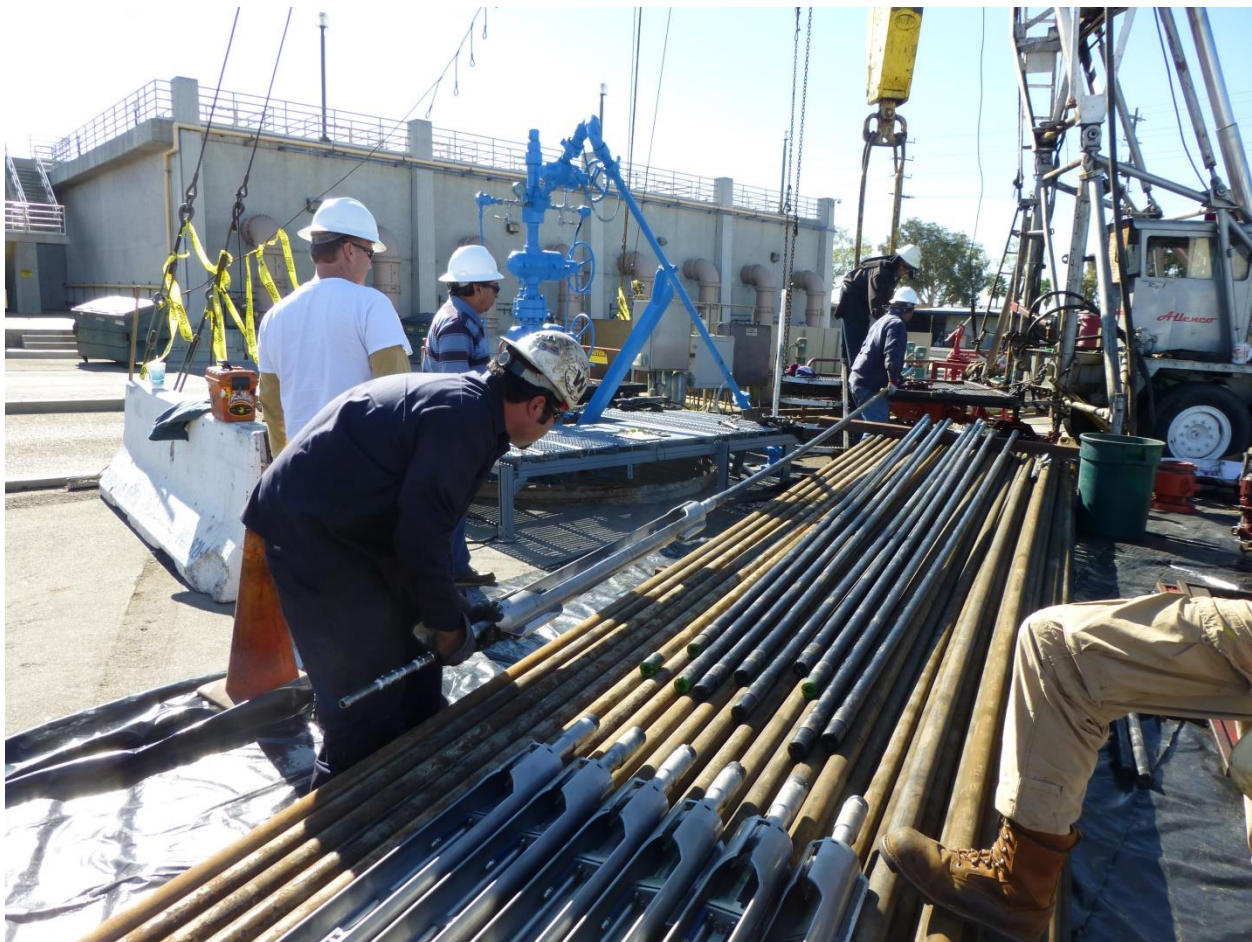


Figure 52. Long Beach, CA. Site and the layout of the equipment for the first field test of the OpticSeis® system.

Prior to deployment the components for the borehole seismic system were laid out in front of the rig and partially assembled to allow efficient deployment into the well.

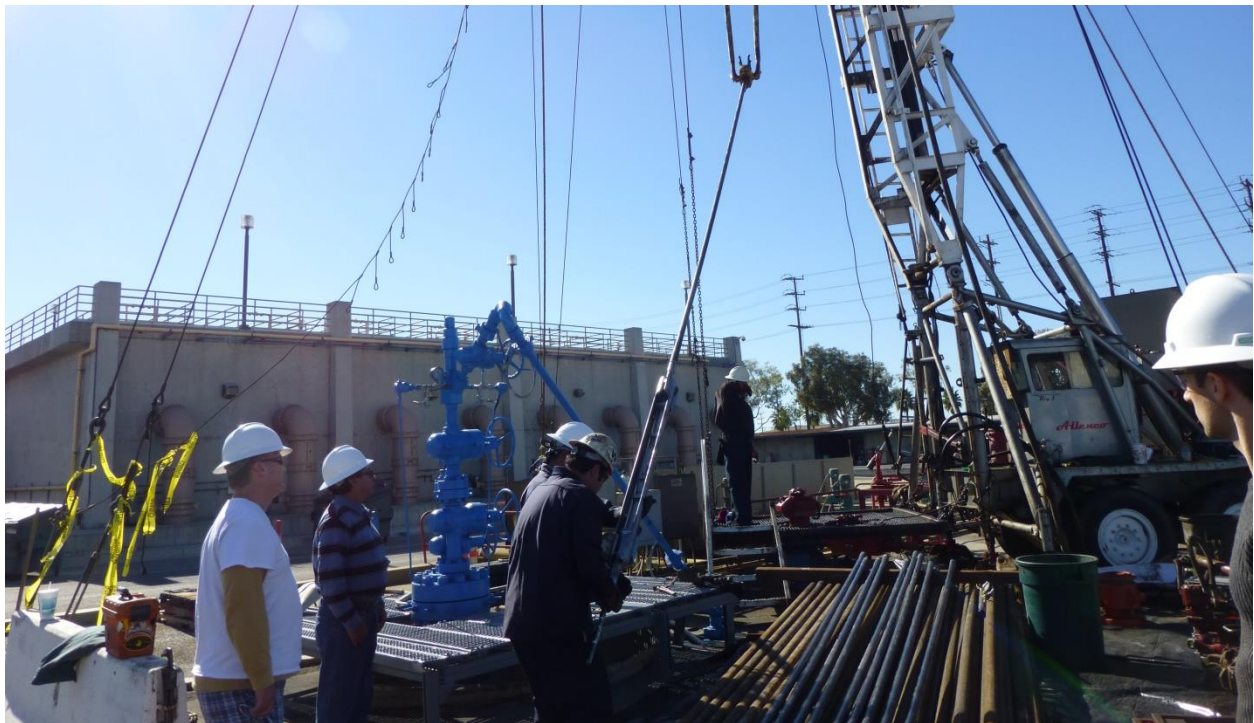


Figure 53. Long Beach, CA. First deployment of the OpticSeis® system.

Figure 53 shows the deployment of the system by lifting the first drill pipe attached to the sensor pod housing. The deployment is identical to deploying normal well tubing or pipe equipment so regular well service crews can be used for deploying the OpticSeis® system.

Figure 54 shows the sensor pod housing hanging from the workover rig. Figure 55 shows the sensor pod after it has been installed into the sensor pod housing.

In order to protect the tubing with optical fiber we designed a sturdy centralizer shown in Figure 56. This centralizer can hold and protect up to six $\frac{1}{4}$ " tubes.

Figure 57 show the assembly of drill pipe using large pipe wrenches. Power tongs can also be used but care as to taken to protect the $\frac{1}{4}$ " tubing containing the fibers.

Figure 58 shows the centralizer and $\frac{1}{4}$ " tubing with fibers being lowered into the well on the drill pipe.

After the system had been lowered to a suitable depth we deployed a 110 lbs. weight impact source. This source is shown in Figure 59.

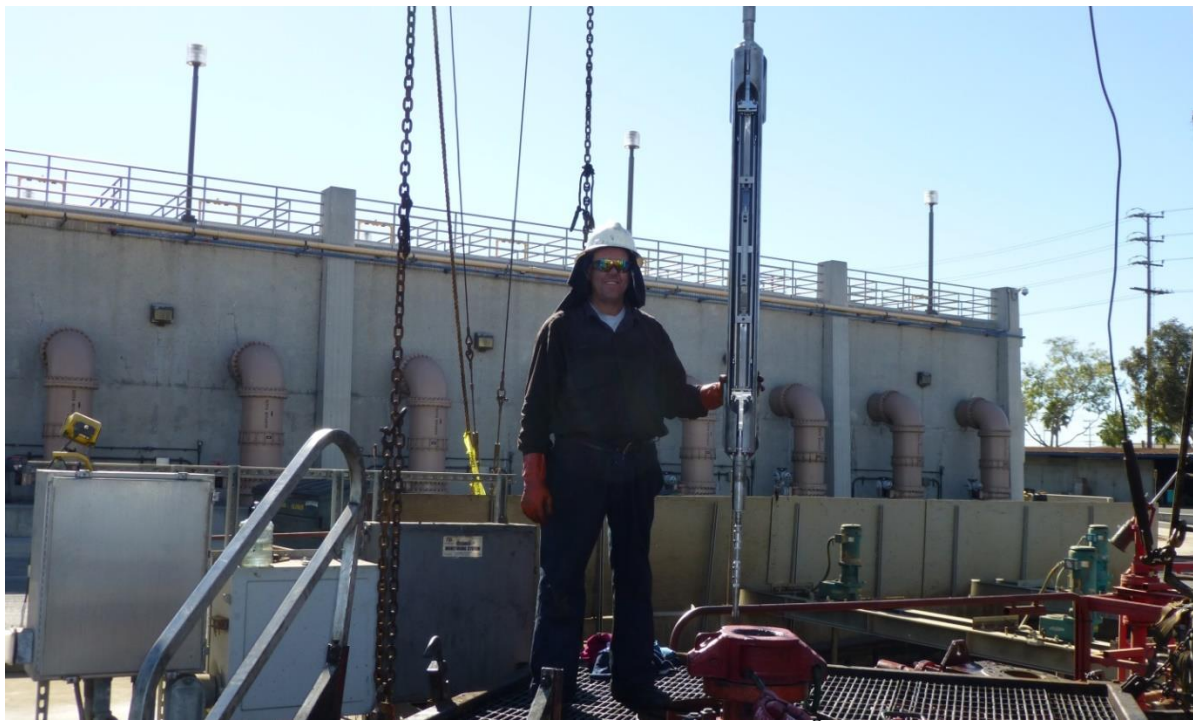


Figure 54. Long Beach, CA. First deployment of the OpticSeis® system. Shown is the sensor pod housing suspended from the 1.660" drill pipe.



Figure 55. Long Beach, CA. The OpticSeis® pod placed in the Sensor Pod Housing unit. The Sensor Pod Housing protects the sensor pod during the deployment and also houses the clamping mechanism which securely clamps the sensor pods to the inside of the borehole wall.



Figure 56. Long Beach, CA. This figure shows the centralizer placed on the small diameter drill pipe. The centralizer is holding and protecting the $\frac{1}{4}$ " steel tubing containing the fibers for the OpticSeis[®] sensors. Space has been made for additional cables and $\frac{1}{4}$ " tubes.

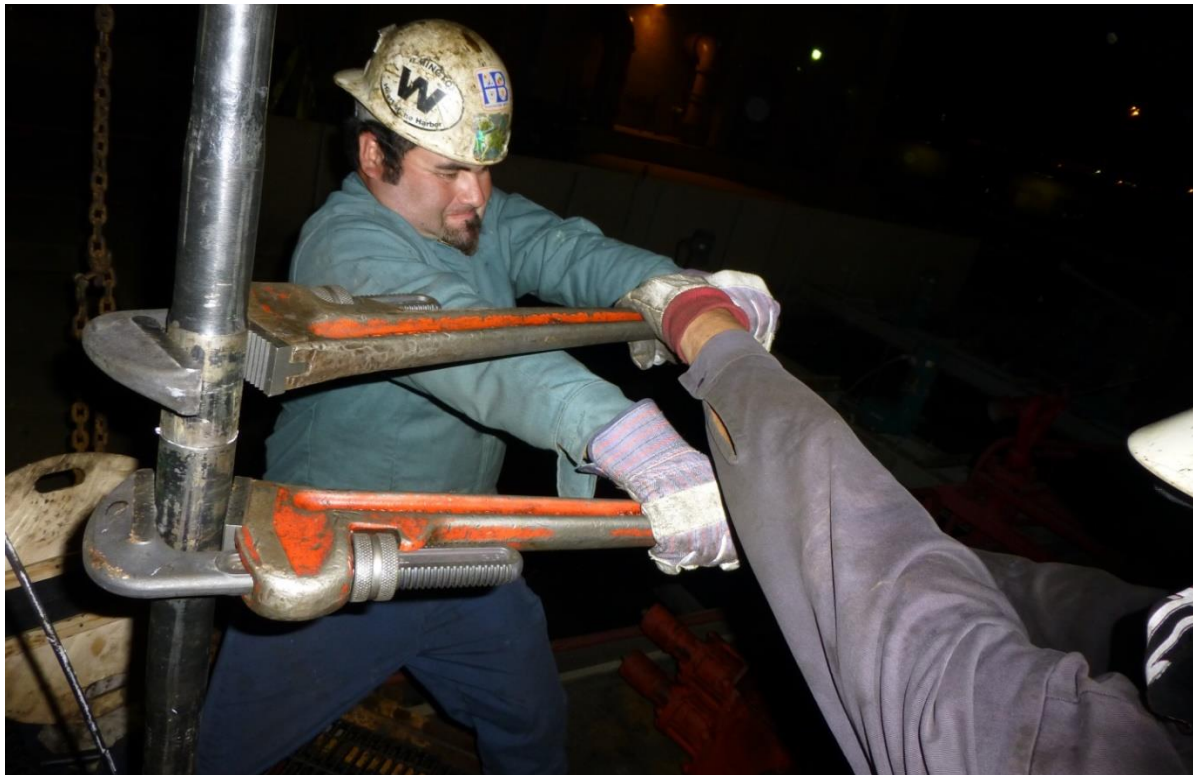


Figure 57. Long Beach, CA. The drill pipe is assembled using large pipe wrenches.



Figure 58. Long Beach, CA. The centralizer is used to protect the $\frac{1}{4}$ " tubing holding the fiber.



Figure 59. Long Beach, CA. The source used for the Long Beach survey was a 110 lbs. solid steel bar with holes drilled for the handles. The zero time was recorded using a time break accelerometer which is mounted near the bottom of the source.

We developed a data QC system as well for this first deployment so we could evaluate the data in the field. The optical system was interrogated on a set of electronics shown in Figure 60. The very first data recorded by the OpticSeis® system can be seen in Figure 61. This record shows that we were successful in recording high quality data despite a small source and a highly attenuating soft formation at the first field test,



Figure 60. Long Beach, CA. Set up of the OpticSeis® interrogator and recording system.

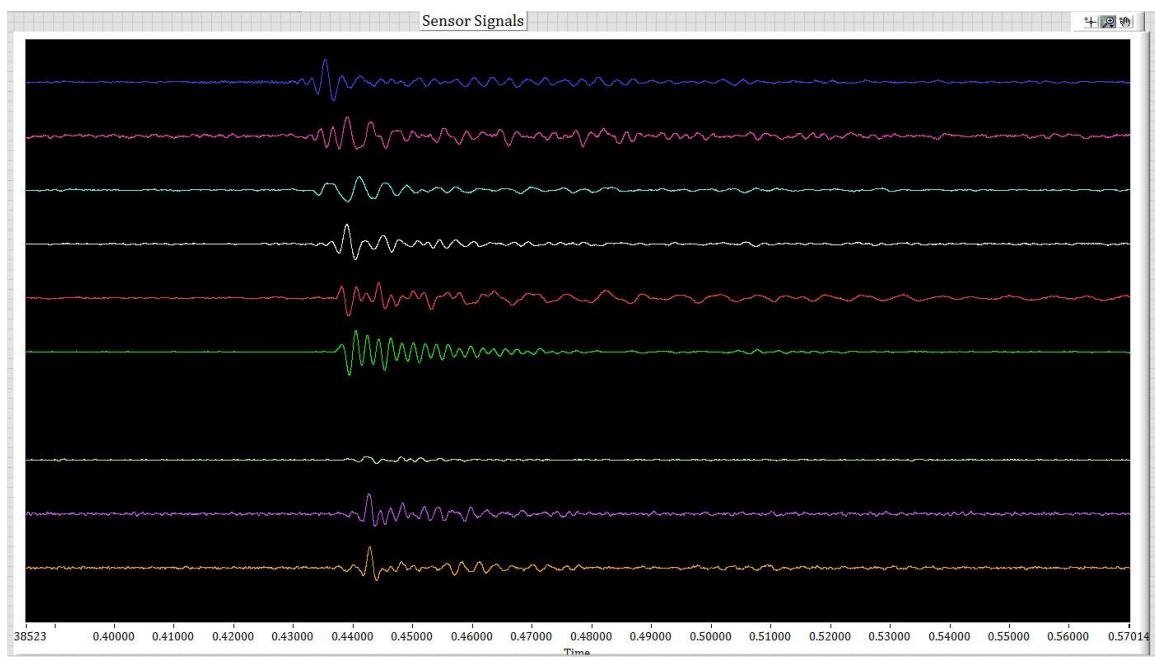


Figure 61. Long Beach, CA. First field data from the OpticSeis® system displayed in the field.



Figure 62. Long Beach, CA. The OpticSeis® system removed from the well after survey has been completed.

After the survey was completed the system was removed from the well as shown in Figure 62. The system was successfully removed from the well, packed and shipped back to our facility without any damage to any of the components.

Processing of Long Beach, CA Data

The survey in Long Beach, CA was the first test of the system in the field so the focus was on operational and data management issues not on generating data for imaging.

A number of tests were conducted over a period of three days. A small walk away survey was recorded and a limited VSP to a depth of about 1,600 ft was recorded. A sample of the offset VSP data rotated to the principal component pointing to the source can be seen in Figure 63. Excellent data was recorded with a frequency content up to 1,000 Hz despite the soft and highly attenuating formation at the test site.

We also did tap tests on the well head to establish the frequency content that could be recorded. The data from the well tap test hitting the well head with a small hammer is shown in Figure 64.

This data has frequencies to about 3,000 Hz showing that the sensors and the sensor pod are capable of recording very high frequencies.

The data recorded from the limited Long Beach field test show that the OpticSeis® system has tremendous potential for recording high frequency high quality borehole seismic data.

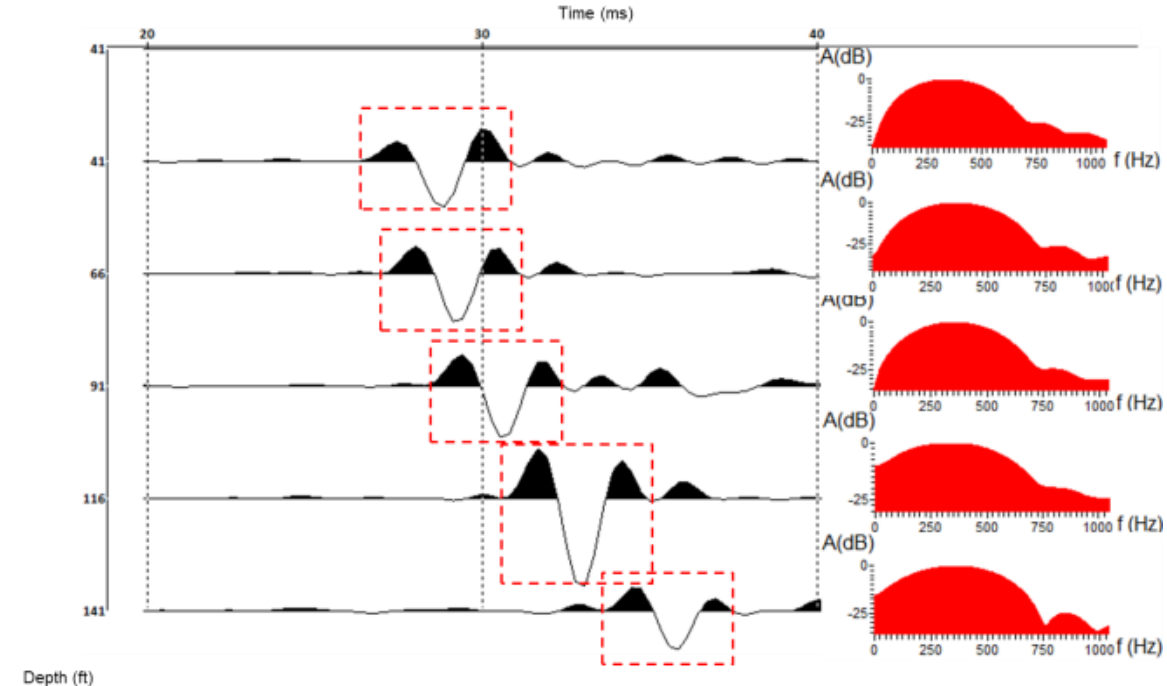


Figure 63. Long Beach, CA. Sample of 160 ft Offset VSP data from Long Beach, CA. The 3C data has been rotated to the Principle Component – i.e. to the direction yielding maximum amplitude. The source used was a 110 lb. steel bar shown in Figure 59.

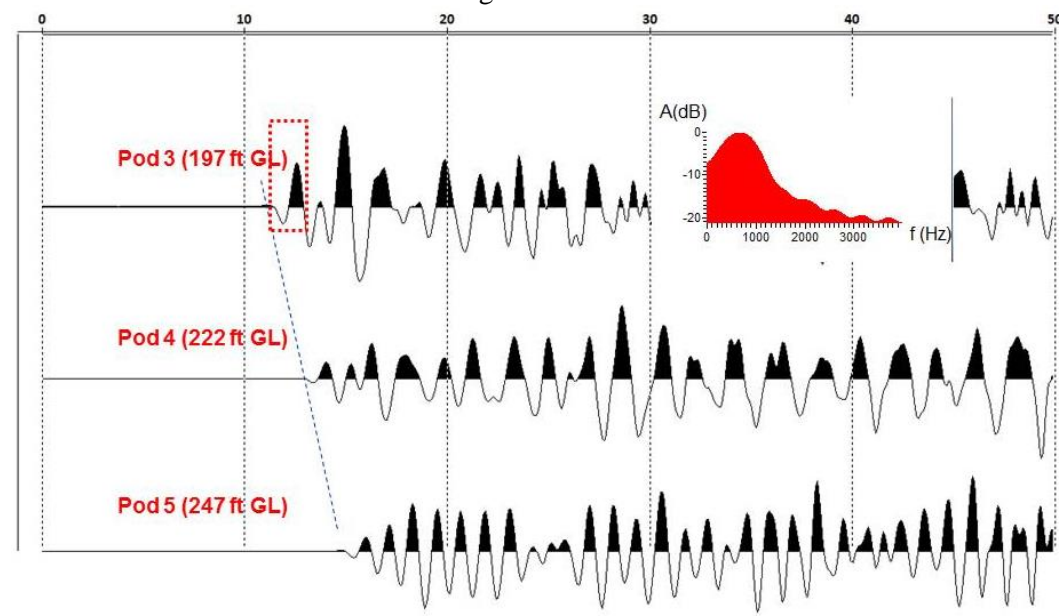


Figure 64. Long Beach, CA. Raw FBG based vector data recorded on the axial component. The data was generated by tapping the well head with a small hammer. The data has been resampled to from 80 kHz to 8 kHz. This data shows that the OpticSeis is capable of recording at least 3,000 Hz data.

The Pearland, TX Field Tests of the OpticSeis® system, June 2013

The second borehole seismic survey with the OpticSeis® system was performed for an operator in June 2013 during a test they commissioned of fiber optic based borehole seismic technologies.



Figure 65. Pearland, TX. The deployment system used for the Pearland, TX VSP survey.

Prior to deployment into the well the entire OpticSeis® deployment system is laid out in front of the well. In Figure 65, from the left, are shown the 19' long drill pipe joints, seven sensor pod housings and one bottom assembly. Properly accounting of the correct number of drill pipe joints is critical to deploying the 3C clamped sensors to the correct depths. The system is partially preassembled on the ground near the well to speed up the deployment of the system.

The first part of the system deployed into the well is the bottom assembly with the nosecone, the fluid intake section, the check valves and the burst disk assembly. This assembly is seen lifted up to the well in Figure 66. Following the bottom assembly are the sensor pod housings attached to a joint of drill pipe. This can be seen in Figure 67.

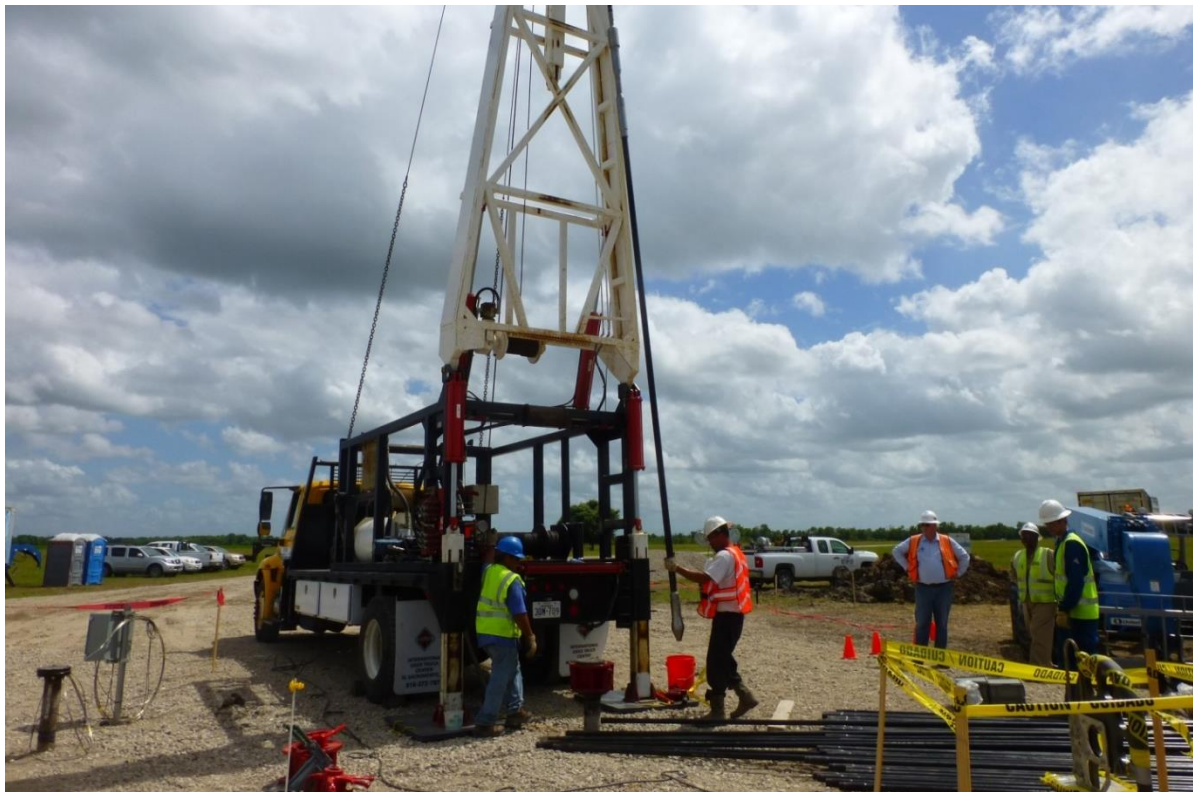


Figure 66. Pearland, TX. The deployment system used for the Pearland, TX VSP survey.

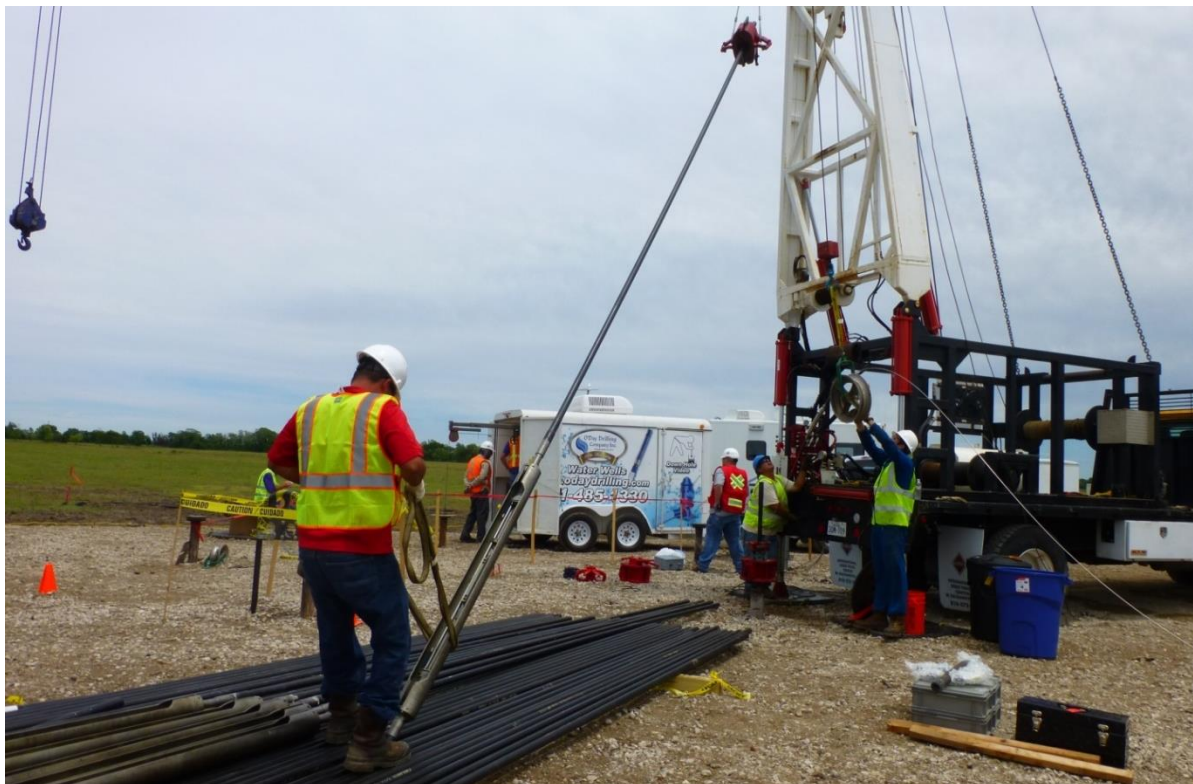


Figure 67. Pearland, TX. The deployment system used for the Pearland, TX VSP survey.

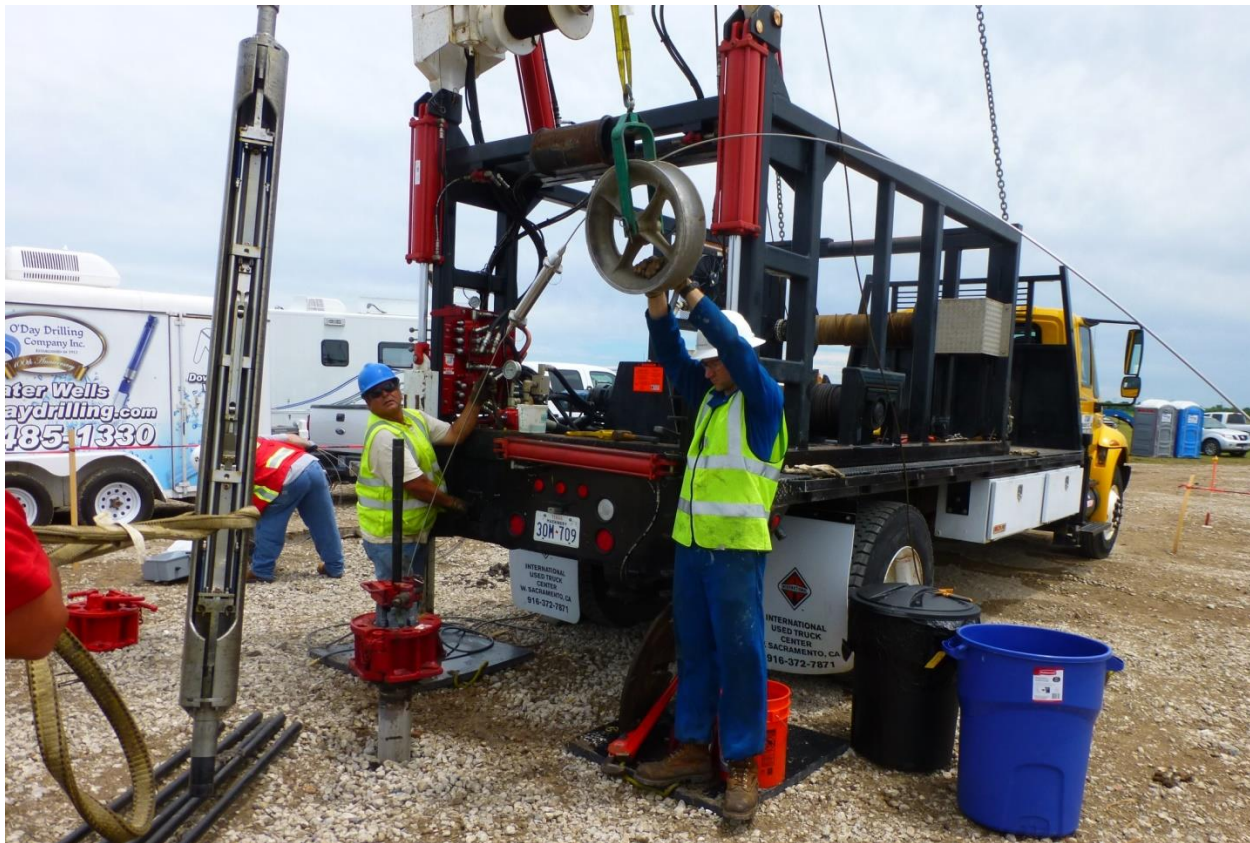


Figure 68. Pearland, TX. The deployment system used for the Pearland, TX VSP survey.



Figure 69. Pearland, TX. The deployment system used for the Pearland, TX VSP survey.

As the drill pipe is lowered into the well the $\frac{1}{4}$ " tube with the fiber must be lowered simultaneously with the drill pipe and attached to the drill pipe with robust centralizers. This process is shown in Figures 68, 70 and 71. After lowering the drill pipe into the well the pipe is hung from a set of slips that are set into a split bowl as shown in Figure 69. To secure the drill pipe a set of "dog collar" is attached to the pipe above the slips. This assures that the pipe will not slip.



Figure 70. Pearland, TX. The deployment system used for the Pearland, TX VSP survey.

After the pipe has been hung from the slips the next sensor pod housing – drill pipe assembly is attached to the drill pipe sticking up from the slips. This sensor pod housing is shown in Figure 70. After the sensor pod housing has been attached to the drill pipe hanging in the well the sensor pod is attached to the sensor pod housing. This process can be seen in Figure 70.

Deployment Speed of OpticSeis® System

We have been able to install a 25 ft long sensor pod housing, drill pipe and sensor pod assembly in about two minutes allowing 30 x 25 ft sets to be deployed in one hour. This will result in a deployment speed of 750 ft per hour. With a 50 ft spaced sensor pods we will be able to deploy 20 sets per hour, or one every 3 minutes, for a deployment speed of about 1,000 ft per hour.



Figure 71. Pearland, TX. The deployment system used for the Pearland, TX VSP survey.

After the sensor pod has been attached to the sensor pod housing, as shown in Figure 71 the assembly is ready to be lowered into the well.

The fully assembled sensor pod housing shown in Figure 71 shows the pod with the 3C fiber optic seismic sensors attached to the sensor pod housing which includes a drill pipe deployed and operated clamping mechanism. This clamping mechanism can be seen behind the sensor pod labeled “OptiSeis™ 3C”

Also seen in Figure 71 is the $\frac{1}{4}$ ” tubing that is attached to the sensor pod. This is the tubing that contains the fibers used to operate the Fiber Optic Seismic Sensors (FOSS)™.



Figure 72. Pearland, TX. One of the sensor pod housings with the sensor pod attached prior to lowering the assembly into the well.

After attaching the pod to the sensor pod housing the assembly is lifted up to clear it from the well head and the slips. Figure 72 shows a sensor pod housing suspended by a joint of drill pipe which is held by the workover rig. Below the sensor pod housing is the string of drill pipe and the sensor pod housings previously deployed into the well. The sensor pod housing has a number of functions. It is part of the structural backbone of the deployment system, it protects the sensor pod during the deployment into the well and it also contains the clamping mechanism.



Figure 73. Pearland, TX. The deployment system used for the Pearland, TX VSP survey.

After the deployment is complete the workover rig is released since it is a significant source of environmental noise. The only equipment that can be seen is a short drill pipe section sticking out of the well. Attached to this short drill pipe is a borehole seismic system top assembly that serves to control the pressure inside the drill pipe which in turn is operating the clamps for the OpticSeis® sensor pods.



Figure 74. Pearland, TX. The well with the OpticSeis® system is seen on the left side of the figure and a MiniVib next to the well in Pearland, TX.

After the deployment the first test to be recorded is usually a Zero Offset VSP (ZOVSP). This can be seen in Figure 74 where the ZOPVSP was recorded with a 24,000 lbs. mini vibrator from ION.



Figure 75. Pearland, TX. The deployment system used for the Pearland, TX VSP survey.

After the successful deployment of the OpticSeis® system the data acquisition was started. The OpticSeis® data acquisition systems are shown in Figure 75.

Processing of Pearland, TX Data

The Pearland survey was a comprehensive survey testing the response of the Fiber Optics Seismic Sensors (FOSS)™ using both surface and downhole seismic sources.

The map of the source points can be seen in Figure 76. The red and white dots on the map represent source points for the surface vibrators. The four purple dots outside the ring of red dots were used for downhole seismic sources.

The data that will be shown in this report is one of the TNT shots that were shot in the well almost straight to the south relative to the center of the wheel of surface seismic source points.

This well is 1,100 ft from the receiver well with the Paulsson OpticSeis® system in the center of the circle of surface seismic source points as seen in Figure 76.

The source was shot at a depth of 300 ft while the receivers were placed at a depth of about 800 ft. The straight line distance between the source and the receiver are thus about 1,200 ft.

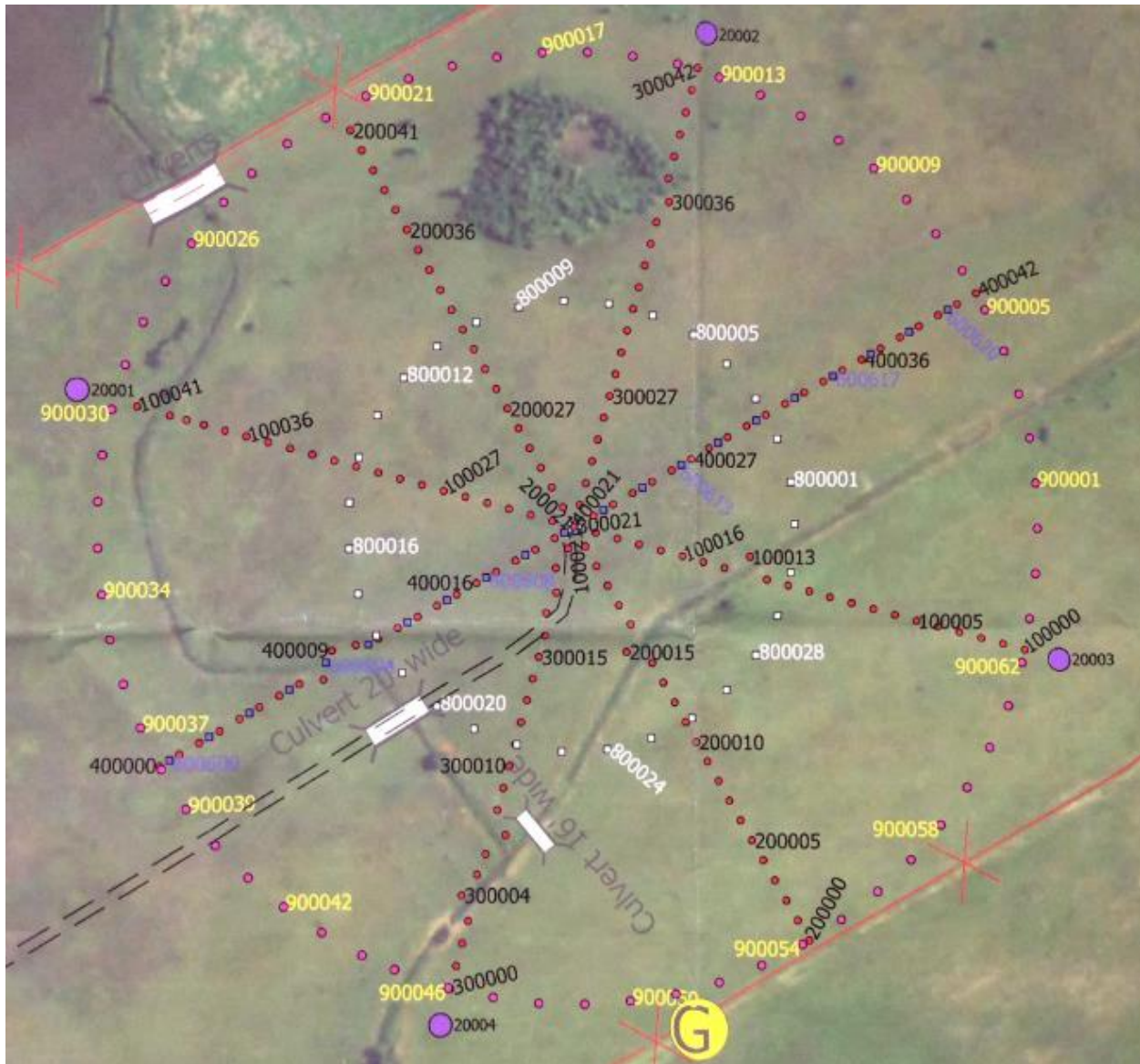


Figure 76. Pearland, TX. The deployment system used for the Pearland, TX VSP survey.

The data displayed in figures 77 to 83 is from a shot of 0.65 gram (650 milligram) of TNT (stringshot) with the TNT was wrapped around a steel pole lowered into the well. Using this technique more than 90% of the effective energy is coupled into tube was and consequently less than 10% is transmitted into seismic body waves.

In Figure 77 we display data from three of the six pods prior to rotation of the data displayed without AGC. The reason for only displaying data from three of the pods is that these three pods all had the latest generation fiber optic seismic sensor. The other three pods had an earlier version of the fiber optic sensors which were not as sensitive.

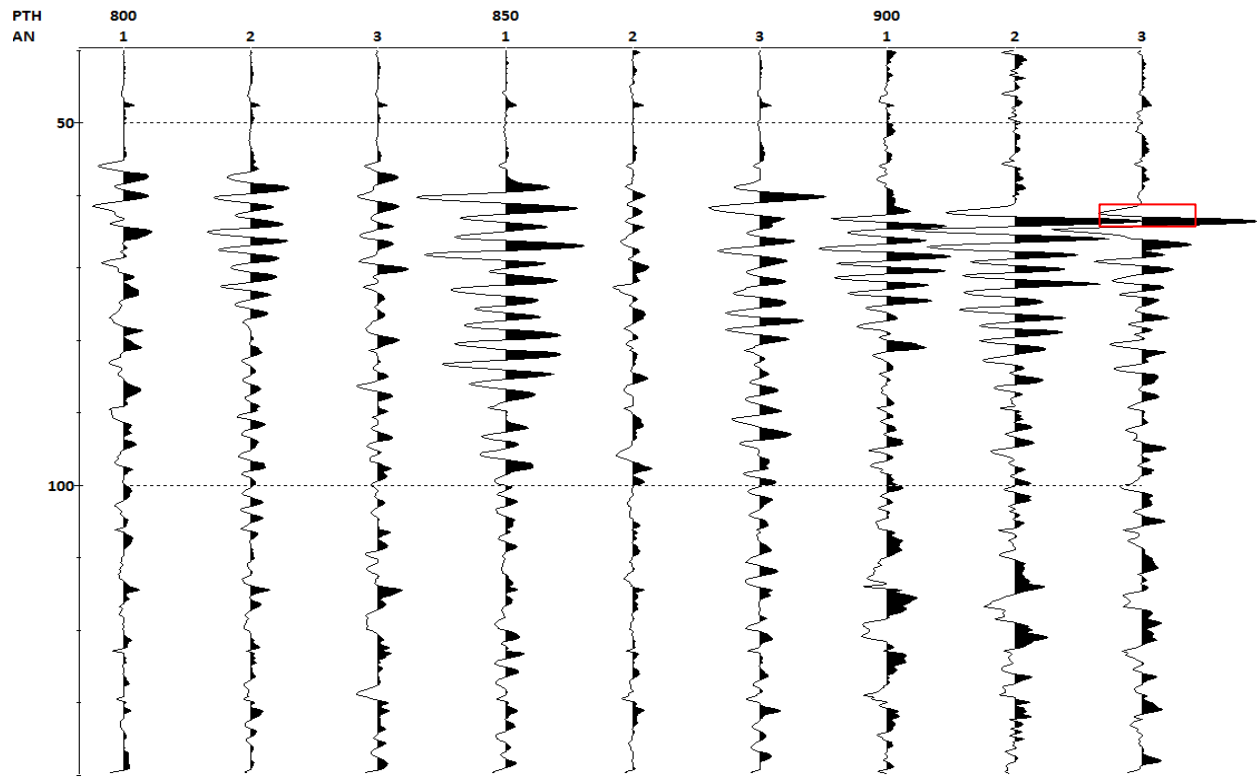


Figure 77. Shot 0.65 gram TNT @ 1,200 ft: Three 3C Pods, Pre-Rotation (Depth 800 – 900 ft, Filter: 80-100-1500-2000 Hz) No AGC. Sensors 3 are the axial sensors.

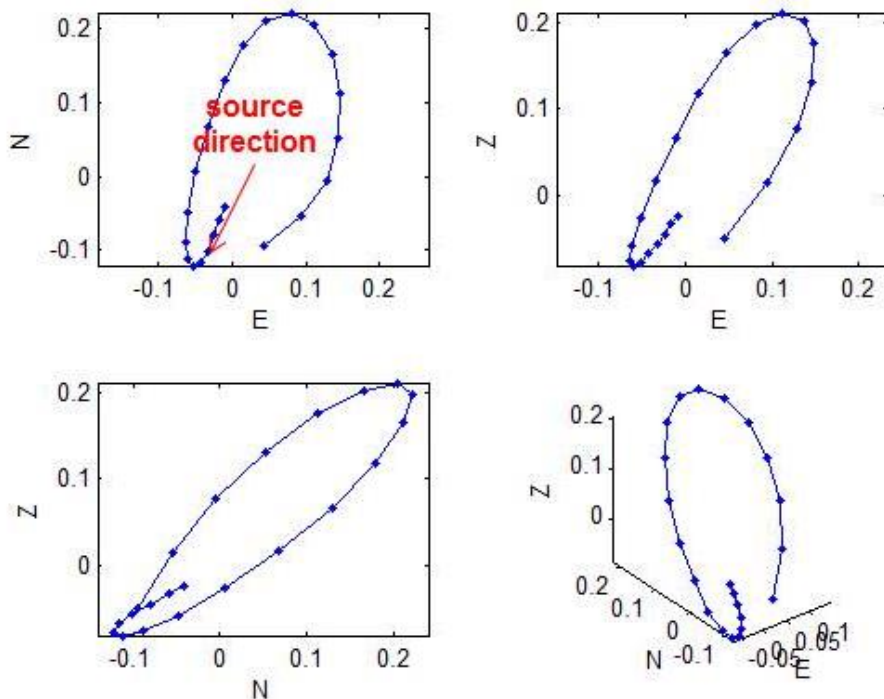


Figure 78. Hodogram analysis of the lowermost pod in the OpticSeis® array. The hodogram shows good 3D vector fidelity. The hodogram points towards the known source point location.

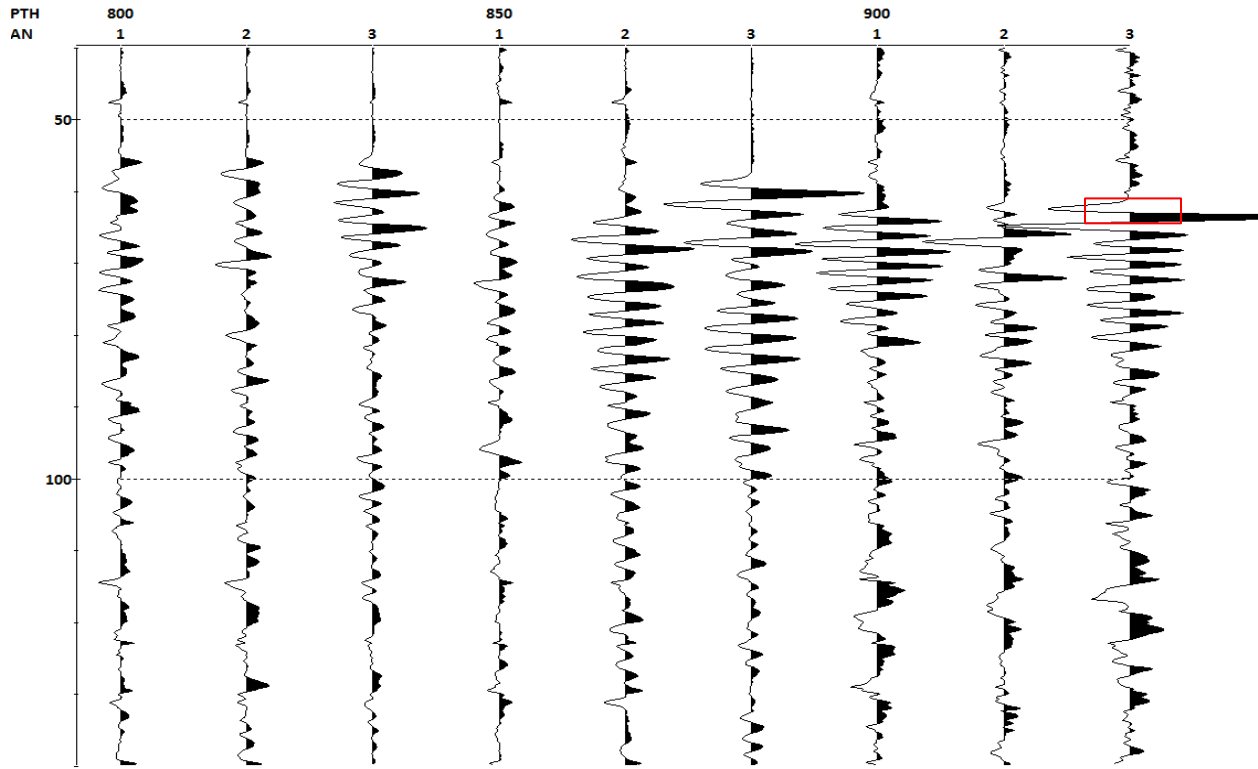


Figure 79. A string shot of 0.65 gram TNT @ 1,200 ft: Three 3C Pods, Post-Rotation (Depth 800 – 900 ft, Filter: 80-100-1500-2000 Hz) No AGC applied. Sensors 3 are the principal components pointing to the source.

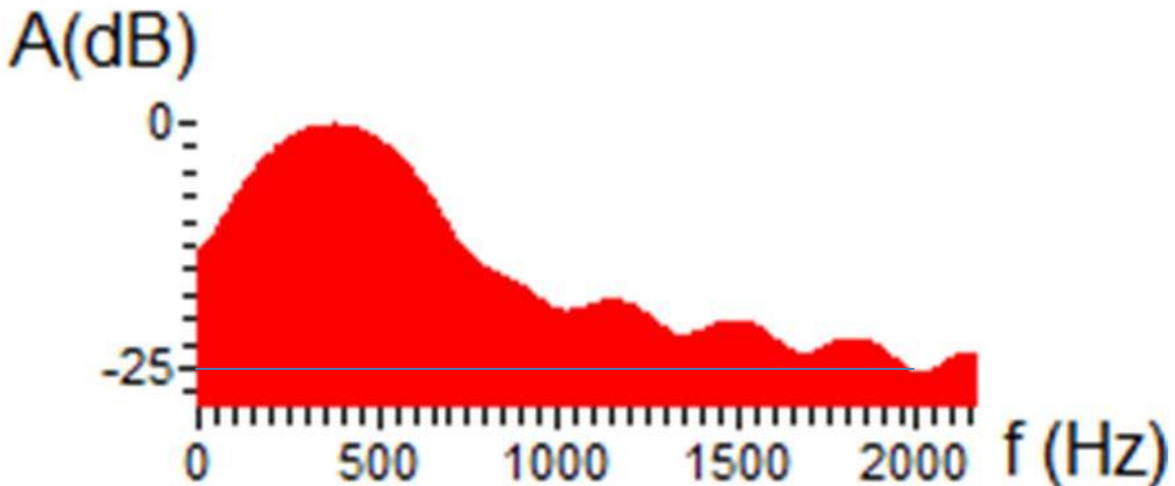


Figure 80. Frequency spectrum of the first arrival wavelet generated by the 0.65 gram shot of TNT at a distance of 1,200 ft between the source and the receivers. The -25dB point is at 2,000 Hz.

The data displayed in Figure 79 is from the 3C pods and the 3C data had been rotated to the principal component for each pod. Sensor 3 is the principal component. The straight line distance between the source point and the receiver location was about 1,200 ft. The Three 3C Pods, Post-Rotation (Depth 800 – 900 ft, Filter: 80-100-1500-2000 Hz). When we did the frequency analysis of the data we found that the - 25 dB point was at 2,000 Hz as seen in Figure 80.

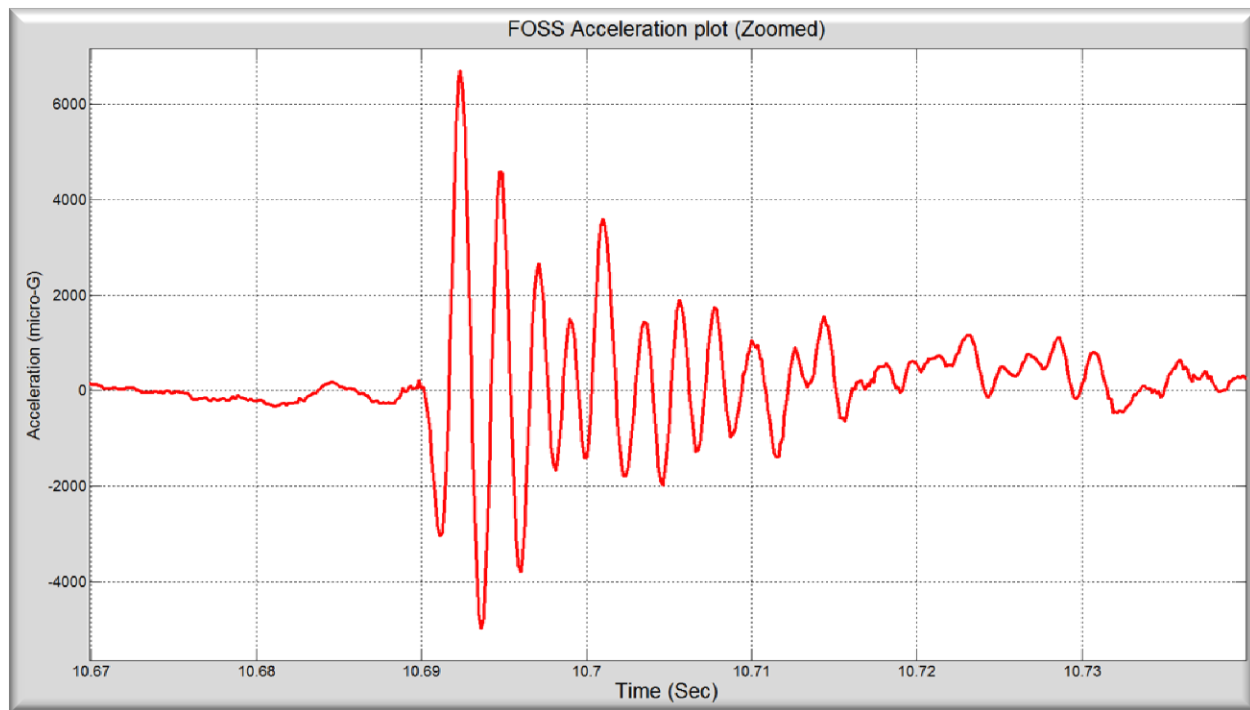


Fig 81. A 3C rotated trace from a 0.65 gram TNT string shot at a distance of 1,200 ft between the shot and the clamped Fiber Optic Seismic Sensor (FOSS)TM pod.

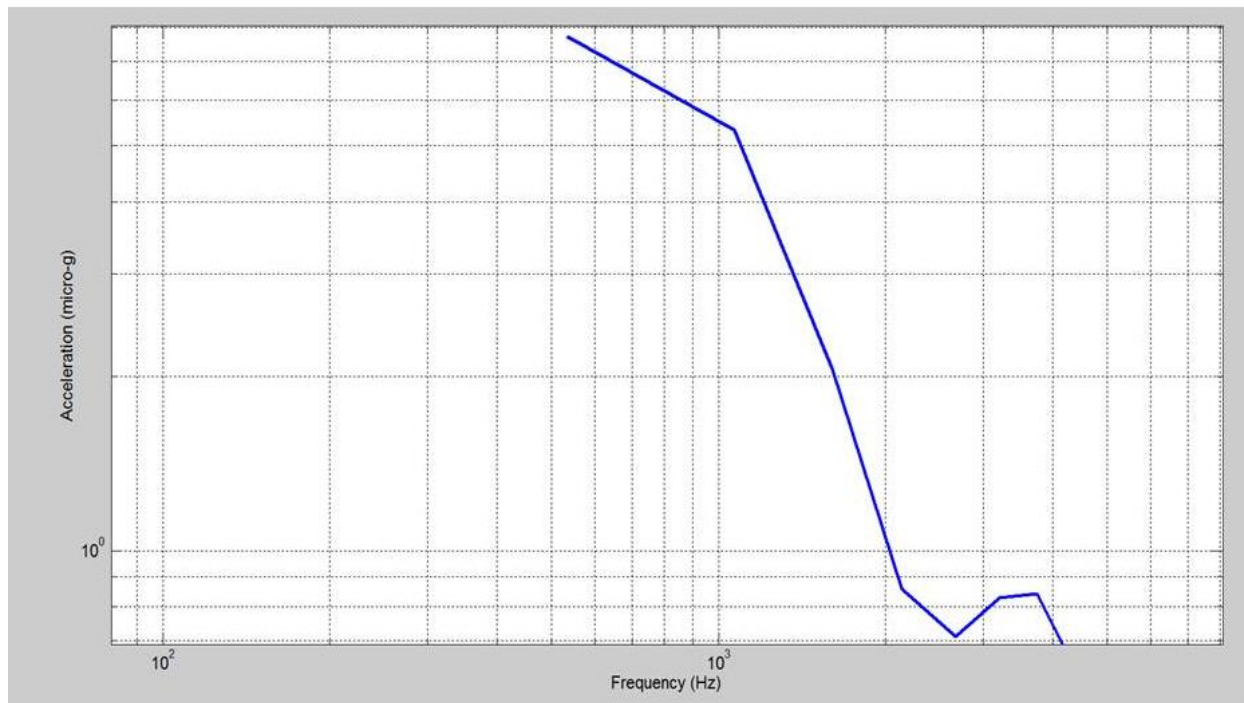


Fig 82. The absolute acceleration spectrum from the seismic record in Figure 81 using the calibrated sensor transfer function.

We are analyzing one of the traces generated by the Our Fiber Optic Seismic Sensors (FOSS)TM . All the sensor amplitude acceleration transfer functions have been calibrated so we can map the optical output amplitude into absolute acceleration. We analyzed the data recorded from the small explosives and compared the data with earthquakes. We calculated that the 0.65 gram of uncoupled TNT in a fluid filled well is equivalent of an earthquake with magnitude -2.6. Small earthquakes do not only have low energy they also generate a lot of high frequencies so any sensor that is deployed to monitor micro seismic events must not only be sensitive but also be able to record high frequencies.

Quantitative Analysis of Data from 0.65 gram of TNT At a distance of 1,200 ft (366 m)	
Frequency (Hz)	Acceleration (μ g)
600	7.3
700	6.7
800	6.2
900	5.8
1,000	5.5
2,000	2.0

Figure 83. Seismic data mapped into absolute acceleration using the calibrated sensor transfer function. Assuming 90% of TNT energy go into tube waves = 200 Joules from 0.65 gram of TNT = Magnitude -2.6

Late Developments

After the field tests were completed in June 2013 further development of the fiber optic sensor was initiated to assess if the sensor could be made even more sensitive. After the analysis the sensor design was updated using the latest findings and FD modeling of the design.

The result is that the latest version of the sensor is now four times more sensitive than the sensor deployed in the June 2013 field test. The increased sensitivity is seen in a comparative test data shown in Figure 84.

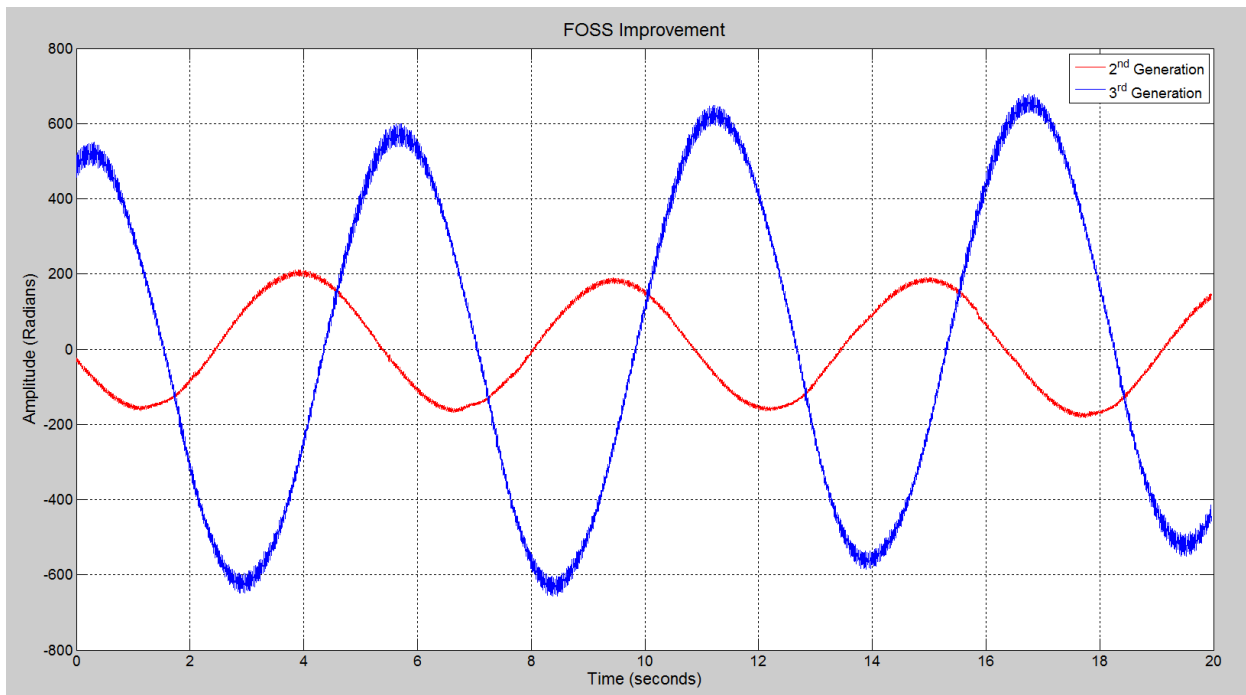


Figure 84. FOSS™ Sensitivity Improvements Red curve tested sensors; Blue curve new sensors

Next steps

We are making the system commercially available. To facilitate this process we have taken the following steps:

We have increased the sensitivity of the fiber optic seismic sensors.

Test the pod performance at high pressure and high temperature: To confirm this modeling we will perform a simultaneous high pressure and high temperature test of the sensor pod. We plan to test the sensor pod to 30,000 psi at 500°F.

We are continuing developing the fiber optic telemetry to make it more compatible with seismic acquisition standards and make the data available for analysis in real time in the field. To achieve this we will automate the transition from an optical data format to a SEGY data format.

The next big step is to build a 200 level 3C borehole seismic array using the technology described in this report. The 200 pods will use a spacing of 25 ft will make the array section 5,000 ft long. We will use a 15,000 ft lead-in for an overall system length of 20,000 ft.

Following the manufacturing of the large array we will deploy the array in a deep on shore well and record a 3DVSP survey and micro seismic data.

Deploy the large array in a deviated/horizontal well and record a 3D VSP survey and micro seismic data.

Process the data to generate images and micro seismic event locations and present results.

Conclusions

A very sensitive, large bandwidth, high temperature vector Fiber Optic Seismic Sensor (FOSS)TM system capable of long term deployment at 30,000 psi and 300°C (570°F) has been developed and integrated into the borehole OpticSeis[®] system.

The Fiber Optic Seismic Sensor (FOSS)TM system discussed in this report was designed and built by Paulsson, Inc. with the support of a number of subcontractors. In the first tests the fiber optic seismic sensors have shown to have superior performance relative to state of the art seismic sensors such as exploration type coil geophones and high performance accelerometers in terms of band width, sensitivity and high temperature performance. The lower noise floor, the flatter spectral response and the higher sensitivity of the new fiber optic seismic sensor will allow for higher resolution imaging and detailed reservoir characterization and monitoring.

The robust design with all electronics placed at the surface will allow the sensors to be deployed at very high temperatures, thus making the sensor a viable sensor for exploration and production and for deep high temperature oil and gas wells. Removing all the electronics from the hostile well environment will also allow the system to be permanently deployed into wells since the fragile component are all installed in a controlled environment where they can be monitored, repaired and replaced.

The new Fiber Optic Seismic Sensor (FOSS)TM represents a breakthrough for the seismic industry and has the potential to challenge the dominance of the regular coil geophone in the most demanding operational environments CCUS reservoir imaging and monitoring and for other demanding high temperature and high pressure applications.

The Fiber Optic Seismic Sensor (FOSS)TM design has the following attributes:

1. Flat frequency response over a very large frequency range
 - a. High Frequency performance: Tested to 6,000 Hz.
 - b. Low frequency performance: Tested to 0.01 Hz (100 second period)
2. Very high sensitivity – capable of recording an earthquake with -2.6M with a S/N > 50
3. High signal to noise ratio – 100 times the S/N ratio compared with geophones
4. Outstanding high temperature performance tested to 320°C (608°F)

A deployment system has been developed and has shown to be strong enough to deploy a 1,000 level 3C borehole seismic array in vertical and horizontal boreholes to a MD of at least 20,000 ft.

First a six and then a sixteen level Fiber Optic Seismic Sensor (FOSS)TM array were manufactured and assembled. The test of the sixteen level array is being planned for mid 2015.

References

Chavarria, J.A., Goertz, A., Karrenbach, M., Paulsson, B., Milligan, P., Soutyrine, V., Hardin, A., and LaFlame, L., (2007), The use of VSP techniques for fault zone characterization: An example from the San Andreas Fault, *The Leading Edge*, June 2007.

Dandridge, A., Tveten, A.B. and Kirkendall, C.K., Development of the Fiber Optic Wide Aperture Array: From Initial Development to Production, 2004 NRL Review, <http://www.nrl.navy.mil/research/nrl-review/2004/optical-sciences/dandridge/>.

Hons, M.S., Stewart, R. R., Lawton, D. C. Bertram, M. B. and Hauer, G., 2008, Field data comparisons of MEMS accelerometers and analog geophones: *The Leading Edge*, 27, 896-903.

Hons, M.S. and Stewart, R. R., 2009, Geophone and MEMS Accelerometer Comparison at Spring Coulee, Alberta, 2009 CSGG, CSEG, CWLS Convention

Kirkendall, C.K., Bartolo, R.E., Tveten, A.B. and Dandridge, A., High-Resolution Distributed Fiber Optic Sensing, 2004 NRL Review, <http://www.nrl.navy.mil/research/nrl-review/2004/optical-sciences/kirkendall/>

Majer, E.L., Daley, T.M., Korneev, V., Cox, D., Peterson, J.E., Queen, (2006), Cost-effective imaging of CO₂ injection with borehole seismic methods, *The Leading Edge*, October 2006.

Müller, K., Paulsson, B.N.P., Soroka, W. L., Marmash, S., Baloushi, M. A., Jeelani, O. A.[2010], 3D VSP Technology - Now a Standard High Resolution Reservoir Imaging Technique; Part- 1 and Part-2, *The Leading Edge*, June 2010

O'Brien, J., Kilbridge, F. and Lim, F. [2004] Time-Lapse VSP Reservoir Monitoring. *The Leading Edge*, Nov. 2004.

Panahi, S.S., Alegria, F. and Manuel, A., 2006, Characterization of a High Resolution Acquisition System for Marine Geophysical Applications, IMTC 2006 – Instrumentation and Measurement Technology Conference

Paulsson, B., Karrenbach, M., Milligan, P., Goertz, A., Hardin, A., O'Brien, J., and McGuire, D., [2004], High resolution 3D seismic imaging using 3C data from large downhole seismic arrays, *First Break*, 22 , no. 10, 73-84

Ramkhelawan, R., Hornby, B., Sugianto, H., Younger, J. (2008), Analysis and interpretation of the largest US onshore 3D VSP, SEG expanded abstract (2008)

Sullivan, Claire, Ross, Allan, Lemaux, James, Urban, Dennis, Hornby, Brian, West, Chris, Garing, John, Paulsson, Björn, Karrenbach, Martin, Milligan, Paul., A 3D Massive VSP Survey at Milne Point, Alaska, Proc., SEG's Annual meeting, Salt Lake City, October 6 - 10, 2002

Wolf, A., Cowles, L.G. and Richardson, W.S., 1938, Vibration Detector, U.S. Patent: 2,130,21